Novel laser energy applications for the treatment of cardiac arrhythmias

Novel laser energy applications for the treatment of cardiac arrhythmias

Proefschrift ter verkrijging van de graad van doctor aan de Universiteit Maastricht, op gezag van de Rector Magnificus, prof. dr. Pamela Habibović, volgens het besluit van het College van Decanen, in het openbaar te verdedigen op

dinsdag 5 juli 2022 om 13:00 uur.

door

Dennis Krist
geboren op 03 juni 1990
te Heerlen

Promotor:

Prof. dr. U. Schotten

Copromotoren:

Dr. D. Linz

Dr. S. Zeemering

Beoordelingscommissie:

Prof. dr. F. Prinzen (Voorzitter)

Prof. dr. K. Vernooy

Prof. T. Jespersen, Copenhagen University, Denmark

M. Mlček PhD, University of Karlovy, Czech Republic

“Declare the past, diagnose the present, foretell the future.”

- Hippocrates -

“A good decision is based on knowledge and not on numbers.”

- Plato -

Table of contents

1 General Introduction

Cardiac Arrhythmias

Cardiac arrhythmias are prevalent among humans across all age ranges, defined as heart rhythms that differ from the normal sinus rhythm, which may occur in the setting of underlying heart disease and structurally normal hearts. The mechanisms responsible for cardiac arrhythmias are divided into two major categories, abnormal impulse formation, and conduction disturbances.

Abnormal impulse formation can result in abnormal frequency, including both reduced automaticity, which causes bradycardia, and increased automaticity, which causes tachycardia. Often the problem is not an abnormal frequency but an abnormal location of impulse formation, leading to irregular cardiac contraction.

Abnormal conduction disturbances most commonly occur when the conduction is delayed or blocked, and the propagating impulse fails to conduct. If the signal fails to succumb and persists, re-entry occurs, re-exciting the heart after the refractory period, leading to an abnormally fast heart rhythm. Treatment options for cardiac arrhythmias include medication, pacemaker placement, cardioversion, and catheter ablation. This thesis discusses the catheter ablation of common cardiac arrhythmias more thoroughly.

Atrial Fibrillation and Flutter

Prevalence Atrial Fibrillation and Atrial Flutter

Atrial fibrillation (AF) and atrial flutter (AFL) are the two most common cardiac arrhythmias encountered in clinical practice, leading to reduced atrial contraction. [1-3] Often, a mix of AF and AFL exists. [3]

The global age standardized prevalence of AF, as estimated per global burden of disease study in 2010, is 596 per 100.000 men and 373 per 100.000 women equating to approximately 33 million people.[4] The prevalence increases from 1-4% among adults below 55 years,[5-7] to more than 13% in persons aged 80 years or older,[7-9] as shown in **Fig. 1.1**. AF is also more common in male than in female subjects (1,1% vs 0,8%; p < 0,001).[10]

Moreover, the prevalence of diagnosed AF is significantly higher in Caucasian individuals (8,0%) compared with African (3,8%), Hispanic (3,6%), and Asian (3,9%) ethnic groups. [11, 12] AFL is less common, with an incidence of 88 per 100.000 persons, but is also more common in men. [13, 14]

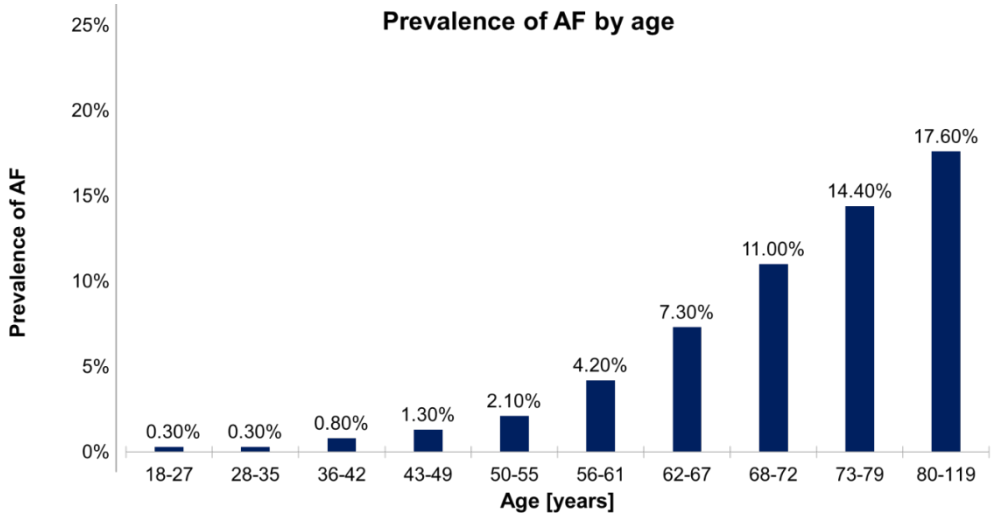

Fig. 1.1 *Increasing prevalence of AF by age. 18-27 years, 0.27% (95% Confidence Interval (CI)); 28-35 years, 0.31% (95%CI); 36-42 years, 0.79% (95%CI); 43-49 years, 1.26% (95%CI); 50-55 years, 2.12% (95%CI); 56-61 years, 4.23% (95%CI); 62-67 years, 7.3% (95%CI); 68-72 years, 10.99% (95%CI); 73-79 years, 14.39% (95%CI); and 80-119 years, 17.56% (95%CI).*[7]

The incidence of AF and AFL increases rapidly due to the ageing population and increased awareness in high-income countries. The future influence of developing countries, such as Brazil, China, India, Indonesia, and Africa, is of particular interest as more people are likely to reach 65 years or older. [10, 15]

Accordingly, the number of AF cases is expected to have doubled by 2050. Affecting at least 1216 million people in the USA by 2050[16]. In Europe, approximately 15 million people will be affected by 2050[8, 17], with 120.000–215.000 newly diagnosed patients per year[8, 18]. In China, 9 million people will be affected by 2050 and 12 million in Africa. [19, 20]

Pathophysiology of AF and AFL

The relationship between AFL and AF can be complex since AFL coexist with or precedes AF.[14] For example, the incidence of AF after successful AFL treatment is up to 56,6% at a three-year follow-up.[21] Commonly shared symptoms for individual AF and AFL patients vary, ranging from asymptomatic to fatigue, palpitations, dyspnoea, hypotension, syncope, heart failure (HF) or general discomfort in the chest.[18]

The development of AF is progressive, with premature atrial contractions progressing to short paroxysms and self-terminating periods of AF. Ranging over several months up to years, the occurrence of AF tends to increase in duration and to become persistent.[22] In comparison, AFL tends to self-terminate within hours to days. **Fig. 1.2** portrays the ECGs of a normal rhythm, AF and AFL.

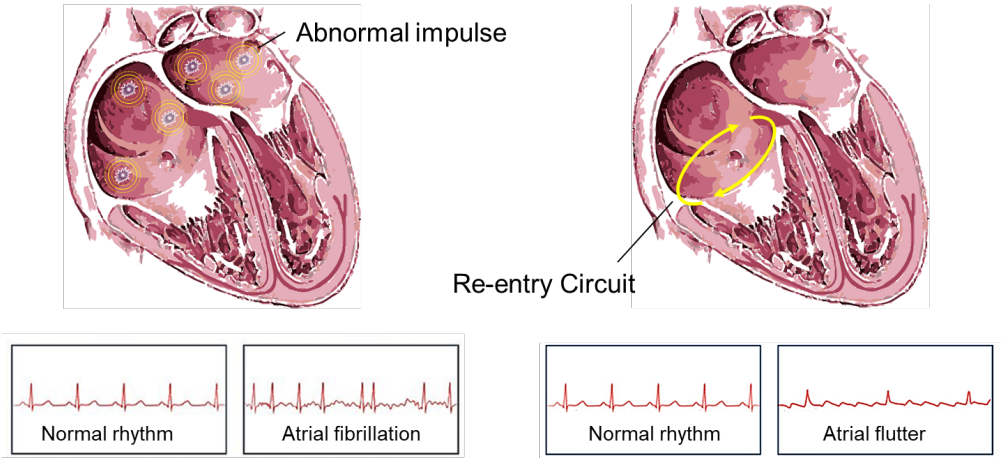

Fig. 1.2 *AF and AFL compared to the normal sinus rhythm. Left: abnormal impulses in case of atrial fibrillation and the ECG of a normal and affected rhythm. Right: re-entry circuit in case of atrial flutter and an ECG of a normal and affected rhythm.*

Although the exact interaction between the factors contributing to the pathogenesis of AF is unknown, it is assumed it involves an interaction between triggers for initiation of the arrhythmia and an abnormal atrial tissue substrate capable of maintaining the arrhythmia. [18, 23] The trigger often occurs as rapidly firing ectopic foci, most commonly located in the myocardial sleeves extending from the left atrium into the proximal parts of pulmonary veins (PV).[24, 25] Interstitial cells[26] and melanocytes[27], both of which have been identified in the PV, provide additional potential sources for abnormal atrial activity.

The mechanisms involved in the production of focal ectopic activity and the exact underlying mechanism of initiation remain to be elucidated. The abnormal atrial substrate, with potentially increased susceptibility to AF, is usually a result of inflammatory infiltration, fibrosis, ion channel alterations, or hypertrophy.[9] Common causes are underlying heart disease associated with hypertension [28, 29], valvular heart disease [30], cardiomyopathies, coronary artery disease (CAD), [31] and HF.

Several extra cardiac risk factors influence the incidence of AF, including obesity [32-34], excessive alcohol and drug consumption[35], hyper-thyroidism[36, 37], and sleep apnea[38], all of which have pathophysiological effects on atrial cellular structure and function. The same characteristics, causes and risk factors underlay AFL.

As opposed to atrial fibrillation, atrial flutter is a macro re-entrant tachyarrhythmia, mostly contained in the right atrium (RA). A single re-entrant circuit sustains it. The cava tricuspid isthmus (CTI), defined as the atrial tissue confined by the inferior vena cava (IVC) and the tricuspid valve (TCV), provides a critical zone of slow conduction, sustaining the re-entrant circuit forms.[39]

Clinical significance of AF and AFL

AF is associated with elevated risks of cardiovascular events and death. Due to stagnant blood in the fibrillating atrium, AF is directly related to an increased occurrence of thromboembolic events, resulting in significant morbidity and mortality. [40-42] AF is associated with a fivefold increase in stroke incidence and a stroke risk increase with age.[43]

Subsequently, a stroke is one of the most debilitating complications. Nearly 15% of all ischemic strokes are directly related to AF[44]. Moreover, ischemic stroke associated with AF is approximately twice as likely to be fatal, and functional deficits are more likely to be severe among survivors than non-AF stroke. [45] Therefore, early recognition and treatment of AF are of utmost importance. Non-stroke outcomes include HF [41], cognitive impairment and dementia [46], myocardial infarction[42], sudden cardiac death[40], and all-cause death. [47]

Ventricular Tachycardia

Prevalence of Ventricular Tachycardia

Ventricular tachycardia (VT) is a cardiac arrhythmia originating in the ventricles and producing an abnormal heart rate above 100 beats per minute. It is a sequence of consecutive premature ventricular beats. The underlying ventricular myocardial scar is the most common etiology, although VT commonly also occurs in the context of severe valvular heart disease or low ejection fraction (EF). Ventricular arrhythmias may also occur in individuals with no apparent structural heart disease. Currently, 10% of all VT diagnoses consist of these idiopathic VT cases. [48]The age- and gender-adjusted incidence of idiopathic ventricular arrhythmias is 52 per 100.000 (95% CI). [49] The incidence increases with age but are similar across genders.

Pathophysiology of VT

Symptoms of VT include fatigue, palpitations, dyspnoea, presyncope, syncope (although rare in PVCs unless in the context of severely depressed cardiac function), and heart failure. [50-52] The mechanisms behind ventricular tachyarrhythmias include enhancing normal automaticity or abnormal automaticity, an activity triggered by early or late afterdepolarizations and re-entry. [53] Depending on the origin of the tachycardia, the rhythm is either monomorphic or polymorphic.

In monomorphic VT, the ventricular activation sequence is constant with a heart rate greater than 100 beats per minute, most caused by re-entry related to ischemic or structural heart disease. These diseases usually lead to scar tissue in either ventricle, disrupting the normal electrical impulses around the scar that result in tachycardia, which is similar to the re-entrant circuits that are the cause of atrial flutter. Contrarily, polymorphic VT presents a variable electrical activation sequence caused primarily by abnormalities of ventricular muscle

repolarization, related to either congenital heart disease or external triggers like drug toxicity or electrolyte abnormalities. **Fig. 1.3** portrays the ECGs of a normal rhythm, monomorphic, and polymorphic VT.

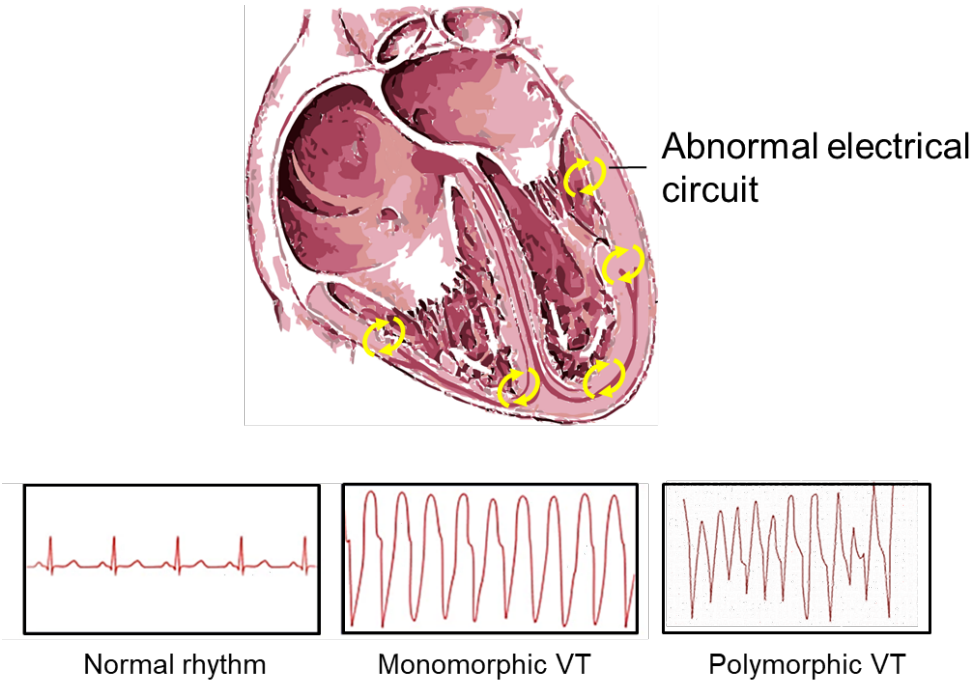

Fig. 1.3 *Abnormal electrical circuits in case of monomorphic and polymorphic VT, and the ECG of a normal and affected rhythms.*

Clinical significance of VT

VT is often short-lived and self-terminating. However, it can be associated with hemodynamic instability and collapse, where acute cardioversion is necessary. Although VT is not a life-threatening abnormal rhythm in people without any structural heart disease, it can be life-threatening. It may impair cardiac output with consequent hypotension, collapse, and acute cardiac failure, if underlying structural heart diseases are present.

In general, VT is a significant cause of sudden cardiac death (SCD), accounting for 80% of SCDs worldwide, equating to 6 million deaths per year [54]. With appropriate drug or surgical treatment, ventricular tachycardia can be controlled in most people.

Treatment of cardiac arrhythmias

Restoring and maintaining sinus rhythm, also known as rhythm control, is an integral part of AF management. Pharmacological or electrical cardioversion restores sinus rhythm in approximately 50% of patients with recent-onset AF. [55, 56] If cardioversion is insufficient and long-term antiarrhythmic treatment is required, antiarrhythmic drugs can be administered, with amiodarone as the most commonly prescribed antiarrhythmic drug (45%). Unfortunately, most antiarrhythmic drugs show many cardiovascular and non-cardiovascular side effects and limited long-term efficacy. [57]

Besides pharmacological treatment of AF, catheter ablation can be first- and second-line therapy of AF, to restore a normal sinus rhythm. In experienced catheter ablation centers, ablation proves more effective than antiarrhythmic drug therapy, with similar complication rates as drug treatment. [58, 59]

For AFL patients, the choice is more straightforward since catheter ablation is superior to rate-control and rhythm-control strategies with antiarrhythmic drugs in restoring sinus rhythm. Therefore, it is commonly chosen as first-line therapy in reasonable candidates.[60]

VT can be treated by antiarrhythmic pharmacotherapy, cardioversion, and catheter ablation, depending on the patients' clinical status. However, the correct treatment strategy decision is complex and depends on the estimated probability of life-threatening VTs and the severity of underlying heart disorders. The primary goal is preventing SCD rather than merely suppressing the arrhythmia.

This objective is accomplished using an implantable cardioverter-defibrillator (ICD).

When the prevention of VTs is essential (e.g., in patients who have an ICD), or when patients do not meet the criteria for ICD implantation, antiarrhythmic pharmacotherapy is initiated.

Alternatively, transcatheter or surgical ablation can be applied, an important treatment choice for patients with VA when antiarrhythmic medications are ineffective, not tolerated, or not desired by the patient. Transcatheter ablation is most used in patients with idiopathic VT and well-defined syndromes.[61]

Catheter ablation of AF and AFL

In patients with paroxysmal AF, pulmonary vein isolation (PVI) is the method of choice. This method is either achieved by circumferential point-by-point radio frequency (RF) ablation of the PV antrum or by single-shot balloon technologies such as the cryo- or laser balloon.

Access to the PV antra is most realized by the entry of the left atrium via a transseptal puncture, after access to the venous system is achieved via the femoral vein. Complete isolation of the PV results in most cases the restoration of NSR.[59]

Conversely, in persistent AF, numerous additional lesions besides PVI can be necessary, ranging from rooflines, mitral isthmus (MI) ablation, ablation of rotor waves and box lesions encircling the posterior LA, including all PVs. In these cases, RF ablation is the gold standard to achieve complex lesion schemes. The most common reason for recurrence of AF after catheter ablation is recovered pulmonary vein conduction of one or more veins. In these cases, RF ablation is an effective strategy for redo procedures supplying a favorable outcome during midterm follow-up.[62]

In patients with AFL, catheter ablation of the CTI is the first-line treatment. Contiguous conduction block between the TCV and IVC is needed at CTI to terminate the re-entrant circuit. Therefore, a contiguous lesion is created between the TCV and IVC to obtain a line of block at CTI, disrupting the circular conduction pattern between the right atrium and the right ventricle.

A radiofrequency ablation catheter creates the lesion with access to the venous system obtained via a femoral puncture. During ablation, the ablation catheter is gradually retracted from the tricuspid valve to the inferior vena cava, [63] with bidirectional CTI block as the desired endpoint.

Epicardial approach in AF and AFL ablation

Besides endocardial ablation, also hybrid and stand-alone epicardial ablation procedures can treat arrhythmias. In general, this treatment is only reserved for patients with prior failed catheter ablation for treatment of paroxysmal AF or symptomatic patients with persistent or long-standing AF.

It is necessary to obtain transmurality or linearity of the CTI and MI ablations by epicardial ablation from the coronary sinus (CS). The hybrid therapy usually consists out of endocardial PVI (1) and epicardial ablation for gap closure, and additional lesions such as roofline (2), inferior line (3), mitral valve isthmus line (4), and RA lines (5) needed to complete the Cox-Maze IV lesion scheme to obtain conduction block as shown in **Fig. 1.4**.

During stand-alone epicardial ablation, all lesions are created via transthoracic access.[64] In both procedures, interoperative measurement of the conduction block with a pacing and sensing device is crucial to increase the efficacy. For epicardial ablation, minimally invasive access to the pericardial space is in most cases obtained by either thoracoscopic or subxiphoidal methods. Although, the

percutaneous subxiphoidal approach is the only access method allowing unrestricted catheter mapping and ablation.[65]

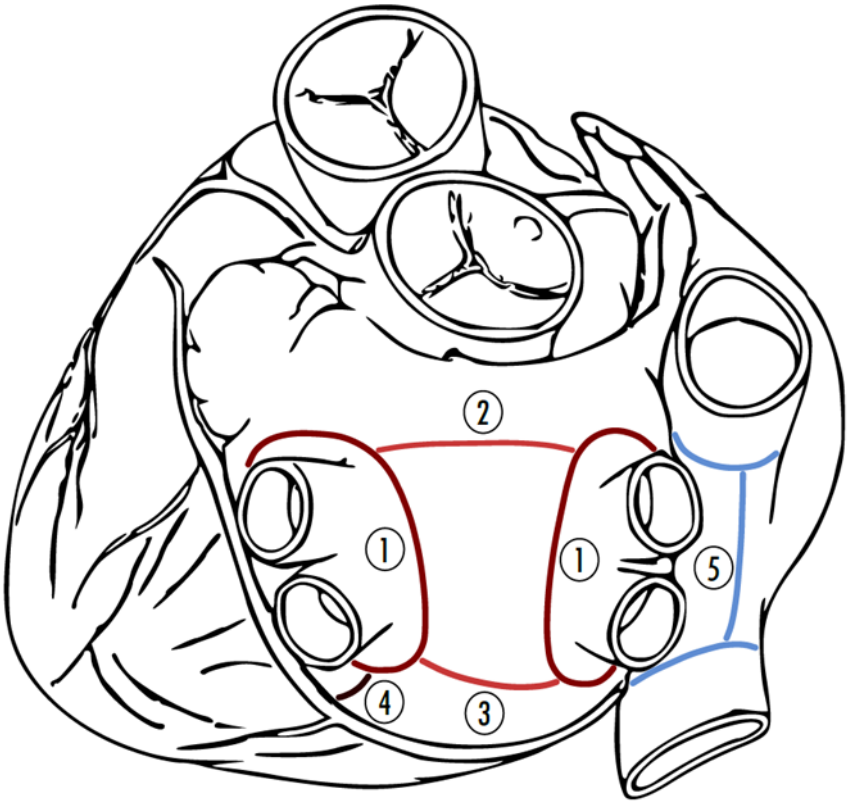

Fig. 1.4 *A common lesion scheme used for hybrid procedures containing PVI (1), roofline (2), inferior line (3), mitral valve isthmus line (4) and RA lines (5).*

Catheter Ablation of VT

Ablation treatment of VT has significantly evolved over the past few decades and is a powerful tool for post-infarction scar homogenization. [66] Ablation of idiopathic VT in the absence of structural heart disease is well accepted as a safe and effective procedure. In post-infarction scar homogenization ablation, no uniform agreement exists on the optimal ablation strategy. However, high-density

delineation of the scar is commonly the first step to eliminate all abnormal electrograms. [67, 68]

More extensive and linear ablation schemes are associated with a better success rate and a lower recurrence rate during ablation of large scar-related ventricular tachycardia.[69]

In contrast, ablation of VT with underlying structural heart disease is more challenging due to the involved heterogeneous re-entrant circuits and the location of the circuits deep inside the scar.[70]

Biophysical limitations of RF ablation are constituted by the thick ventricular walls with transmural circuits, where besides the wall thickness, trabeculations and fat serve as barriers to effective power delivery into the scar.

Aim and outline of the thesis

This thesis aims to illustrate the development of a linear laser ablation technology that can be used in either hybrid or stand-alone epicardial ablation procedures for the treatment of cardiac arrhythmias.

In *Chapter 2,* the technical development of a laser ablation catheter with lateral emission is described, including investigations regarding the laser-tissue interaction and a therapeutical dose-finding study. Subsequently, a proof-of-concept study was conducted to investigate the atrial and ventricular lesion formation by a 20mm linear laser ablation catheter.

Chapter 3 discusses the results of the lesion depth, and tissue damage is reported. In these investigations, laser energy was applied in a continuous fashion. However, indications show that a pulsed laser application could possess beneficial properties regarding lesion formation and thermally induced blood clot formation.

The significance of pulsed wave laser applications on the minimally invasive treatment of cardiac arrhythmias was investigated in *Chapter 4*.

Chapter 5 addresses the differences in the lesion formation principle between RF and laser ablation catheters on the required energy to achieve transmural tissue lesions. In the ablative treatment of cardiac arrhythmias, lesion continuity is crucial for procedural success.

In *Chapter 6,* the suitability of reflectance spectroscopy to assess lesion formation directly was investigated.

References

[1] Cox JL, Boineau JP, Schuessler RB, Ferguson TB Jr, Cain ME et. al. Successful surgical treatment of atrial fibrillation. Review and clinical update. JAMA. 1991 Oct 9;266(14):1976-80.

[2] Takahashi Y, Iesaka Y, Takahashi A, Goya M, Kobayashi K et. al. Reentrant tachycardia in pulmonary veins of patients with paroxysmal atrial fibrillation. J Cardiovasc Electrophysiol. 2003 Sep;14(9):927-32. doi: 10.1046/j.1540-8167.2003.03094.x.

[3] Granada J, Uribe W, Chyou PH, Maassen K, Vierkant R et. al. Incidence and predictors of atrial flutter in the general population. J Am Coll Cardiol. 2000 Dec;36(7):2242-6. doi: 10.1016/s0735-1097(00)00982-7.

[4] Chugh SS, Havmoeller R, Narayanan K, Singh D, Rienstra M et. al. Worldwide epidemiology of atrial fibrillation: a Global Burden of Disease 2010 Study. Circulation. 2014 Feb 25;129(8):837-47. doi: 10.1161/CIRCULATIONAHA.113.005119.

[5] Colilla S, Crow A, Petkun W, Singer DE, Simon T, Liu X. Estimates of current and future incidence and prevalence of atrial fibrillation in the U.S. adult population. Am J Cardiol. 2013 Oct 15;112(8):1142-7. doi: 10.1016/j.amjcard.2013.05.063.

[6] Naccarelli GV, Varker H, Lin J, Schulman KL. Increasing prevalence of atrial fibrillation and flutter in the United States. The American journal of cardiology 2009 Dec; 104(11):1534-9. Doi: 10.1016/j.amjcard.2009.07.022.

[7] Barrios V, Calderón A, Escobar C, de la Figuera M. Patients with atrial fibrillation in a primary care setting: Val-FAAP study. Rev Esp Cardiol (Engl Ed). 2012 Jan;65(1):47-53. English, Spanish. doi: 10.1016/j.recesp.2011.08.008.

[8] Krijthe BP, Kunst A, Benjamin EJ, Lip GY, Franco OH et. al. Projections on the number of individuals with atrial fibrillation in the European Union, from 2000 to 2060. Eur Heart J. 2013 Sep;34(35):2746-51. doi: 10.1093/eurheartj/eht280.

[9] Rahman F, Kwan GF, Benjamin EJ. Global epidemiology of atrial fibrillation. Nat Rev Cardiol. 2014 Nov;11(11):639-54. doi: 10.1038/nrcardio.2014.118.

[10] Go AS, Hylek EM, Phillips KA, Chang Y, Henault LE et. al. Prevalence of diagnosed atrial fibrillation in adults: national implications for rhythm management and stroke prevention: the AnTicoagulation and Risk Factors in Atrial Fibrillation (ATRIA) Study. JAMA. 2001 May 9;285(18):2370-5. doi: 10.1001/jama.285.18.2370.

[11] Hernandez MB, Asher CR, Hernandez AV, Novaro GM. African american race and prevalence of atrial fibrillation:a meta-analysis. Cardiol Res Pract. 2012;2012:275624. doi: 10.1155/2012/275624.

[12] Dewland TA, Olgin JE, Vittinghoff E, Marcus GM. Incident atrial fibrillation among Asians, Hispanics, blacks, and whites. Circulation. 2013 Dec 3;128(23):2470-7. doi: 10.1161/CIRCULATIONAHA.

[13] Bauerle H, Japha T, Gonska BD. Katheterablation von isthmusabhängigem Vorhofflattern [Catheter ablation of typical atrial flutter]. Herzschrittmacherther

Elektrophysiol. 2008 Jun;19(2):60-7. German. doi: 10.1007/s00399-008-0001-x.

[14] Bun SS, Latcu DG, Marchlinski F, Saoudi N. Atrial flutter: more than just one of a kind. Eur Heart J. 2015 Sep 14;36(35):2356-63. doi: 10.1093/eurheartj/ehv118.

[15] Moran A, Gu D, Zhao D, Coxson P, Wang YC et. al. Future cardiovascular disease in china: markov model and risk factor scenario projections from the coronary heart disease policy model-china. Circ Cardiovasc Qual Outcomes. 2010 May;3(3):243-52. doi: 10.1161/CIRCOUTCOMES.

[16] Miyasaka Y, Barnes ME, Gersh BJ, Cha SS, Bailey KR et. al. Secular trends in incidence of atrial fibrillation in Olmsted County, Minnesota, 1980 to 2000, and implications on the projections for future prevalence. Circulation. 2006 Jul 11;114(2):119-25. doi: 10.1161/CIRCULATIONAHA.105.595140.

[17] Stefansdottir H, Aspelund T, Gudnason V, Arnar DO. Trends in the incidence and prevalence of atrial fibrillation in Iceland and future projections. Europace. 2011 Aug;13(8):1110-7. doi: 10.1093/europace/eur132.

[18] Kirchhof P, Benussi S, Kotecha D, Ahlsson A, Atar D et. al. 2016 ESC Guidelines for the management of atrial fibrillation developed in collaboration with EACTS. Eur Heart J. 2016 Oct 7;37(38):2893-2962. doi: 10.1093/eurheartj/ehw210.

[19] Tse HF, Wang YJ, Ahmed Ai-Abdullah M, Pizarro-Borromeo AB, Chiang CE et. al. Stroke prevention in atrial fibrillation--an Asian stroke perspective. Heart Rhythm. 2013 Jul;10(7):1082-8. doi: 10.1016/j.hrthm.2013.03.017.

[20] Stambler BS, Ngunga LM. Atrial fibrillation in Sub-Saharan Africa: epidemiology, unmet needs, and treatment options. Int J Gen Med. 2015 Jul 31;8:231-42. doi: 10.2147/IJGM.S84537.

[21] Jin MN, Song C, Kim TH, Uhm JS, Pak HN et. al. CHA_2DS_2-VASc Score in the Prediction of Ischemic Stroke in Patients after Radiofrequency Catheter Ablation of Typical Atrial Flutter. Yonsei Med J. 2018 Mar;59(2):236-242. doi: 10.3349/ymj.2018.59.2.236.

[22] Natale A, Jalife J. Atrial Fibrillation. Humana 2008. ISBN-13 : 978-1588298560

[23] Markides V, Schilling RJ. Atrial fibrillation: classification, pathophysiology, mechanisms and drug treatment. Heart. 2003 Aug;89(8):939-43. doi: 10.1136/heart.89.8.939.

[24] Haïssaguerre M, Jaïs P, Shah DC, Takahashi A, Hocini M et. al. Spontaneous initiation of atrial fibrillation by ectopic beats originating in the pulmonary veins. N Engl J Med. 1998 Sep 3;339(10):659-66. doi: 10.1056/NEJM199809033391003.

[25] Schotten U, Verheule S, Kirchhof P, Goette A. Pathophysiological mechanisms of atrial fibrillation: a translational appraisal. Physiol Rev. 2011 Jan;91(1):265-325. doi: 10.1152/physrev.00031.2009.

[26] Gherghiceanu M, Hinescu ME, Andrei F, Mandache E, Macarie CE et. al. Interstitial Cajal-like cells (ICLC) in myocardial sleeves of human pulmonary veins. J Cell Mol Med. 2008 Sep-Oct;12(5A):1777-81. doi: 10.1111/j.1582-4934.2008.00444.x.

[27] Levin MD, Lu MM, Petrenko NB, Hawkins BJ, Gupta TH et. al. Melanocyte-like cells in the heart and pulmonary veins contribute to atrial arrhythmia triggers. J Clin Invest. 2009 Nov;119(11):3420-36. doi: 10.1172/JCI39109.

[28] Thacker EL, McKnight B, Psaty BM, Longstreth WT Jr, Dublin S et. al. Association of body mass index, diabetes, hypertension, and blood pressure levels with risk of permanent atrial fibrillation. J Gen Intern Med. 2013 Feb;28(2):247-53. doi: 10.1007/s11606-012-2220-4.

[29] Mitchell GF, Vasan RS, Keyes MJ, Parise H, Wang TJ et. al. Pulse pressure and risk of new-onset atrial fibrillation. JAMA. 2007 Feb 21;297(7):709-15. doi: 10.1001/jama.297.7.709.

[30] Chiang CE, Naditch-Brûlé L, Murin J, Goethals M, Inoue H et. al. Distribution and risk profile of paroxysmal, persistent, and permanent atrial fibrillation in routine clinical practice: insight from the real-life global survey evaluating patients with atrial fibrillation international registry. Circ Arrhythm Electrophysiol. 2012 Aug 1;5(4):632-9. doi: 10.1161/CIRCEP.112.970749.

[31] Kannel WB, Abbott RD, Savage DD, McNamara PM. Coronary heart disease and atrial fibrillation: the Framingham Study. Am Heart J. 1983 Aug;106(2):389-96. doi: 10.1016/0002-8703(83)90208-9.

[32] Wang TJ, Parise H, Levy D, D'Agostino RB Sr, Wolf PA et. al. Obesity and the risk of new-onset atrial fibrillation. JAMA. 2004 Nov 24;292(20):2471-7. doi: 10.1001/jama.292.20.2471.

[33] Wanahita N, Messerli FH, Bangalore S, et al. Atrial fibrillation and obesity--results of a meta-analysis. American Heart Journal. 2008 Feb;155(2):310-315. DOI: 10.1016/j.ahj.2007.10.004.

[34] Frost L, Hune LJ, Vestergaard P. Overweight and obesity as risk factors for atrial fibrillation or flutter: the Danish Diet, Cancer, and Health Study. Am J Med. 2005 May;118(5):489-95. doi: 10.1016/j.amjmed.2005.01.031.

[35] Kodama S, Saito K, Tanaka S, Horikawa C, Saito A et. al. Alcohol consumption and risk of atrial fibrillation: a meta-analysis. J Am Coll Cardiol. 2011 Jan 25;57(4):427-36. doi: 10.1016/j.jacc.2010.08.641.

[36] Cappola AR, Fried LP, Arnold AM, Danese MD, Kuller LH et. al. Thyroid status, cardiovascular risk, and mortality in older adults. JAMA. 2006 Mar 1;295(9):1033-41. doi: 10.1001/jama.295.9.1033.

[37] Selmer C, Olesen JB, Hansen ML, Lindhardsen J, Olsen AM et. al. The spectrum of thyroid disease and risk of new onset atrial fibrillation: a large population cohort study. BMJ. 2012 Nov 27;345:e7895. doi: 10.1136/bmj.e7895.

[38] Mehra R, Benjamin EJ, Shahar E, Gottlieb DJ, Nawabit R et. al. Association of nocturnal arrhythmias with sleep-disordered breathing: The Sleep Heart Health

Study. Am J Respir Crit Care Med. 2006 Apr 15;173(8):910-6. doi: 10.1164/rccm.200509-1442OC.

[39] Daoud EG, Morady F. Pathophysiology of atrial flutter. Annu Rev Med. 1998;49:77-83. doi: 10.1146/annurev.med.49.1.77.

[40] Chen LY, Sotoodehnia N, Bůžková P, Lopez FL, Yee LM et. al. A. Atrial fibrillation and the risk of sudden cardiac death: the Atherosclerosis Risk in Communities Study and Cardiovascular Health Study. JAMA Intern Med. 2013; 173:29–35

[41] Wang TJ, Larson MG, Levy D, Vasan RS, Leip EP, et al. Temporal relations of atrial fibrillation and congestive heart failure and their joint influence on mortality: the Framingham Heart Study. Circulation. 2003; 107:2920–2925.

[42] Soliman EZ, Safford MM, Muntner P, Khodneva Y, Dawood FZ et al. M. Atrial fibrillation and the risk of myocardial infarction. JAMA Intern Med. 2014; 174:107–114.

[43] Wolf PA, Abbott RD, Kannel WB. Atrial fibrillation as an independent risk factor for stroke: the Framingham Study. Stroke. 1991 Aug;22(8):983-8. doi: 10.1161/01.str.22.8.983.

[44] Healey JS, Connolly SJ, Gold MR, Israel CW, Van Gelder IC et. al. Subclinical atrial fibrillation and the risk of stroke. N Engl J Med. 2012 Jan 12;366(2):120-9. doi: 10.1056/NEJMoa1105575.

[45] Lin HJ, Wolf PA, Kelly-Hayes M, Beiser AS, Kase CS et. al. Stroke severity in atrial fibrillation. The Framingham Study. Stroke. 1996 Oct;27(10):1760-4. doi: 10.1161/01.str.27.10.1760.

[46] Kalantarian S, Stern TA, Mansour M, Ruskin JN. Cognitive impairment associated with atrial fibrillation: a meta-analysis. Ann Intern Med. 2013; 158(pt 1):338–346.

[47] Benjamin EJ, Wolf PA, D'Agostino RB, Silbershatz H, Kannel WB, Levy D. Impact of atrial fibrillation on the risk of death: the Framingham Heart Study. Circulation. 1998; 98:946–952.

[48] Brooks R, Burgess JH. Idiopathic ventricular tachycardia. A review. Medicine (Baltimore) 1988;67:271–294. doi: 10.1097/00005792-198809000-00001.

[49] Sirichand S, Killu AM, Padmanabhan D, Hodge DO, Chamberlain AM et. al. Incidence of Idiopathic Ventricular Arrhythmias: A Population-Based Study. Circ Arrhythm Electrophysiol. 2017 Feb;10(2):e004662. doi: 10.1161/CIRCEP.116.004662.

[50] Brugada P, Gürsoy S, Brugada J, Andries E. Investigation of palpitations. Lancet. 1993 May 15;341(8855):1254-8. doi: 10.1016/0140-6736(93)91155-f.

[51] Latchamsetty R, Bogun F. Premature Ventricular Complex-Induced Cardiomyopathy. JACC Clin Electrophysiol. 2019 May;5(5):537-550. doi: 10.1016/j.jacep.2019.03.013.

[52] Singh SM, Kadmon E, Suszko A, Chauhan VS. Syncope triggered by a premature ventricular complex: a case of atrial fibrillation and paroxysmal atrioventricular block. Heart Rhythm. 2012;9:1650–1651.

[53] Cherry EM, Fenton FH, Gilmour RF. Mechanisms of ventricular arrhythmias: a dynamical systems-based perspective. Am J Physiol Heart Circ Physiol. 2012 Jun 15;302(12):H2451-63.

[54] Mehra R. Global public health problem of sudden cardiac death. J Electrocardiol. 2007 Nov-Dec;40(6 Suppl):S118-22. doi: 10.1016/j.jelectrocard.2007.06.023.

[55] Chen WS, Gao BR, Chen WQ, Li ZZ, Xu ZY et. al. Comparison of pharmacological and electrical cardioversion in permanent atrial fibrillation after prosthetic cardiac valve replacement: a prospective randomized trial. J Int Med Res. 2013 Aug;41(4):1067-73. doi: 10.1177/0300060513489800.

[56] Gitt AK, Smolka W, Michailov G, Bernhardt A, Pittrow D, Lewalter T. Types and outcomes of cardioversion in patients admitted to hospital for atrial fibrillation: results of the German RHYTHM-AF Study. Clin Res Cardiol. 2013 Oct;102(10):713-23. doi: 10.1007/s00392-013-0586-x.

[57] Zimetbaum P. Antiarrhythmic drug therapy for atrial fibrillation. Circulation. 2012 Jan 17;125(2):381-9. doi: 10.1161/CIRCULATIONAHA.111.019927.

[58] Cosedis Nielsen J, Johannessen A, Raatikainen P, Hindricks G, Walfridsson H et. al. Radiofrequency ablation as initial therapy in paroxysmal atrial fibrillation. N Engl J Med. 2012 Oct 25;367(17):1587-95. doi: 10.1056/NEJMoa1113566.

[59] Mont L, Bisbal F, Hernández-Madrid A, Pérez-Castellano N, Viñolas X et. al. Catheter ablation vs. antiarrhythmic drug treatment of persistent atrial fibrillation: a multicentre, randomized, controlled trial (SARA study). Eur Heart J. 2014 Feb;35(8):501-7. doi: 10.1093/eurheartj/eht457.

[60] January CT, Wann LS, Alpert JS, Calkins H, Cigarroa JE et. al. 014 AHA/ACC/HRS guideline for the management of patients with atrial fibrillation: a report of the American College of Cardiology/American Heart Association Task Force on Practice Guidelines and the Heart Rhythm Society. J Am Coll Cardiol. 2014 Dec 2;64(21):e1-76. doi: 10.1016/j.jacc.2014.03.022.

[61] Al-Khatib SM, Stevenson WG, Ackerman MJ, Bryant WJ, Callans DJ et. al. 2017 AHA/ACC/HRS Guideline for Management of Patients With Ventricular Arrhythmias and the Prevention of Sudden Cardiac Death: A Report of the American College of Cardiology/American Heart Association Task Force on Clinical Practice Guidelines and the Heart Rhythm Society. J Am Coll Cardiol. 2018 Oct 2;72(14):e91-e220. doi: 10.1016/j.jacc.2017.10.054.

[62] Kettering K, Gramley F. Catheter ablation of atrial fibrillation: Radiofrequency catheter ablation for redo procedures after cryoablation. World J Cardiol. 2013 Aug 26;5(8):280-7. doi: 10.4330/wjc.v5.i8.280.

[63] Knecht S, Burch F, Reichlin T, Spies F, Mühl A et. al. First clinical experience of a dedicated irrigated-tip radiofrequency ablation catheter for the ablation of cavotricuspid isthmus-dependent atrial flutter. Clin Res Cardiol. 2018 Apr;107(4):281-286. doi: 10.1007/s00392-017-1180-4.

[64] Vroomen M, Pison L. Hybrid ablation for atrial fibrillation: a systematic review. J Interv Card Electrophysiol. 2016 Dec;47(3):265-274. doi: 10.1007/s10840-016-0183-9.

[65] Aryana A, d'Avila A. Epicardial Catheter Ablation of Ventricular Tachycardia. Card Electrophysiol Clin. 2017 Mar;9(1):119-131. doi: 10.1016/j.ccep.2016.10.009.

[66] Aryana A, Tung R, d'Avila A. Percutaneous Epicardial Approach to Catheter Ablation of Cardiac Arrhythmias. JACC Clin Electrophysiol. 2020 Jan;6(1):1-20. doi: 10.1016/j.jacep.2019.10.016.

[67] Di Biase L, Santangeli P, Burkhardt DJ, Bai R, Mohanty P et. al. Endo-epicardial homogenization of the scar versus limited substrate ablation for the treatment of electrical storms in patients with ischemic cardiomyopathy. J Am Coll Cardiol. 2012 Jul 10;60(2):132-41. doi: 10.1016/j.jacc.2012.03.044.

[68] Vergara P, Trevisi N, Ricco A, Petracca F, Baratto F et. al. Late potentials abolition as an additional technique for reduction of arrhythmia recurrence in scar related ventricular tachycardia ablation. J Cardiovasc Electrophysiol. 2012 Jun;23(6):621-7. doi: 10.1111/j.1540-8167.2011.02246.x.

[69] Ghanem MT, Ahmed RS, Abd El Moteleb AM, Zarif JK. Predictors of success in ablation of scar-related ventricular tachycardia. Clin Med Insights Cardiol. 2013 May 7;7:87-95. doi: 10.4137/CMC.S11501.

[70] Nair M, Kataria V, Yaduvanshi A. Radiofrequency Catheter Ablation of Ventricular Tachycardia in Structural Heart Disease: Single team Experience with

follow-up upto 5 years Arrhythmia: Open Access. January 2016Interventional Cardiology 08(01). DOI: 10.4172/Interventional-Cardiology.1000520

2 Development of a novel linear laser catheter

Dennis Krist, Ulrich Schotten, Stef Zeemering, Dominik Linz, M. Hettkamp

Abstract

In the thermo-ablative treatment of cardiac arrhythmias, laser energy can be used to achieve durable lesions in the cardiac tissue. This chapter summarizes the basics to laser-tissue interaction and the utilization of laser energy to treat cardiac arrhythmias. With this information and knowledge from existing laser ablation devices, a deflectable 20mm linear laser catheter was developed for endo- and epicardial ablations with state-of-the-art requirements to ablation catheters in the treatment of cardiac arrhythmias.

We investigated the properties of laser on tissue interaction to select the appropriate laser wavelength for the ablative treatment of cardiac arrhythmias. A spectroscopic analysis of the molecular tissue components showed that 980nm provides the ideal wavelength with an adequate balance between penetration depth and absorption. An *ex vivo* dose-finding study was conducted with an existing laser lasso catheter with a length of 45mm to assess the effect of applied power and application time on the thermal coagulation of cardiac tissue to provide a proper baseline for the catheter development. Subsequently, electrodes were fitted to this catheter's the laser active area, allowing recording of local EGM data, 3D mapping, and navigation.

A second dose-finding study showed that the lesion depth remained unaffected in the therapeutic setting window. An *in vivo* study confirmed the advantages of electrodes, including reductions of local EGM data during power application, providing some degree of lesion confirmation.

With this information, a deflectable 20mm linear laser catheter was developed, suitable for transfemoral CTI ablation and ablation of the epicardium via subxiphoidal access. The laterally emitted energy density was increased to 0,49W/mm^2 while maintaining a homogeneous emission profile to increase the maximum lesion depth.

An *ex vivo* dose-finding study confirmed the increase of lesion depth with the same lesion depth predictability as the lasso catheter.

In conclusion, a 20mm linear laser ablation catheter was developed, well able to create deep and homogeneous lesions over the entire length of the 20mm laser-active area. The electrodes placed in the laser active area enabled the usage of state-of-the-art 3D electro-anatomical mapping and navigation systems, without affecting the catheter's lesion depth or safety profile.

Introduction

Laser tissue interaction

In the thermo-ablative treatment of cardiac arrhythmias by laser energy, the targeted tissue is heated by laser absorbtion until a transmural lesion is formed. This absorption of laser energy is related to the optical properties of the targeted tissue, determining whether the light is absorbed, reflected, scattered, or transmitted. In case of absorption, the energy of a photon causes a quantized state at the affected particles, resulting in a changed vibrational mode of the molecule. The energy that triggers the change of vibrational mode is converted to thermal energy and additionally heating of the tissue. The scattering of the light in the tissue influences the achievable lesion depth.

The probability function expressed by the anisotropy factor g[1] describes the directional change of photons in tissue evoked by scattering. The anisotropy factor defines the scattering characteristics between isotropic scattering $g = 0$ and forwards scattering $g = 1$. In human cardiac tissue, this value is between 0.88 and 0.99[2], indicating forward scattering into the tissue. In cardiac tissue, most of the light is absorbed in the near-infrared (NIR) wavelength range by molecular components, such as water, chromophores (i.e., porphyrin, melanin, flavin, and

hemoglobin), nucleic acids, deoxyribonucleic acid (DNA), and ribonucleic acid (RNA).[3] The ideal wavelength for thermal ablation of cardiac tissuecan be determined by absorption spectroscopy of all aforementioned components.

Fig. 2.1 shows the absorption spectroscopy between 200 and 10.000nm for water, fat, Hemoglobin, and Oxyhemoglobin.

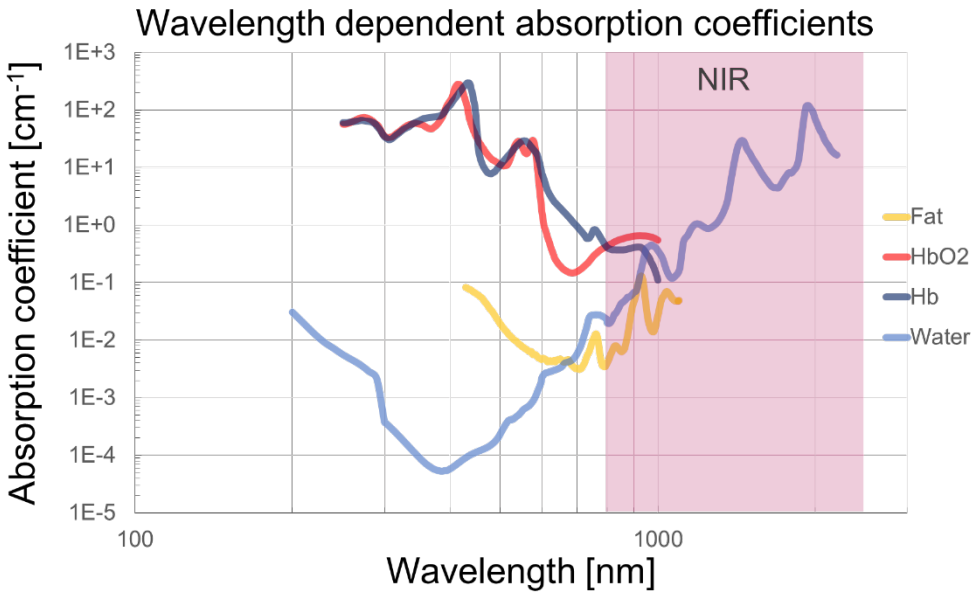

Fig. 2.1 *Estimated absorption coefficients of the main absorbing tissue components like water, fat and haemoglobin as a function of wavelength.*

Since most cardiac structures contain water or components consisting of water, the absorption of laser light is dominated by these aqueous components. Simultaneously, the absorption by (Oxy)hemoglobin should be low in endocardial applications to prevent coagulum formation. The NIR region provides an exciting bandwidth regarding high absorption by water and lower absorption by (oxy)hemoglobin. Therefore, the spectral range between 700nm and 1100 nm is commonly used in medical laser applications, due to a beneficial combination of absorption and penetration ratio. As earlier studies have shown, a wavelength of

980nm ± 1% provides the most suitable therapeutic window for cardiac ablation treatments.[4]

The delivered thermal dose must exceed the threshold defined by the Arrhenius equation to achieve irreversible tissue damage. The Arrhenius equation defines the relationship between exposure time, exposure temperature, and thermal necrosis of the tissue[5] (i.e., an exposure of at least 10s at a temperature of 60°C, leads to tissue necrosis.) **Fig. 2.2** displays this relationship, which is essential to define the therapeutic dose of an ablation catheter.

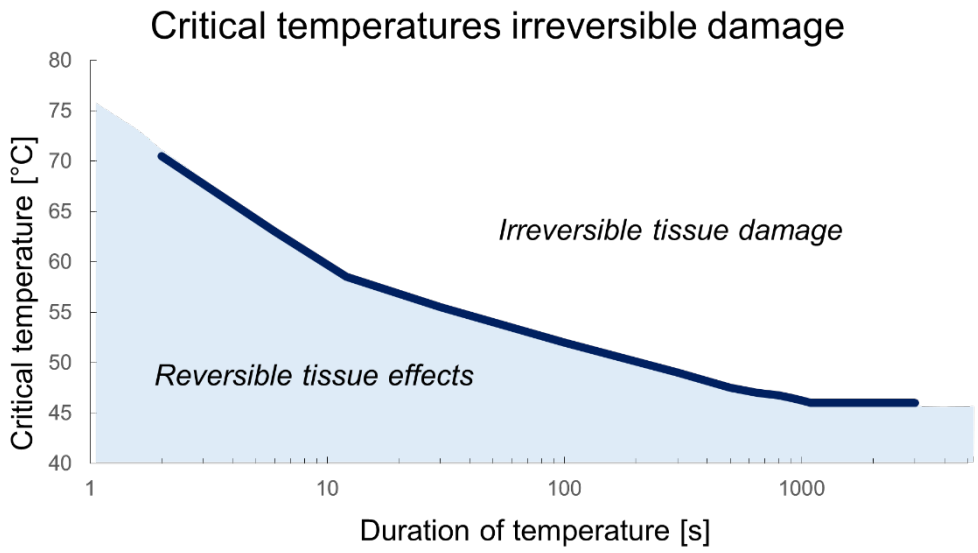

Fig. 2.2 *Critical threshold for irreversible tissue damage that results in cell necrosis.[5]*

Laser ablation technology

The first laser was established in May 1960 at Hughes Research Laboratories by Theodore H. Maiman using a ruby crystal.[6, 7] Since then multiple applications in surgery and medicine have been developed with various laser types. The first investigations with laser energy applications in the treatment of cardiac arrhythmias were conducted in 1985.[8] High energy pulsed Nd-YAG laser was applied to

canine hearts resulting into lesions with a central vaporized crater surrounded by a rim of necrotic tissue. In lower energy settings no crater formation was observed.

In 1989 the effects of a water-cooled argon gas laser in the endocardial ablation of ventricular tachycardia were investigated in an intra-operative clinical evaluation in 20 patients. [9] The study showed the clinical efficacy of focal endocardial laser ablation. The same efficacy was obtained in the epicardial ablation of ventricular tachycardia using a Nd-YAG laser to treat nine patients.[10]

Up to this point the laser ablation studies were conducted with a tip emitting catheter for focal ablation. In 2000 a linear laser ablation was attempted in the canine right ventricle with use of an irrigated linear diffuser and 50W Nd-YAG laser source. By the inclusion of titanium particles along the length of distal active element a lateral scattering was achieved. The studies demonstrated to produce linear transmural conduction block without char formation or tissue disruption.[11]

While prior studies demonstrated the efficacy of pulsed and relatively high energy endocardial and epicardial laser in the treatment of ventricular tachycardia, the arrival of a continuous lower energy diode laser facilitated the formation of controllable and precise lesions. This was demonstrated in a dog model, creating large, deep lesions without hazardous tissue damage using a low energy diode laser light.[12] The first report describing the pathological and histological findings using this type of diode laser energy source was published in 2006[13]. A surgical laser ablation procedure was performed encircling the pulmonary veins in a canine model. Electrophysiological effectiveness was judged by pacing, subsequent histological examination of the excised hearts confirmed all lesions to be transmural.

The earlier diffuser and reflector technology used to create linear lesions was improved by these novel diode laser sources. Linear lesions were created in a sheep model with a 980nm diode laser source demonstrating electrical isolation in all sheep. Histological assessment showed extensive epi- and endocardial

necrosis verifying the effectiveness in minimal invasive creation of transmural cardiac lesions.[14]

With the introduction of ablation devices based on balloon technologies, a laser balloon catheter was developed focussing on the electrical isolation of the pulmonary vein antra und visual guidance. The first-in-human study established the feasibility balloon-based laser ablation, with direct visualization to guide the catheter ablation.[4] The latest generation of laser balloon devices have currently been adopted to clinical routine in atrial fibrillation ablation providing a highly effective and safe tool for pulmonary vein isolation. [15] **Tab. 2.1** provides an historical overview of the laser-based ablation catheters.

Tab. 2.1 *Historical overview of laser-based ablation catheters regarding energy source, wavelength, lesion form, irradiation type and cooling.*

Year	Energy Source	Wavelength	Lesion Form	Irradiation Type	Cooling Type
1960	Ruby Crystal	694.3nm	-	-	-
1985	Nd-YAG	1064nm	Focal	Direct	-
1989	Argon	514nm	Focal	Direct	External Saline
1996	Nd-YAG	1064nm	Focal	Direct	External Saline
1999	Diode	805nm	Focal	Indirect	External Saline
2000	**Nd-YAG**	**1064nm**	**Linear**	**Indirect**	**External Saline**
2006	Diode	980nm	Focal	Indirect	External Saline
2008	**Diode**	**980nm**	**Linear**	**Indirect**	**External Saline**
2009	Diode	980nm	Circular	Direct	Internal Saline
2021	Diode	980nm	Circular	Direct	Internal Saline
Novel device of this thesis	**Diode**	**980nm**	**Linear**	**Direct**	**Internal Saline**

Concept 20mm Linear laser ablation catheter

The 20mm linear laser ablation catheter developed in the frame of this thesis was based on the technology and design used for the Vimecon endocardial ablation catheter. Vimecon has developed a laser lasso catheter that homogeneously emits contentious wave (CW) laser light of a wavelength of 980nm, over a length between 45 and 70mm(Patents: US 2018/0021089, US 2011/0230941, US 2011/0230871).

The laser light is transmitted from the diode laser source (1) into the heart by an optical fiber (2) with a core diameter of 100 - 600µm. Optical fibers typically include a core surrounded by a transparent cladding material with a lower index of refraction. the light is kept in the core by total internal reflection at the transition between the core and the cladding before lateral emission at the active ending. The laser light is emitted laterally(3) over a certain length in a circular or straight shape, adaptable to the physician' individual needs via the central lumen(4). This lateral extraction of laser light in a linear fashion is achieved by selective removal of the cladding(5) in the distal region of the fiber, allowing the light to escape from the core. The openings need to be arranged so that a homogeneous unilateral emission pattern is formed. However, the openings can only make out 10% to 20% of the cladding diameter to maintain the stability of the optical fiber.[16] Any residual energy remaining in the fiber is dissipated at the catheters' tip(6). The schematical drawing of **Fig. 2.3** shows the principle of lateral emission via openings in the fiber cladding in comparison to an old catheter, using titanium dioxide particles(7) to produce scattered radiation.

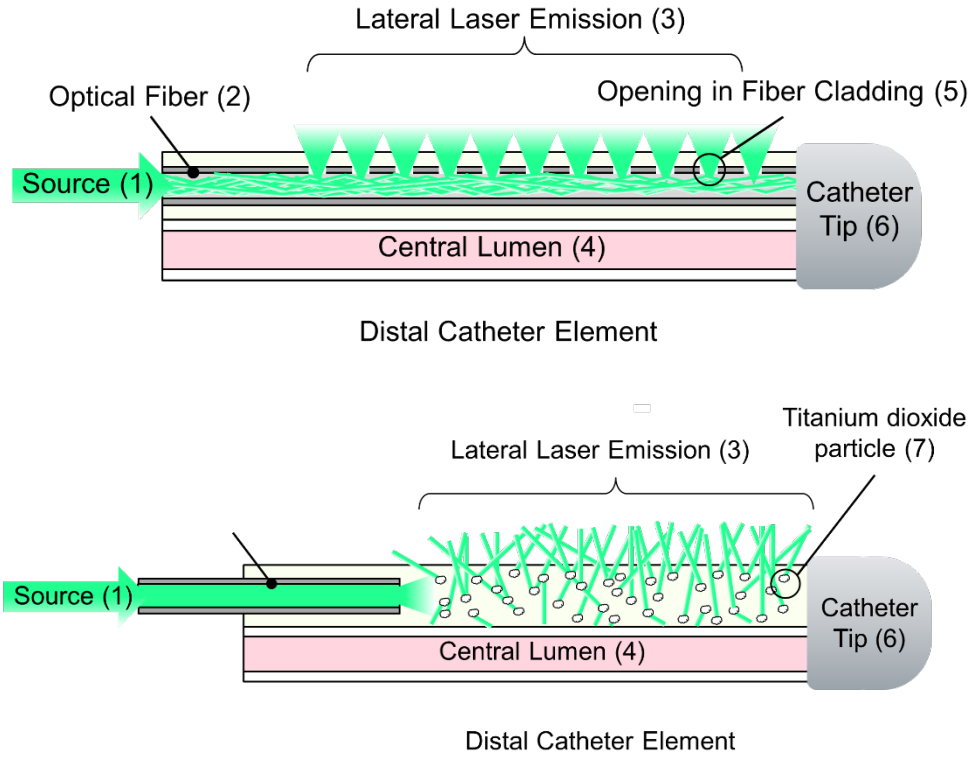

Fig. 2.3 Top: *Schematic drawing of the 20mm linear laser ablation catheter demonstrating the later emission via openings in the fiber cladding. Bottom: old linear ablation catheter based on lateral emission by scattering via titanium dioxide particles.*

This kind of lateral emission and associated direct linear irradiation of tissue is unique in comparison to existing devices that rely on focal point-by-point ablation or reflective particles to create linear lesions. The direct irradiation allows a very controllable linear energy application directly into the tissue resulting into homogeneous lesions in both endocardial and epicardial procedures.

In general, the 20mm linear laser catheter is developed as flexible and multipurpose ablation catheter for endo- and epicardial applications. The use of a linear catheter could reduce ablation times for endocardial procedures that require linear lesions schemes. Currently these lines are created by point-by-point RF or Cryo ablations.

In epicardial procedures the device can create deep and linear lesions in a minimal invasive manner. In its difficulty to create a secure linear conduction block on a beating heart from the epicardial side many focal lesions required resulting in long procedural times. It is the aim of this device to shorten the procedure times by creating linear lesion in one shot in comparison to point-by-point RF or Cryo ablations. The unidirectional energy delivery of the laser catheter also contributes to the protection of surrounding tissues against collateral ablation damage.

Development 20mm laser ablation catheter

During the catheter development various procedural aspects were addressed, including access method, catheter dimensions, catheter steering, and the necessary features in electrophysiology. From a procedural point of view, it is desirable if the catheter orientation is easily identifiable, if wall contact can be confirmed, electro cardiac data can be captured, and if the ablation leads to well-defined deep lesions. Additionally, the catheter must enable state-of-the-art 3D navigation and mapping tools to create a virtual electro-anatomical map of the heart. This section addresses the individual aspects of the catheter development.

Epicardial access methods

Foremost, the desired pericardial access method was identified, providing the boundaries and physical limitations of the catheter. Minimal invasive access is possible based on the experiences with the 8.5 Fr endocardial lasso catheter design. Most commonly, access to the pericardium is achieved by a subxiphoidal approach.[17] For this access method, a needle is inserted in the angle between the xiphoid process and the left costal margin, and advanced at an angle towards the left shoulder. Under fluoroscopy, the needle is advanced into the pericardial space, and its position is confirmed by the contrast agent.[18] Based upon

preprocedural CT and with the aid of echocardiography and fluoroscopy, the ideal trajectory is determined.

The subxiphoid approach is also preferred to insert the epicardial laser ablation catheter into the pericardial sac. This method allows free access to the entire ventricular surfaces, the RA, and the majority of the LA.[19] A multifunctional catheter design is preferred to facilitate endocardial CTI, MI, roof- and bottom lines, in addition to the epicardial ablation of the ventricular surface. An 8.5 Fr bidirectional steerable catheter combined with a steerable sheath is identified as the preferred concept. The length of the laser-active area is set at 20mm, providing an adequate balance between the needed number of applications, maneuverability, and handling.

A bipolar couple of electrodes will mark the beginning and end of the laser-active area. The catheter tip can either be open with saline flushing, or closed with internal flushing. Flushing cannot be omitted in this kind of laser catheter. The flushing is required as the cooling medium, dissipating residual laser energy at the tip. shows the final design of the 20mm linear laser ablation catheter. A low-energy 532nm laser diode is used to highlight the lateral emission between the electrodes in green.

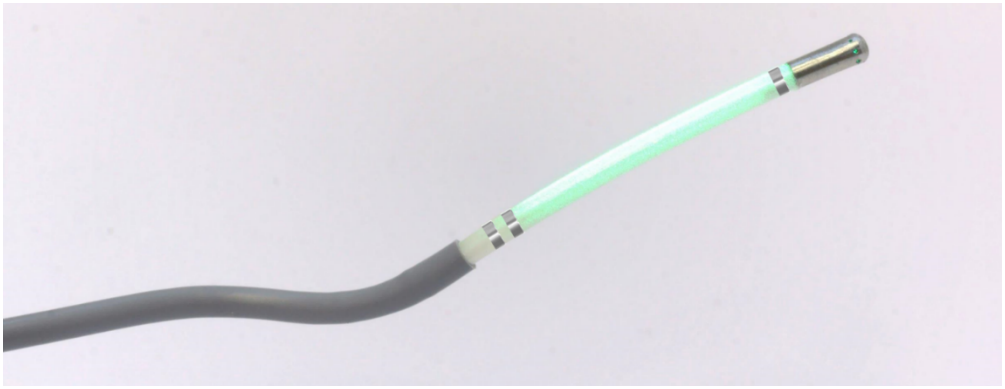

Fig. 2.4 *The final design of the 20mm linear laser ablation catheter. A low-energy 532nm laser diode is used to highlight in green the lateral emission between the electrodes.*

Sensing and pacing electrodes in the laser-active area

The electrophysiology market has shown significant technological development involving 3D mapping of voltages and anatomy, 3D navigation, and high-quality signal recording. The ability to map and navigate in 3D is essential, especially for epicardial ablations.

The incorporated electrodes are used in the intraprocedural fluoroscopic navigation but moreover for impedance-based electro-anatomical mapping and navigation. The individual spatial location of each electrode can be determined by measurement of the voltage gradient between two electrodes if an electrical field is applied and, thus, achieve intracardiac catheter visualization.

The state-of-the-art electroanatomic mapping and navigation systems also provide a reconstruction of the geometry of the catheter allowing precise placement and orientation of the catheter.[20, 21] displays the schematic principle of three orthogonal electrical fields and a catheter found in this field.

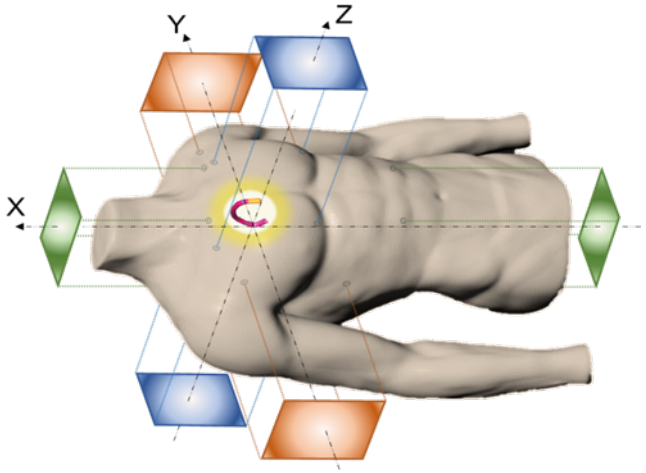

Fig. 2.5 *Schematic illustration of the principle behind impedance-based visualization, with 3 orthogonal electrical fields x, y, and z. By measuring the voltage gradient, the position of each electrode can be determined in this electrical field, thus defining the position of the catheter.*

Besides mapping and navigation, the electrodes in the laser-active area can also provide information about the lesion formation during the power application. The intracardiac potentials, measured by the electrodes, supply local EGM data to verify wall contact of the entire laser-active area. Compared to RF, no electrical interference is caused during energy delivery. The main challenge is the placement of the electrodes in the laser-active area. Electrode placement may not change lesion formation or reduce procedural safety due to thermocoagulation of blood. To prevent excessive heating of the electrodes by direct irradiation the lateral laser emission was locally reduced.

Methods

Base-line existing laser ablation catheter

An *ex vivo* dose-finding study was conducted to establish a lesion depth predictability for the existing 45mm linear laser ablation catheter. This study also serves a baseline for the development of the 20mm linear laser ablation catheter. The lesion depth function of the applied power and application time was investigated under controlled conditions. An 8.3 Fr irrigated tip laser lasso catheter with a total laser-active area of 45mm and lasso diameter of 28mm was used to apply the laser light with a wavelength of 980nm to the *ex vivo* tissue model. The catheters were opposed to avian tissue heated in a saline bath at a controlled temperature of 37 ± 2°C. Due to the strong demarcation between treated and untreated tissue, avian tissue is preferred for the macroscopic estimation of the lesion depth compared to bovine or porcine tissue. A contact force of 22 ± 5g was set by use of a calibrated force sensor. The power settings were varied between 20W and 30W, respectively 45s to 120s.

Electrode placement in the laser active area

To assess the influence of electrodes in the laser active area of the catheter a dose-finding study was conducted with the same power settings and setup as for the existing laser ablation catheter. The results of both dose-finding studies are displayed as scatter plots. To assess the differences in lesion depth between both scatterplots a t-test was conducted per energy setting with a significance level of 5%.

Endocardial *in vivo* experiment with integrated electrodes

An *in vivo* animal study was conducted to assess the compatibility of the existing lasso catheter with the current state-of-the-art electro anatomical mapping system and investigate the capabilities of recording local EGM data. The experiments were performed at the Cardiac Physiology Experimental Lab of the

Charles University and Na Homolce Hospital (Albertov 5, 128 00 Prague, Czech Republic), the experimental protocol was compliant with the local guidelines for animal experiments. Female swine with a weight between 40 and 60kg and approximately 4–6 months old were used for the study.

Standard femoral vein access with transseptal puncture was used to introduce a steerable sheath and a laser lasso catheter with eight electrodes in the LA. The primary endpoint of this proof-of-concept investigation was to show the compatibility with the NavX™ Ensite™ system of St. Jude Medical and record local EGM data during the power application.

Optimizing the lateral emission profile for 20mm lesions

The lateral emission of laser light is a defining aspect of the linear laser ablation catheter. By careful distribution of openings in the fiber cladding a homogeneous emission profile can be created.

The hole distribution of the 20mm linear catheter is derived from a compacted distribution scheme of the existing 45mm laser lasso catheter. By step-wise adjustments of the hole distribution algorithm a homogeneous lateral emission over 20mm can be achieved. To assess the homogeneity of the created distribution scheme a small amount of laser energy is applied to the modified fiber while an IR-camera records the emission. Freely available image analysis software was used to plot the emission over the length as grey values (ImageJ Version 1.52, public domain). The recorded grey values are plotted over the length of the catheter for comparison between distribution schemes.

Dose-finding 20mm linear laser ablation catheter

To investigate the created emission profile's homogeneity and assess the lesion depth a dose-finding study was conducted. A similar set up as the 45mm laser

lasso catheter was used. Equivalently, the catheters were opposed to avian tissue with a temperature of 37±2°C. Contrastingly, the ablations were performed outside of the saline bath to simulate epicardial ablations. The power settings were varied between 20W and 30W; the time was set between 60s and 150s.

The homogeneity of the lesion was decided by a comparison of the lesion depth between the proximal and distal areas. The relative deviation (Δ_{rel}) between distal ($t_{dist.}$) and proximal ($t_{prox.}$) area against the average lesion depth ($t_{average}$) was estimated by the following function:

$$\Delta_{rel} = \frac{\left| t_{prox.} - t_{dist.} \right|}{t_{average}} \cdot 100\%$$

Comparison of data

To compare the lesion depth between the existing 45mm lasso catheter and the novel 20mm linear laser catheter, the applied energy was corrected to energy per mm of laser active area and plotted against the average lesion depth in one graph.

Results

Base-line existing laser ablation catheter

In total, 295 ablations with five different catheters were performed, resulting in 1180 measurements of lesion length and depth.

The study found the lesion length to be constant at approximately 46,7 ± 2,81mm. **Fig. 2.6** display the lesion depth as a function of power and time as a box plot. The plot portrays a quasi-linear increase of lesion depth by increasing either power or time, with lesion depths ranging from 1mm to 6mm.

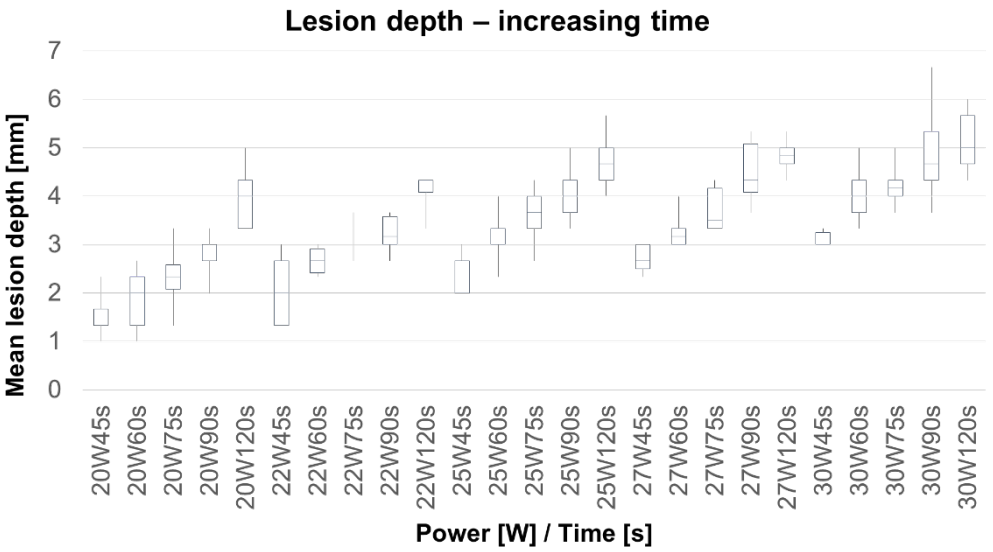

Fig. 2.6 *Measured lesion depth of power and application time. In this graphical presentation, the effect of increasing time is portrayed, by clustering according to applied power.*

Electrode placement in the laser active area

The retention of the lesion formation properties was confirmed by an additional dose-finding study. The scatterplots of catheter with and without electrodes in the laser active area are displayed in **Fig. 2.7**. No significant difference in lesion depth was noticed between both designs in the therapeutic window ($p = 0.735$ and $p = 0.259$). In the low-energy range, the design with electrodes showed significantly reduced lesion depth ($p = 0.012$ and $p = 0.014$). Contrastingly, in the high-energy range, the design with electrodes showed significantly increased lesion depth ($p = 0.004$).

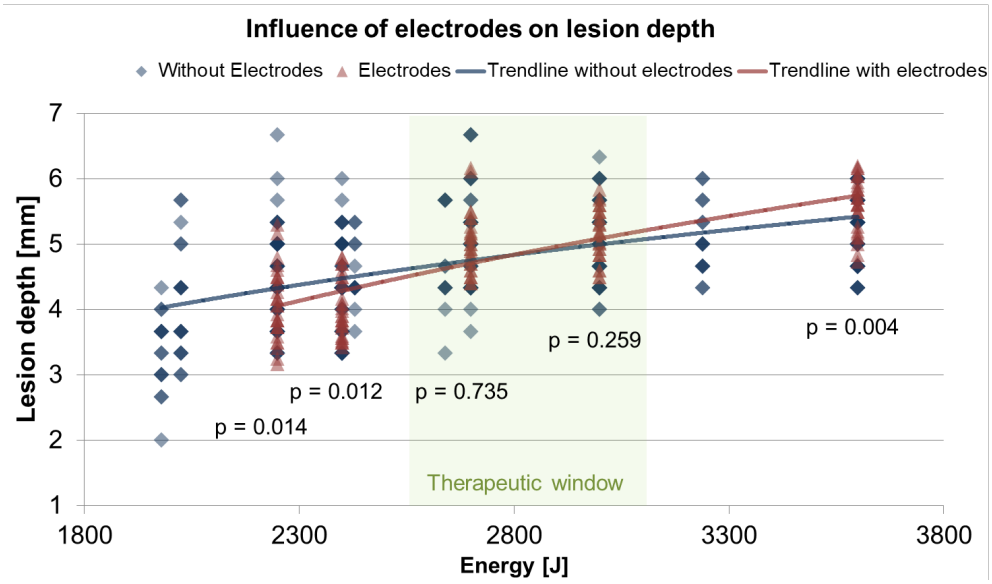

Fig. 2.7 *Comparison of the dose-finding studies with and without electrodes in the laser-active area. In the therapeutic window no significant difference could be observed* (p = 0.735 and p = 0.259). *In the case of lower of higher applied energy, the difference was significant.*

Endocardial *in vivo* experiment with integrated electrodes

The recorded local EGM data and the created anatomical maps are visualized in **Fig. 2.8**. The images A and C depict the local EGM data during the ablation procedure, showing a clear reduction in the recorded potential after 40s power application between all electrode pairs, indicating electrical isolation at the endocardial tissue surface. This presents a confirmation of the lesion formation process over the entire length of the catheter. During the procedure, no adverse events related to the power application were recorded.

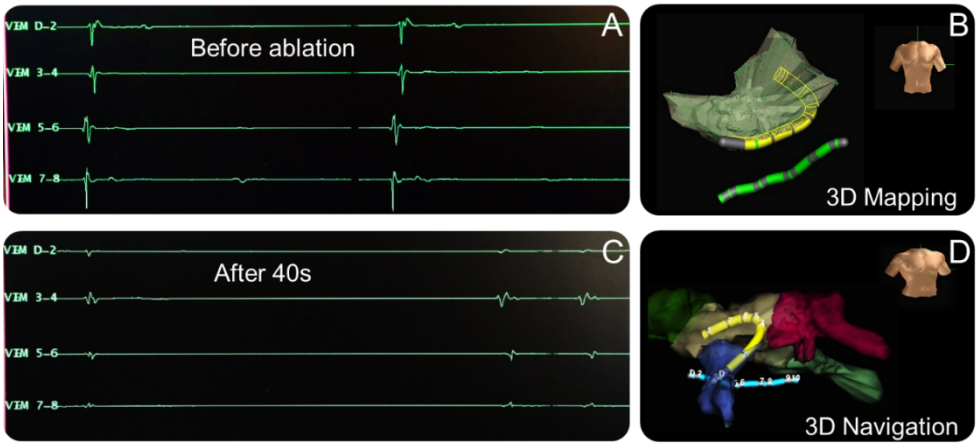

Fig. 2.8 *Recorded local EGM data and the created anatomical maps. A and C: local EGM data during the ablation procedure, with a clear reduction of the recorded potential after 40s of power application. B and D: mapping and 3D navigation with the lasso catheter.*

Moreover, no signs of clotting or bubbles were observed during ICE observations (AcuNav 10F Ultrasound catheter of Siemens Healthineers AG, Erlangen, Germany). The ICE catheter was placed in the upper part of the RA. No signs of charring were observed on the catheter's surface, during and after retraction from the sheath. Correspondingly, no signs of clotting or endocardial tissue damage were observed during the macroscopic analysis of the ablation site. The mapping and navigation in NavX™ Ensite™ could be performed without any issues, and the catheters' behavior was resembling the current state-of-the-art catheters.

Lateral emission profile 20mm linear ablation catheter

Fig. 2.9 shows in A the lateral emission of the compacted distribution scheme of the 45mm catheter and in B the adjusted algorithm for homogeneous emission for the 20mm linear catheter. By compacting the lesion scheme the energy density could be increased from 0,22 W/mm^2 for the 45mm laser lasso catheter to

0,49 W/mm² for the 20mm catheter. In this case the increase is desired to achieve deeper lesions for epicardial ventricle ablations.

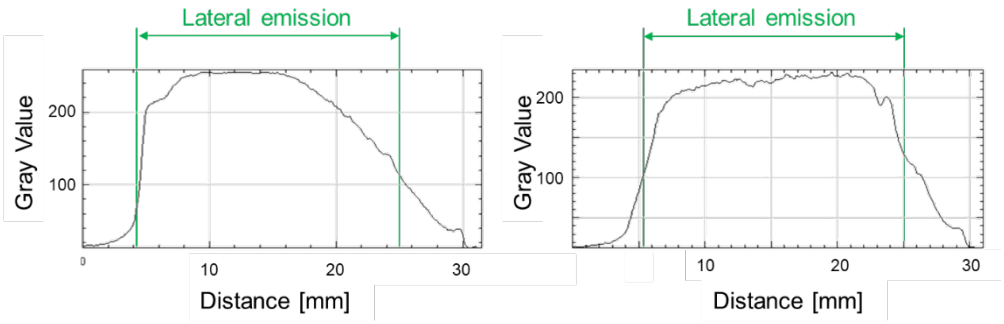

Fig. 2.9 *Algorithm development for optimal lateral emission. Left image: the lateral emission is displayed as recorded by an infrared camera over the entire length of the laser-active area. It can be seen that the emission (recorded Gray value) is not homogeneous over the entire length of 20mm. Right image: the lateral emission of the final algorithm is displayed, showing a plateau with constant emission.*

Dose-finding 20mm linear laser ablation catheter

In total, 138 energy applications were performed with five different catheters to assess the average power and time-dependent lesion depth. The measured lesion depths varied between 3mm and 9mm and are displayed as box plot in **Fig. 2.10**. The plot shows a quasi-linear increase of lesion depth by increasing either power or time, which is comparable to the linearity noticed in the 45mm laser-lasso catheter. Overall, the lesion length showed to be constant at 25.7±1.27mm.

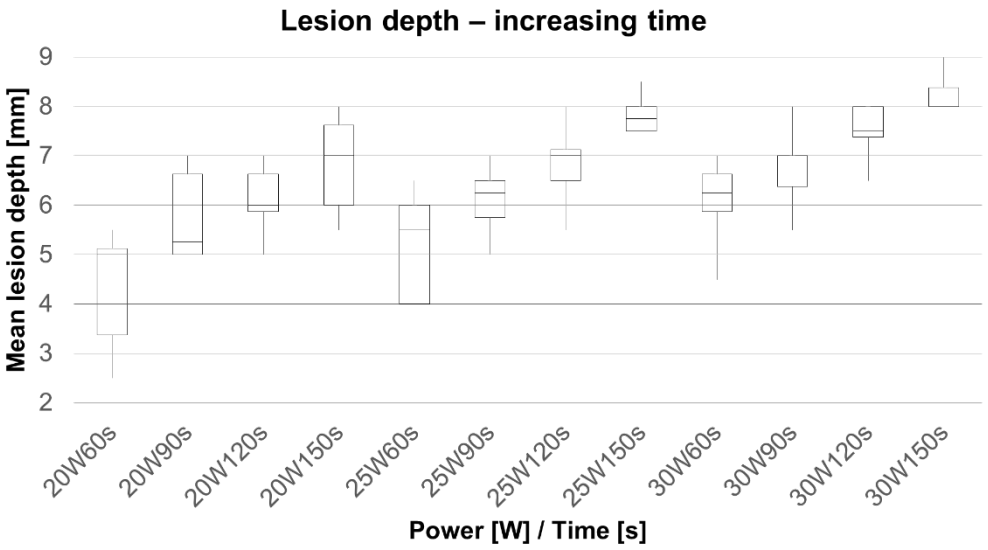

Fig. 2.10 *Measured lesion depth of power and application time. In this graphical presentation, the effect of increasing power is portrayed by clustering according to application time.*

An average relative deviation (Δ_{rel}) between the proximal ($t_{prox.}$) and distal ($t_{dist.}$) lesion depth against the average depth($t_{average}$) of 6.16% was calculated from the 138 energy applications of the dose-finding study. This deviation of 6.16% was homogeneous, considering this difference in lesion depth would be negligible in clinical settings.

Comparison of data

Fig. 2.11 shows the lesion depth of both studies, plotted against the energy per mm. The data 20mm linear laser catheter data points seem to be an extension to the values of the endocardial lasso catheter.

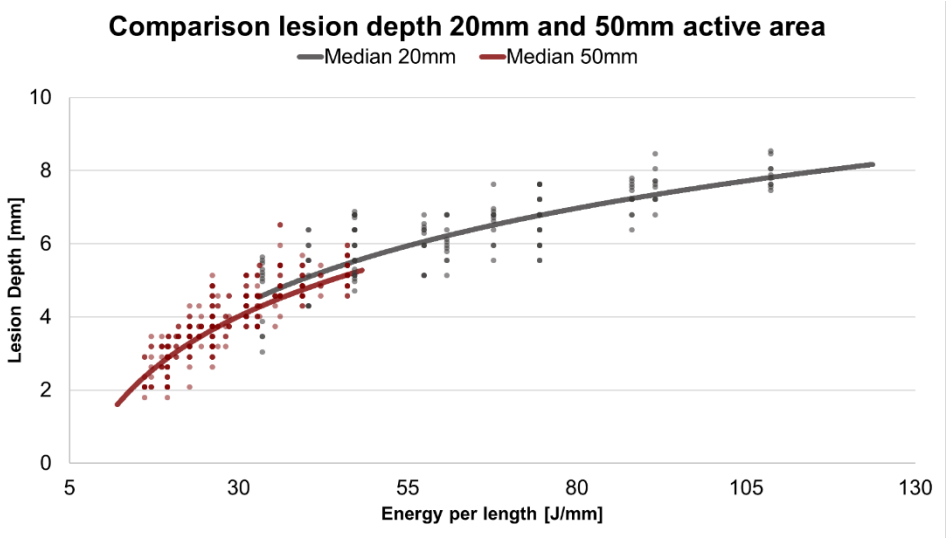

Fig. 2.11 *Recorded lesion depth of the applied energy per mm (individual observations and median line) for the 45mm lasso catheter and the 20mm linear catheter. The graph depicts the increased energy density of the 20mm linear laser catheter and increased lesion depth.*

Discussion

In this chapter we described the principles behind laser ablation and presented a short overview of past and current laser ablation devices. In the past, laser energy was already explored as feasible energy source for the treatment of cardiac arrhythmias. Based on this knowledge and an already existing linear laser ablation catheter, a 20mm linear laser ablation catheter was developed.

As baseline for the 20mm linear laser ablation catheter a dose-finding study was conducted with the existing 45mm laser lasso catheter showing a linear relationship between applied energy and lesion depth. Subsequently electrodes were placed on the 45mm lasso catheter allowing *in vivo* recording of local EGM data and anatomical mapping with the NavX Ensite system. Compatibility with mapping systems is inadmissible in current ablation procedures and integral part of cardiac arrhythmia treatment. The possibility to record the cardiac signals

during power application is real benefit and provides another measure of ablation success.

By modification of the 45mm emission profile a linear laser catheter with a length of 20mm was developed. The dose-finding study showed a linear relationship between applied energy and lesion depth reaching depths between 3 and 10mm. Due to an increase of emitted energy density in comparison to the existing lasso catheter, deeper lesion could be produced. The catheter design in combination with the achieved lesions depths allow both endo- and epicardial ablations of the atria and ventricles. Though this catheter shows good initial results, further investigation is required to assess catheter handling, navigation, and *in vivo* performance. To evaluate these properties and to validate the *ex vivo* investigations an *in vivo* study is required targeting endocardial and epicardial substrates in-line with current ablation strategies.

The ability to directly irradiate the tissue over a length of 20mm in a homogeneous fashion via a modified optical fiber makes this catheter also unique from a technological point of view. Currently no other device exists allowing high power lateral emission from an optical fiber over a certain length whilst maintaining the original flexibility of the fiber.

References

[1] Cheong WF, Prahl S, and Welch AJ; A Review of the Optical Properties of Biological Tissues. IEEE Journal Of Quantum Electronics, Vol. 26. No. 12, December 1990

[2] Steiner R. In book: Laser and IPL Technology in Dermatology and Aesthetic Medicine (pp.23-36). October 2011, DOI: 10.1007/978-3-642-03438-1_2

[3] Raulin C and Karsai S. Laser and IPL Technology in Dermatology and Aesthetic Medicine. Springer 2011. ISBN 978-3-642-03438-1

[4] Reddy VY, Neuzil P, Themistoclakis S, Danik SB, Bonso A et. al. Visually-guided balloon catheter ablation of atrial fibrillation: experimental feasibility and first-in-human multicenter clinical outcome. Circulation. 2009 Jul 7;120(1):12-20. doi: 10.1161/CIRCULATIONAHA.108.840587.

[5] Jürgen Eichler and Theo Seiler. Lasertechnik in der Medizin. Springer 1991. ISBN: 978-3-662-08272-0

[6] Maiman TH. Optical and microwave-optical experiments in ruby. Phys. Rev Lett. 1960;4:564-6

[7] Maiman TH. Biomedical lasers evolve toward clinical applications. Hosp Manage. 1966;101(4):39-41

[8] Lee BI, Gottdiener JS, Fletcher RD, Rodriguez ER, and Ferrans VJ. Transcatheter ablation: comparison between laser photoablation and electrode shock ablation in the dog. Circulation 1985;71:579-586

[9] Saksena S, Gielchinsky I, Tullo NG. Argon laser ablation of malignant ventricular tachycardia associated with coronary artery disease. Am J Cardiol. 1989 Dec 1;64(19):1298-304.

[10] Pfeiffer D, Moosdorf R, Svenson RH, Littmann L, Grimm W, Kirchhoff PG, Lüderitz B. Epicardial neodymium. YAG laser photocoagulation of ventricular

tachycardia without ventriculotomy in patients after myocardial infarction. Circulation. 1996 Dec 15;94(12):3221-5.

[11] Fried NM, Lardo AC, Berger RD, Calkins H, Halperin HR. Linear lesions in myocardium created by Nd:YAG laser using diffusing optical fibers: Ex vivo and in vivo results. Lasers in Surgery and Medicine 2000;27(4):295-304

[12] Ware DL, Boor P, Yang C, Gowda A, Grady JJ, and Motamedi M. Slow Intramural Heating With Diffused Laser Light. A Unique Method for Deep Myocardial Coagulation. Circulation. 1999;99:1630–1636

[13] Williams MR, Casher JM, Russo MJ, Hong KN, Argenziano M and Oz MC. Laser Energy Source in Surgical Atrial Fibrillation Ablation: Preclinical Experience. Ann Thorac Surg 2006;82:2260-2264.

[14] Doll N, Suwalski P, Aupperle H, Walther T, Borger MA, Schoon HA, Mohr FW. Endocardial laser ablation for the treatment of atrial fibrillation in an acute sheep model. J Card Surg. 2008 May-Jun;23(3):198-203.

[15] Chun JKR, Bordignon S, Last J, Mayer L, Tohoku S et. al. Cryoballoon Versus Laserballoon. Insights From the First Prospective Randomized Balloon Trial in Catheter Ablation of Atrial Fibrillation. Circulation: Arrhythmia and Electrophysiology 2021;14(2).

[16] Wehner M, Niessen M, Poprawe, R. Flexibler Laserapplikator. Patent: DE102006039471B3; 2008

[17] Miyamoto K, Noda T, Aiba T, Kusano K. Parasternal intercostal approach as an alternative to subxiphoid approach for epicardial catheter ablation: A case report. HeartRhythm Case Rep. 2015 Apr 23;1(3):150-155. doi: 10.1016/j.hrcr.2014.12.014.

[18] d'Avila A, Koruth JS, Dukkipati S, Reddy VY. Epicardial access for the treatment of cardiac arrhythmias. Europace. 2012 Aug;14 Suppl 2:ii13-ii18. doi: 10.1093/europace/eus214.

[19] Boyle NG, Shivkumar K. Epicardial interventions in electrophysiology. Circulation. 2012 Oct 2;126(14):1752-69. doi: 10.1161/CIRCULATIONAHA.111.060327.

[20] Bhakta D, Miller JM. Principles of electroanatomic mapping. Indian Pacing Electrophysiol J. 2008 Feb 1;8(1):32-50.

[21] Estner HL, Hessling G, Luik A, Reents T, Konietzko A et. al. Einsatz des Navigationssystems NavX bei der Ablationsbehandlung von Vorhofflimmern [Use of the NavX navigation system in ablation of atrial fibrillation]. Herzschrittmacherther Elektrophysiol. 2007;18(3):131-9. German. doi: 10.1007/s00399-007-0573-x.

3 A novel laser energy ablation catheter for endocardial cavo-tricuspid isthmus ablation and epicardial ventricular lesion formation: An in vivo proof-of-concept study.

Dennis Krist, Ulrich Schotten, Stef Zeemering, Dominik Linz, Dwayne Leenen

Krist D, Linz D, Schotten U, Zeemering S and Leenen D (2022) - A Novel Laser Energy Ablation Catheter for Endocardial Cavo-Tricuspid Isthmus Ablation and Epicardial Ventricular Lesion Formation: An in vivo Proof-of-Concept Study. *Front. Med. Technol.* 4:834856. doi: *10.3389/fmedt.2022.834856*

Abstract

Aim: This proof-of-concept study aimed to investigate atrial and ventricular lesion formation by a 20mm linear laser ablation catheter, regarding lesion depth and tissue damage.

Methods: Six female swines underwent standard femoral vein access to introduce a novel 20mm linear laser ablation catheter in the right atrium to perform endocardial cavo-tricuspid isthmus (CTI) ablations. The navigation took place under fluoroscopy with additional visualization by intracardiac echocardiograph. Epicardial ablations were performed on the surface of the left ventricle (LV), right ventricle (RV) and right atrial appendage (RAA) via a sternotomy. Procedural safety was assessed by registration of intraprocedural adverse events and by macroscopic examination of the excised hearts, for presence of charring or tissue disruption at the lesion site.

Results: Altogether 39 lesions were created, including eight endocardial CTI (mean lesion length 20.6±1.65mm), 26 epicardial ventricle (mean lesion length LV: 25.3±1.35mm, RV: 24.9±2.40mm) and five epicardial appendage ablations (mean lesion length RAA: 26.0±3.16mm). Transmurality was achieved in all CTI and atrial appendage ablations, in 62% of the RV ablations and in none of the LV ablations. No perforation or steam pop occurred, and no animal died during the procedure.

Conclusion: In this porcine study, the 20mm linear laser ablation catheter has shown excellent results for endocardial cavo-tricuspid isthmus ablation and resulted in acceptable lesion depth during atrial and ventricular epicardial

ablation. The absence of tissue charring, steam pops, or microbubbles under the experimental conditions, suggests a high degree of procedural safety.

Introduction

Typical right atrial flutter is a common abnormal heart rhythm and often occurs in patients with atrial fibrillation. For the minimal invasive treatment of atrial flutter, a linear conduction block is created at the cavo-tricuspid isthmus (CTI). Ablation of the isthmus prevents conduction at the narrowest point of the circuit and therewith, usually terminates atrial flutter, as the block is being completed. The use of a linear ablation catheter could improve procedure times and minimize conduction gaps.

In the area of epicardial procedures, linear ablations could also be beneficial in the treatment of ventricular tachycardias (VT) or persistent atrial fibrillation. [1] Currently no uniform agreement exists on the optimal VT ablation strategy. However, high-density delineation of the scar is commonly the first step.[2] Various ablation strategies can be applied to reduce the scar-related recurrent VT. Scar homogenization is an important trend to eliminate all abnormal electrograms by extensive and diffuse ablation at the scar. [3,4] More extensive and linear ablations of large scar-related ventricular tachycardia are associated with better success rate and lower recurrence rate.[5]

Biophysical limitations of RF ablation are constituted by the thick ventricular walls with transmural circuits. Apart from the wall thickness, trabeculations and fat, act as barriers to effective power delivery into the scar. Laser could provide an improved technique to create deep and linear lesions. Besides, the unidirectional emission of laser light does not damage any surrounding tissue, such as the phrenic nerve, the lungs, and the parietal pericardium. Therefore, deep linear

lesions would allow epicardial substrate modification in the setting of a post-infarct scar re-entry VT but could also provide an additional method for epicardial left atrial ablations in the treatment of longstanding persistent atrial fibrillation.[6,7]

This proof-of-concept study was designed to investigate the performance of a novel deflectable 20mm linear laser ablation catheter, to create transmural endocardial CTI lesions and epicardial atrial and ventricular lesions with focus on lesion depth, tissue damage and general procedural safety in a porcine experimental model. Additionally, this data was used to validate the ex vivo models of the preclinical dose-finding studies.

Material and Methods

Animal Preparation

The experiments were performed at the Cardiac Physiology Experimental Lab of the Charles University and Na Homolce Hospital (Albertov 5, 128 00 Prague, Czech Republic).

The experimental protocol was compliant with the local guidelines for animal experiments. The study used female swines with a weight between 40 and 60kg and approximately four to six months of age for the experiments. Animals were inspected by a veterinarian for health status and exclusion criteria, fasted 12 hours prior to the procedure with unlimited access to water. An acute non-survival protocol was applied with euthanization prior to recovering from anesthesia.

Pre-anesthesia was initiated by an intramuscular injection of ketamine and midazolam. After the effect, venous access was secured. In the operating room, the

animal was placed in a supine position on the X-Ray table and the ECG was attached. Total intravenous anesthesia (propofol, midazolam, morphine) was induced and continued throughout the procedure to maintain surgical level of anesthesia.

Orotracheal intubation was performed and mechanical ventilation was initiated. Heparin maintained anticoagulation to reach target ACT of 350s, checked hourly. Antibiotic bolus was applied when the expected experiment duration exceeded four hours. Body temperature was controlled by heating or cooling the mattress to maintain 38°C. Standard femoral vein access was used to introduce a steerable sheath in the RA and to insert an ICE catheter (AcuNav 10F Ultrasound catheter of Siemens Healthineers AG, Erlangen, Germany) in the upper part of the RA. Via the jugular vein a CS catheter was positioned.

After the endocardial atrial ablations, a sternotomy was created, and the pericardial sac was opened to gain access to the epicardial surface of the LV, RV, and RAA. After euthanization the hearts were excised for macroscopy.

Laser Ablation Catheter

Vimecon GmbH designed the experimental 20mm linear laser catheter (Herzogenrath, Germany) (Patents: US 2018/0021089, US 2011/0230941, US 2011/0230871). It has a bidirectional steerable 8.2F shaft with a deflection angle of approx. 180° in both directions. The 20mm laser active area is shaped slightly convex, to optimize wall contact.
A saline irrigated tip was used to dissipate remaining energy in the optical fiber. Typical energy densities during the experiments were between 75 J/mm (for CTI ablation) and 150 J/mm (for LV ablation), as defined per a priori *ex vivo* dose-finding study.

Fig. 3.1 *Visualization of the laser active area by use of a low energy green laser diode, depicting the linear lateral emission of the catheter.*

Using a low-energy green laser diode, the laser active area was visualized as depicted in **Fig. 3.1**, demonstrating the lateral emission of the catheter. This design emitted laser light with a divergence of approx. 85°, with its highest intensity over the longitudinal axis of the catheter. Due to the large divergence, wall contact is indispensable to achieve well-formed lesions. During a successful ablation, the tissue absorbs the laser light, leading to thermally induced coagulation of the targeted substrate.

A priori *Ex vivo* Dose-finding Study

An *ex vivo* dose-finding study defined the power and time settings for transmural. Avian tissue and freshly excised porcine hearts with a thickness > 10mm were used as substitute tissue model to estimate the energy dependent lesion depth. The tissues samples were heated and kept at a temperature of 37°C ± 2°C in a saline-solution bath.

The lesion depth could be assessed macroscopically by a section at the target site due to the strong and clear border demarcation of the coagulated area. The

power settings were varied between 20W and 30W; the time was set between 60s and 150s.

A total of 138 energy applications were performed on avian tissue and 38 applications on porcine cardiac tissue. This animal study investigation validated the suitability of *ex vivo* investigations for the prediction of *in vivo* lesion formation.

Statistical Analysis

For comparison of data, the following tests were used with a significance cut-off set at 5%: the Pearson's correlation coefficient was determined to investigate the relationship between applied energy and lesion depth and the Kruskal-Wallis test was used to assess the *ex vivo* and *in vivo* tissue models. For the statistical analysis, invalid *in vivo* measurements were omitted if strong ventricular contractions caused substantial movement of the catheter during the ablation procedure.

Procedure Details

Six female animals were prepared for the experimental ablations with the linear laser catheter. First, the endocardial ablations were performed by transfemoral access to the RA. The use of a 82cm, 8.5F steerable sheath (Agilis Nxt, Dual-Reach, St. Jude Medical, Saint Paul, United States of America) enabled free movement in the RA and the steerability of the catheter allowed good positioning of the catheter. The navigation took place under fluoroscopy and with added visualization by usage of ICE.

Fig. 3.2 displays the recorded ICE and fluoroscopy images during navigation. To perform CTI ablation the catheter was inserted partially into the RV over the tricuspid valve (TCV) as displayed in image A and E. Followed by stepwise

retraction towards the inferior vena cava (IVC) to create a linear lesion, extending from inside the TCV to the IVC as depicted in images B-D and F-H.

The slight convex shape of the laser-active area allowed good wall-contact over the entire length, adjustable via the bidirectional steering mechanism. The power and time settings were defined at 25W/60s, as per dose-finding. During the power application the catheter was kept at the same location as much as possible to assure transmurality.

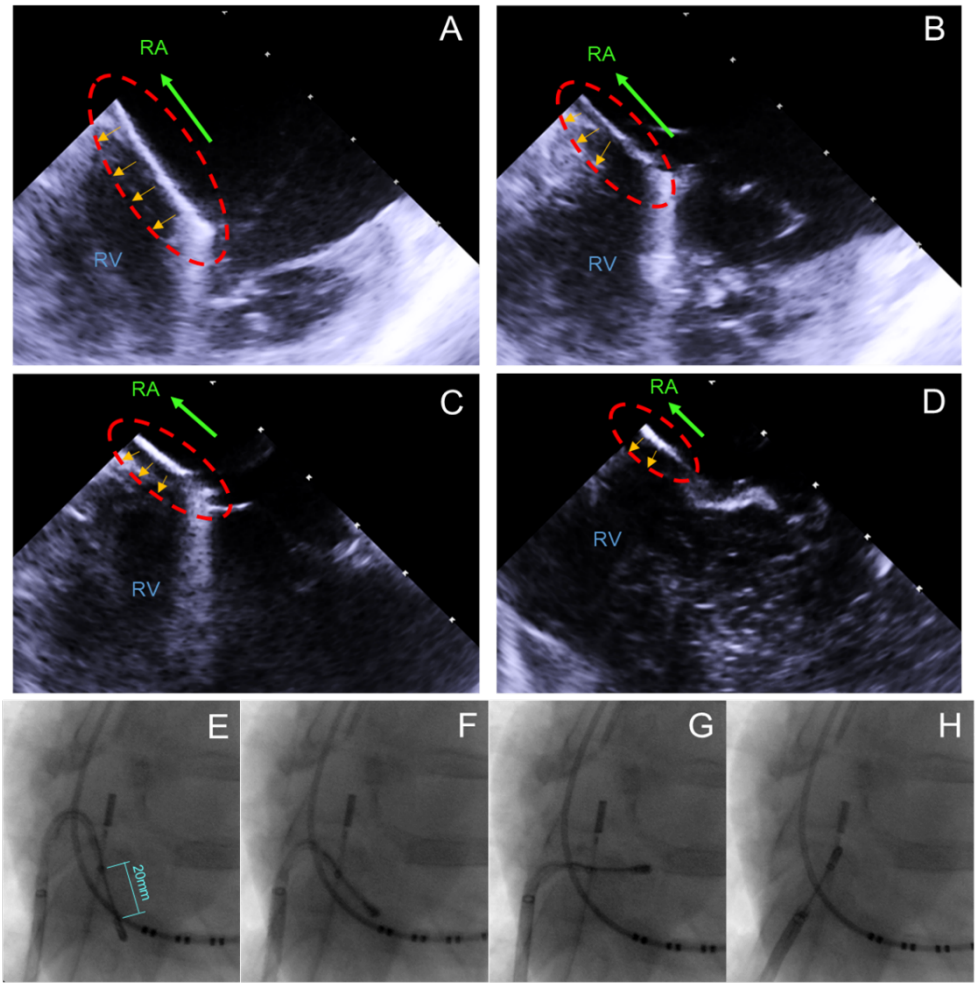

Fig. 3.2 *ICE/X-ray recordings captured during the CTI ablation, visualizing the stepwise retraction from the RV/TCV towards the IVC. A: Initial position with the catheter partially in the RV and on the TCV. B-D: Stepwise retraction into the IVC. E: Initial position with the catheter partially in the RV and on the TCV. F-H: Stepwise retraction into the RA.*

The epicardial ablations of the RAA, RV and LV were conducted under direct visualization via a full sternotomy, allowing free access to the atria and ventricles. The lesions were created with an adequate distance between the applications, to

prevent lesion overlapping to assess the length and depth per individual power application.

Procedural Safety

The procedural safety was assessed by awareness and recording of steam pops, acute procedural complications with respect to the vascular access site, severe arrhythmias and pericardial effusion or tamponade. During the power application, the target site was inspected for signs of micro bubbles and clotting by use of ICE. Post procedural inspection of the catheter, lesion site, and surrounding tissues was conducted to confirm the absence of charring and damage to surrounding tissue structures.

Results

Endocardial CTI Ablation

In three of the six animals, CTI ablations were attempted with the 20mm linear ablation catheter. ICE proved to be a useful tool to assess the exact location of the catheter and to verify wall contact. All ablations (n=8) were transmural, with a mean lesion length of 20.6±1.65mm. A full CTI lesion from the TCV up to the IVC was obtained in two of three animals. In the third animal the lesions did not connect between the IVC and TCV due to gaps in the ablation line. The CTI ablation was well tolerated, no sustained arrhythmias were induced during energy application.

Fig. 3.3 shows the macroscopic analysis of the CTI ablations in the excised hearts. In none of the performed ablations, charring of the tissue surface, steam-pops, or tissue disruptions were observed at the lesion site. Intraprocedural

visualization of the ablation site with ICE also showed no signs of microbubbles during the power application. The researcher found no signs of charring or coagulation on the catheter. Macroscopic analysis of the surrounding tissue structures showed no signs of laser ablation related tissue damage. Autopsy of the lungs also showed no signs of emboli.

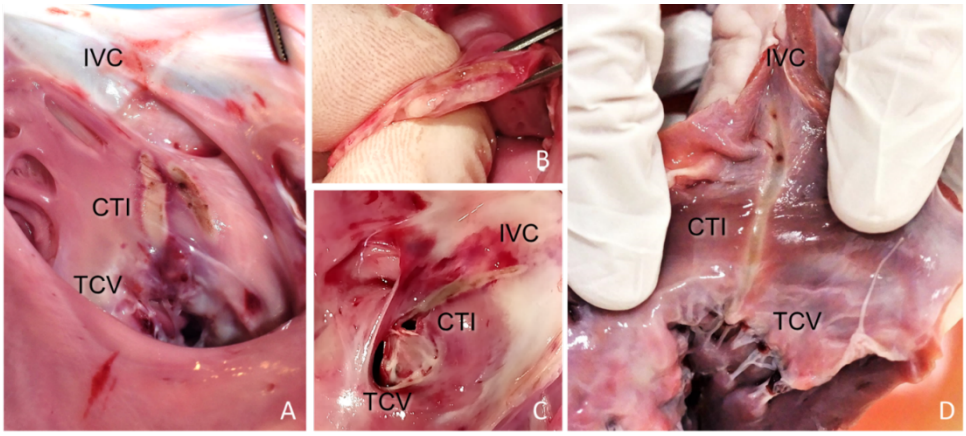

Fig. 3.3 *Endocardial view of the RA specimens displaying the pale linear lesion. A: Incomplete CTI ablation, showing the created lesions of four power applications at 25W for 60s. One application was set parallel to the rest. B-C: Full CTI ablation including axial section, confirming transmurality and linearity. The lesion extended from the CV towards the IVC. D: Full CTI ablation, requiring only two energy applications of 25W/60s to complete the lesion.*

Epicardial Ablations

In all six animals epicardial ablations were performed on the ventricles and on the right atrial appendage. This resulted into 13 left ventricle, 13 right ventricle, and five appendage ablations, with a mean lesion length of 25.3±1.35mm (LV), 24.9±2.40mm (RV), and 26.0±3.16mm (RAA).

Power and time settings were varied between 15 to 30W and 60 to 180s. Comparable to the *ex vivo* dose-finding, the time settings had more impact on the achieved lesion depth than power. The largest lesion depth, estimated at 9mm, was achieved after 120s regardless of 25 or 30W of energy applied. The findings correlate with the gathered *ex vivo* data, also showing a maximum lesion depth of approximately 9mm. In most RV ablations, transmurality was easily observed by clearly visible discoloration of the endocardial tissue surface, as depicted in **Fig. 3.4**.

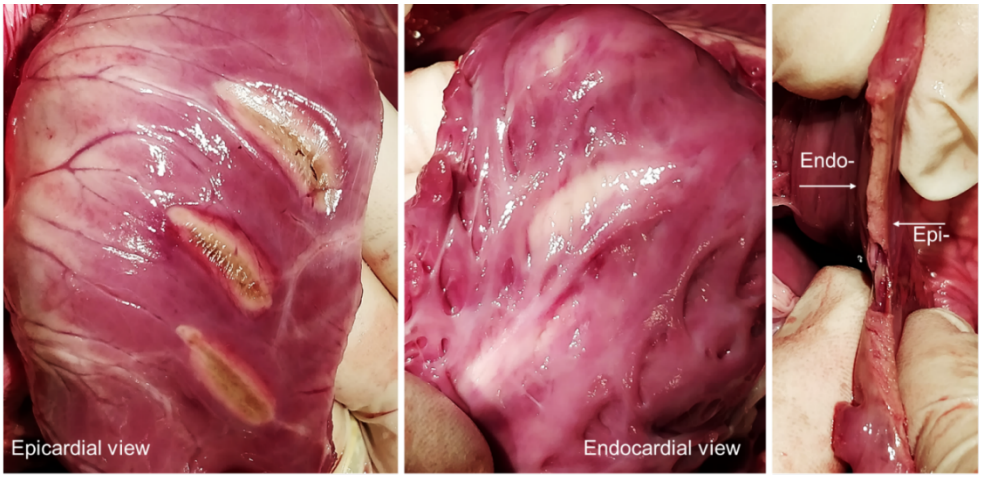

Fig. 3.4 *(Left and Middle Panel) Epi-and endocardial view of three epicardial RV ablations. (Right Panel) Axial section of a lesion, displaying the transmurality and linearity.*

The presence of endocardial trabeculations mostly prevented full lesion transmurality due to the increased tissue thickness and additional convective cooling. In general, transmurality was not achieved if the wall thickness surpassed 10mm. Subsequently transmurality could not be obtained in left ventricular ablations. All lesions showed equal homogeneity and linearity over the length of the laser active area. The macroscopic analysis of the LV ablations (Panel B) and the intraprocedural catheter positioning (Panel A) are depicted in **Fig. 3.5**.

Under the experimental conditions, none of the performed ablations showed evidence of charring on the tissue surface, steam-pops, or tissue disruptions at the lesion site, suggesting a high degree of procedural safety. Non-sustained VTs and ventricular premature contractions were often induced from the second ventricle ablation or onwards.

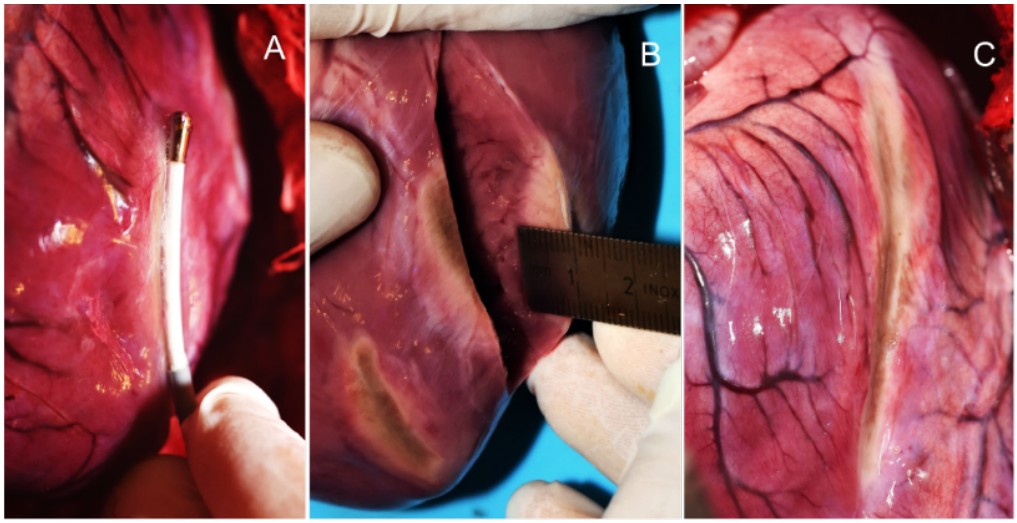

Fig. 3.5 *A: Epicardial ablation of the LV with the laser ablation catheter. B: Axial section of the excised heart and macroscopic estimation of the lesion depth. C: 4 connected ablations with approx. length of 80mm.*

In vivo validation of the a priori *ex vivo* dose-finding studies

In **Fig. 3.6** (Left Panel) all 39 lesions from this animal investigation were plotted against the estimated wall thickness of the targeted substrate. A transmural line was added, to visualize the transmurality per lesion. For epicardial LV ablations the association between wall thickness, applied power, and application time was displayed individually.

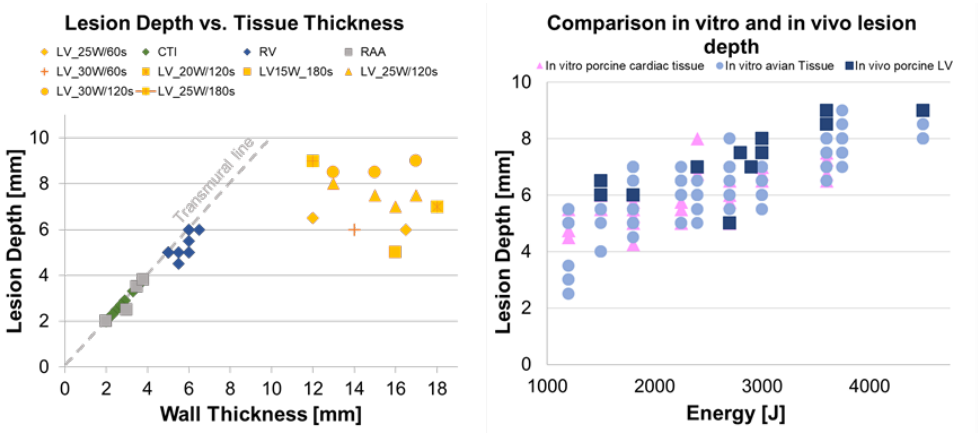

Fig. 3.6 *(Left Panel) Overview of the performed CTI and epicardial ventricle ablations, with a differentiation between transmural and non-transmural ablations. (Right Panel) Three scatter plots, representing the ex vivo avian tissue model, the ex vivo porcine cardiac tissue model, and the results from the in vivo study.*

In the right panel a scatter plot was created representing the generated data from this *in vivo* investigation and the antecedental conducted *ex vivo* dose-finding studies concerning energy dependent lesion depth. A Pearson's product-moment correlation was applied to assess the relationship between applied energy and lesion depth for all groups. A strong positive correlation between the applied energy and the lesion depth was shown, with a Pearson correlation factor of $r=0.706$, $p<0.001$ for the *ex vivo* porcine tissue, $r=0.798$, $p<0.001$ for the *ex vivo* avian tissue, and $r=0.659$, $p=0.027$ for the *in vivo* left ventricles.

Tab. 3.1 lists the results for the Kruskal-Wallis test, comparing the *ex vivo* and *in vivo* models concerning energy dependent lesion depth. No significant difference in energy-dependent lesion depth was indicated between the *in vivo* and *ex vivo* studies.

Tab. 3.1 *Statistical analysis. A Kruskal-Wallis Test was conducted to compare the energy-dependent lesion depth of this in vivo animal study and antecedental conducted ex vivo dose-finding studies on porcine and avian tissue. No significant difference was shown with p>0.05.*

Kruskal-Wallis test					
Tissue sample	**N**	**Median**	**Median Rank**	**H- Value**	**P-Value**
In vitro porcine	6	6.306	8.2		
In vivo LV	6	6.750	11.7	H = 1.51	P = 0.470
In vitro avian	6	6.438	8.7		

Discussion

In this proof-of-concept study, we investigated the capability to create transmural lesions during CTI ablation and epicardial atrial and ventricular power applications with a deflectable 20mm linear laser ablation catheter. To this aim, an *in vivo* animal study was conducted, which also considered the procedural safety. The laser catheter showed to be effective in creating well demarcated transmural endocardial CTI lesions, without negatively affecting the procedural safety. Although all atrial lesions were transmural, this translates not directly into procedural success, since the main objective of atrial flutter ablation remains conduction block at the isthmus. In a setting without 3D electroanatomical activation and voltage mapping systems, this confirmation of lesion contiguity proved to be difficult. In future studies, the use of these systems is inevitable to proof the effectiveness of this laser catheter. At the same time, the direction of the lateral laser emission could be visualized. Since the laser ablation catheter already possesses an optical fiber, spectroscopy could be used to directly visualize the tissue and lesion formation. This principle was already proven feasible in several studies combining radiofrequency ablation and optical spectroscopy[8-10]. Allowing detection of wall contact, prior lesions and tissue defects.

Navigation was no issue during the epicardial ablations, performed under direct visualization of the catheter and the target site, as result of the midline sternotomy. The epicardial atrial and ventricle ablations created linear lesions, without evidence of charring, steam-pops, or tissue disruptions. In the right ventricle, transmurality was obtained in more than halve of the ablations. In the left ventricle this could not be achieved due to the high wall thickness of up to 18mm.

In comparison to previous epicardial RF ablation studies [11,12], the laser ablation resulted into deeper and more homogeneous lesions. Ex vivo studies already showed that increasing the power above 30W did not create deeper lesions. To reach lesion depths beyond 9mm, a different or additional wavelength could be used. Past investigations have shown that 800nm has at least 50% more penetration depth in comparison to 980nm, providing an alternative to achieve transmural lesions in the left ventricle.[13-15] Increased penetration depths have also been achieved by the use of pulsed wave laser light, leading to reduced energy absorption in the superficial layers of the myocardium.[15] A different wavelength and pulsed laser applications are easily implementable in the current catheter design, since the same fiber optic components can be used.

An interesting observation was made, comparing the lesion length of endo- and epicardial ablations. Showing a reduced length of approximately 5mm for the endocardial ablations. This can be explained by the convex shape of the applicator and the convective cooling of the outer edges of the target site. The circulating blood in the right atrium cools the tissue around the catheter. Therewith, only directly irradiated areas are heated. The scattered energy beyond the area of direct irradiation is dissipated. Without the effects of convective cooling, the lesion length increases as observed in the epicardial ablations.

The macroscopic analysis of the excised hearts showed no edema formation after endo- and epicardial laser ablation. This could benefit the long-term freedom of AFL and procedural efficacy. Reversible acute conduction block induced by edema formation, which is indistinguishable from complete tissue necrosis, can be prevented.[16,17] This way conduction gaps formed with passing of time are obviated. In future studies this potential lack of edema induced false conduction block needs to be investigated and observed more thoroughly.

Overall, the deflectable 20mm linear laser catheter showed good performance regarding lesion depth and procedural safety in endo- and epicardial ablations. The achieved maximum ventricular lesion depths are slightly deeper than the conventional RF- and Cryo devices[11, 12], but also compared to upcoming technologies like pulsed field ablation[18]. As for all thermal ablation devices, achieving tissue contact is critical for lesion formation when delivering energy. The linearity of the lesion, could be beneficial towards RF power applications, reducing the needed amount of power applications and therewith reducing procedure times. In epicardial ablations, the unilateral laser emission holds a benefit in comparison to RF- and Cryo applications, since only the targeted tissue will be treated, protecting the surrounding tissue.

Besides the ablation of the cavotricuspid isthmus, in patients with typical right atrial flutter, also the mitral isthmus (MI) could be targeted, as commonly applied in patients with atypical left atrial flutter.[19] This also applies for the various application possibilities in epicardial ablation procedures, besides the aforementioned scar-related therapies.

In closing, the achieved lesion depths of the LV ablations were used to validate the applied *ex vivo* tissue models regarding lesion depth, as used in preclinical dose-finding studies. No significant difference in lesion depth was observed between *in vivo* and *ex vivo* lesion. Therefore, the used *ex vivo* models are a valid substitute to predict the lesion depth and therewith to define the therapeutic ablation settings, to achieve transmurality in case of laser applications. The benefits of laser-based catheter ablation extend beyond the lesion formation process. Laser additionally allows online monitoring of the laser effects on the myocardium.

This immediate and real-time verification of ablation success would be extremely beneficial to increase procedural success.

Limitations

The ablations with the 20mm linear catheter were always conducted as part of an animal trial study of the endocardial laser lasso catheter. Therefore, no ablations were performed in (endocardial) and on (epicardial) the LA, to prevent any contamination of the created lesion with the lasso catheter. Accordingly, only the RV, RA, RAA and LV were targeted during the combined endo- and epicardial ablations.

One aspect that could not be accounted for in this animal study, is the usually challenging isthmus anatomy in humans.[20] Common anatomical peculiarities like prominent Eustachian ridge, pouchlike recesses and pectinate muscles are not observed in young swines, where the surface is usually smooth and without trabeculations. The effects of these tissue structures on the lesion transmurality could therefore not be assessed. A more flexible catheter design could better suitable for difficult anatomies or by adding tip emission, enabling point-by-point ablation in pouches.

As swines do not tolerate ventricle ablations very well, only a few ventricle ablations could be performed *in vivo*, i.e. with perfused tissue. Though, the gathered data regarding epicardial lesion formation in the ventricles, provides a good basis for further investigations. The endo- and epicardial atrial ablations on the other hand were well-tolerated. It needs to be mentioned, that due to the small sample size of the *in vivo* ablations, more research is required to further substantiate the results of the study.

Moreover, the epicardial ablations were performed in an ideal setting, i.e. with opened thorax. Thus, good contact force was always achieved under visual navigation. Ablations were solely performed to the healthy ventricular tissue and therewith the effect on ventricular scar tissue could not be assessed. Though, the effect can be estimated by studies conducted in the past on scar tissue. In future studies these aspects could be investigated more specifically.

Conclusion

The 20mm linear laser ablation catheter has shown excellent results for endocardial cavotricuspid isthmus ablation and resulted in acceptable lesion depth during atrial and ventricular epicardial ablation. There was no evidence of tissue charring, steam pops, or microbubbles under the experimental conditions, suggesting a high degree of procedural safety. Laser as energy sources for catheter-based epicardial ablation is promising but requires technical optimization of catheter design. Further studies are needed to assess long-term efficacy and safety.

References

[1] Matsuo S, Wright M, Knecht S, I. Nault I, Lellouche N, K. Lim K, et. al. Peri-mitral atrial flutter in patients with atrial fibrillation ablation. Hearth Rhythm Society. 2010;7:2-8.

[2] Tung R. Evolution of ventricular tachycardia ablation in structural heart disease. Journal of Arrhythmia. 2014;30:250-261.

[3] di Biase L, Santangeli P, Burkhardt DJ, Bai R, Mohanty P, Carbucicchio P, et. al. Endo-Epicardial Homogenization of the Scar Versus Limited Substrate Ablation for the Treatment of Electrical Storms in Patients With Ischemic Cardiomyopathy. Journal of the American College of Cardiology. 2012;60:132-141.

[4] Vergara P, Trevisi N, Ricco A, Petracca F, Baratto F, Cireddu M, et. al. Late potentials ablation as an additional technique for reduction of arrhythmia recurrence in scar related ventricular tachycardia ablation. Journal of Cardiovascular Electrophysiology. 2012;6:621-627.

[5] Ghanem M, Ahmed R, Moteleb A and Zarif J. Predictors of Success in Ablation of Scar-Related Ventricular Tachycardia. Clinical Medicine Insights: Cardiology. 2013;7:87-95.

[6] Compier MG, Braun J, Tjon A, Zeppenfeld K, Klautz R, M. Schalij M, et. al.. Outcome of stand-alone thoracoscopic epicardial left atrial posterior box isolation with bipolar radiofrequency energy for longstanding persistent atrial fibrillation. Netherlands Heart Journal. 2015;24:143-151.

[7] Probst J, Jideus L, Blomström P, Zemgulis V, Wassberg E, Lönnerholm S, et. al. Thoracoscopic epicardial left atrial ablation in symptomatic patients with atrial fibrillation. Europace. 2016;18(10):1538-1544.

[8] Moon RS and Hendon CP. Cardiac tissue characterization using near-infrared spectroscopy. SPIE Volume 8926, Photonic Therapeutics and Diagnostics X, 89263N (4 March 2014), https://doi.org/10.1117/12.2036320

[9] Moon RP, Marboe CC, and Hendon CP. Near-infrared spectroscopy integrated catheter for characterization of myocardial tissues: preliminary demonstrations to radiofrequency ablation therapy for atrial fibrillation. Biomedical optic express. 2015;6(7):2494-11.

[10] Demos SG and Sharareh S. Real time assessment of RF cardiac tissue ablation with optical spectroscopy. Optics Express. 2008;16(19):15286-96.

[11] Tung R. Epicardial Approach to Catheter Ablation of Ventricular Tachycardia. Elsevier, Part 7 – Catheter ablation of ventricular tachycardia 2017;Chapter 33:649-670.

[12] Nazer B, Walter TE, Duggirala S and Gerstenfeld E. Feasibility of Rapid Linear-Endocardial and Epicardial Ventricular Ablation Using an Irrigated Multipolar Radiofrequency Ablation Catheter. Circulation: Arrhythmia and Electrophysiology. 2017;10:1-9.

[13] Hudson DE, Hudson DO, Wininger J and Richardson B. Penetration of Laser Light at 808 and 980nm in Bovine Tissue Samples. Photomedicine and Laser Surgery. 2013;31(4):163-168.

[14] Vuylsteke M and Mordon S. Endovenous Laser Ablation: A Review of Mechanisms of Action. Annals of Vascular Surgery Inc. 2012;26:424-433.

[15] Henderson T and Morries L. Near-infrared photonic energy penetration: can infrared phototherapy effectively reach the human brain? Neuropsychiatric Disease and Treatment. 2015;11:2191-2208.

[16] D'Silva A and Wright M. Advances in Imaging for Atrial Fibrillation Ablation. Radiology Research and Practice. 2011; https://doi.org/10.1155/2011/714864.

[17] Barnett A, Bahnson T, and Piccini J. Recent Advances in Lesion Formation for Catheter Ablation of Atrial Fibrillation. Circulation: Arrhythmia and Electrophysiology. 2016;9(5).

[18] Koruth J, Kuroki K, Iwasawa J, Viswanathan R, Brose R, Buck E, et. al. Endocardial ventricular pulsed field ablation: a proof-of-concept preclinical evaluation. EP Europace. Volume 22, Issue 3, March 2020, Pages 434–439

[19] Seiichiro Matsuo, Matthew Wright, Sébastien Knecht, Isabelle Nault, Nicolas Lellouche et. al. Peri-mitral atrial flutter in patients with atrial fibrillation ablation. Heart Rhythm 2010 Jan;7(1):2-8.

[20] Cabrera JA, Sanchez-Quintana D, Ho SY, Medina A and Anderson RH. The architecture of the atrial musculature between the orifice of the inferior vena caval vein and the tricuspid valve: the anatomy of the isthmus. Circulation. 1998;9:1186-1195.

4 The effect of pulsed wave laser application on thermocoagulation of cardiac tissue and blood.

Dennis Krist, Ulrich Schotten, Stef Zeemering, Dominik Linz

Abstract

Purpose: This investigation addressed the significance of pulsed wave (PW) laser applications in the minimal invasive treatment of cardiac arrhythmias compared to continuous wave (CW) applications. This study investigated two areas of interest: the thermocoagulation of cardiac tissue and the thermocoagulation of blood under the influence of PW laser.

Methods: A complete factorial test plan was created to find adequate pulsing parameters for frequency and duty cycle to achieve thermal tissue coagulation. These settings were used to compare the thermocoagulation properties of PW and CW laser applications in a dose-finding study on freshly excised porcine hearts. The PW applications were applied with a frequency of 40Hz, a varying duty cycle between 72.5% and 85%, and varying power between 20W and 35W. The PW and CW laser effects on thermally induced blood clot formation were assessed by applying laser energy directly into stagnant porcine blood with varying hematocrit between 35% and 55%. An iterative scheme with an incremental increase of power and application time was used to define the clotting point for two different catheter types.

Results:

In total, 52 PW power applications were applied to the freshly excised hearts. No significant difference in lesion depth was observed between pulse settings of 40Hz and 85% duty cycle and CW applications ($p=0.053$). Significant differences were found between PW applications at 40Hz and 72.5% duty cycle, PW applications at 40Hz and 85% duty cycle, and CW applications ($p=0.003$ and $p<0.001$). In contrast to CW, no steam pops were observed by PW laser in ablation of fat-

covered tissue achieving equal lesion depth ($p = 0.216$). Application of PW laser had no effect on the thermocoagulation of blood in catheters with an energy density of 0,22W/mm^2. Catheters with an energy density of 0,40W/mm^2 allowed increased power application for PW applications with a duty cycle of 72.5%.

Conclusion: Pulsed wave application is a good extension to current CW laser applications. Benefits in the ablation of adipose cardiac tissue were obtained by preventing steam-pops as seen in CW applications. Additionally, PW laser could increase procedural safety of endocardial ablations by reduced susceptibility to laser-induced clot formation in high power applications.

Introduction

Percutaneous catheter ablation of atrial fibrillation (AF) is most commonly achieved by endocardial application of radiofrequency (RF) or cryothermal energy to the atrial tissue.[1, 2] Alternative energy forms include microwave, high-intensity focused ultrasound, and laser energy. All therapies relying on thermal ablative modalities encounter the same safety and lesion formation challenges. Recent investigations suggested a possible come-back of direct current applications through pulsed-field ablation (PFA) due to its nonthermal ablative modality to restrict these negative properties. [3-5] PFA creates short-pulsed electrical fields destabilizing cell membranes by forming irreversible nano-scale pores, called irreversible electroporation, and cell contents' leakage, resulting in apoptosis. [6-8]

Clinical studies [3, 4] and preclinical experiments [5, 9] have shown reduced PV stenosis, phrenic nerve injury, and esophageal injury with PFA delivered even

directly atop those structures [10-12]. Similar effects on the safety profile, selective tissue necrosis, and increased procedural efficacy may be observed with pulsed wave (PW) laser applications.

Most commonly continuous wave (CW) laser ablation devices are used in the laser-based treatment of cardiac arrhythmias. [13-15] Early investigations [16] already showed the feasibility of selective tissue heating by PW applications, preventing denaturation of the surrounding tissue by allowing a thermal relaxation time. Depending on the size of the targeted substance, this relaxation time varies between nanoseconds for subcellular organelles to milliseconds for vessels and small structures. The pulsing frequency and duty cycle [1] are to be adjusted accordingly for the desired effect.

Herein, we investigated the effects of PW laser on lesion formation and thermocoagulation of blood compared to continuous wave (CW) laser. The investigation regarding thermocoagulation of tissue focusses on the lesion formation process to find suitable pulse parameters and to assess the effect on cardiac tissue. The investigation regarding thermocoagulation of blood focusses on the safety profile of endocardial procedures to reduce the thermal effect on blood coagulation by using pulsed laser.

Material and methods

To investigate the effect of pulsed wave laser on tissue three separate investigations were required (1) to (3). In (1) a parameter finding to find suitable pulse

[1] *The pulsing duty cycle is the percentage of the ratio of pulse duration to the total period of the waveform. Duty Cycle = Pulse Width (sec) * Repetition Frequency (Hz) * 100%*

parameters, in (2) a dose-finding with the determined pulsing parameters assessing the effect on lesion depth, and in (3) the effect of pulsing on catheter temperature and ablation of adipose tissue-covered substrates were investigated.

The effect of pulsed wave laser on the thermocoagulation of blood was investigated in (4).

Experimental set up for pulse parameter finding (1)

In pulsed-wave laser applications, energy is applied in pulses with predetermined pulse duration and repetition rate. A parameter finding study was conducted to define the ideal pulse duration and repetition rate. A full factorial blocked test plan with the addition of center points was created to assess the influence of applied power, duty cycle, frequency, and application time on the lesion depth. Each run was conducted independently twice as part of the blocked design to increase precision. The high and low levels of factorial analyses were defined at power between 4W and 8W, duty cycle between 60% and 85%, frequency between 5Hz and 40Hz, and application time between 30s and 90s.

A 40W, 976nm diode laser module (M1F-SS2.1, Dilas Diodenlaser GmbH, Mainz, Germany) was used as energy source for this investigation. A diode driver (LDD 600, Lumina Power, Bradford (MA), United States of America) powered the laser diode, and a laser controller (LDDC 1550, Quantum Composers, Bozeman (MT), United States of America) controlled it.

The tissue was irradiated with a 200µm Hard Plastic Clad Silica optical fiber with a numerical aperture of 0,39 (HWF 200T, CeramOptec GmbH, Bonn, Germany). The tip was protected by a glass shell with internal flushing, which minimizes the effects of conductive tissue heating via the glass shell. The setup was calibrated

by measuring the emitted power from the tip with a power sensor compensating possible laser energy dissipation by absorption (i.e., reflection and refraction by the glass).

Due to the low absorbance of 980nm laser Deuterium was preferred as a flushing medium in contrast to water or saline. Non-perfused avian tissue was used as a tissue model for this *ex vivo* study. The sharp demarcation between coagulated and untreated tissue makes avian tissue most suitable to assess the influence of varying pulse parameters on tissue coagulation. Upon power delivery, the glass tip was placed against the tissue. The experimental setup is depicted in **Fig. 4.1**.

A midline section at the lesion site facilitated the macroscopic estimation of the lesion depth. The estimated lesion depth represents the response value of the full factorial experiment.

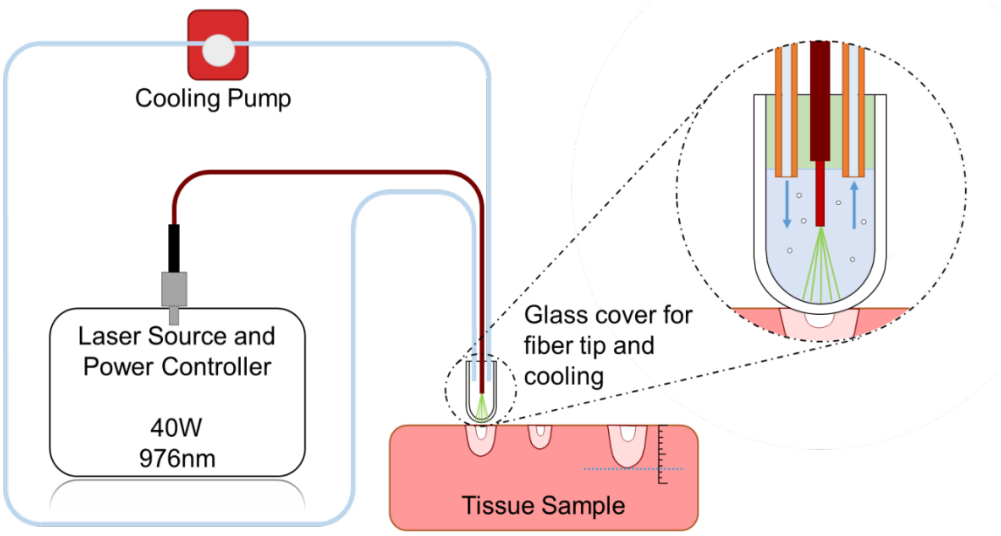

Fig. 4.1 *Experimental setup as used for the parameter finding, investigating the influence of PW laser parameters on the lesion depth.*

Experimental setup for the assessment of thermocoagulation of tissue (2)

An *ex vivo* dose-finding study was conducted to investigate the effects of PW laser on catheter-based tissue ablation. In this regard the lesion depth for applications with varying application time and power settings. In total, ten freshly excised porcine hearts were used, extracted less than six hours before the investigation, and kept at 37°C in a saline solution bath. The hearts were taken from the saline bath promptly before the power application on the epicardial surface of the left ventricle.

The in Chapter 2 developed experimental 20mm linear laser catheter with slightly convex laser-active area to optimize wall contact was used. A contact

force of 25±3g was applied ensuring adequate tissue contact over the entire length of the active area. The pulse parameter combinations 40Hz at 85% duty-cycle and 40Hz at 72.5% duty-cycle were tested. The power and time settings varied between 20W for 60s and 35W for 150s in steps of 5W and 30s. The same power source used in the parameter findings was selected. The applications parameters (Power, Time, Frequency, Duty Cycle) were transformed to energy per mm to promote comparability between CW and PW applications.

Experimental setup ablation-related tissue damage (3)

Carbonization of cardiac tissue is primarily caused by excessive heating of the superficial tissue layers due to absorption of laser energy and conductive heating via the catheter's surface. This investigation estimated the influence of pulsed wave laser on the carbonization of cardiac tissue and in ablation of adipose-tissue covered substrates.

To assess the influence of PW laser on the catheter surface temperature a thermal recording of the catheter was created with an infrared imaging camera (Model PI 640, Spectral range 7,5 to 13µm, Temperature range 0°C - 250°C, Optris GmbH, Berlin, Germany) during power application. PW and CW laser energy was applied at 10W, 15W, 20W, 25W, and 30 W; with the catheter placed in a shielded box emitting in normal air towards the camera. The recording was stopped once a stable temperature was attained.

The overall influence of PW laser on the thermal damage of the tissue surface was assessed by comparing the ventricular surface carbonization for continuous and pulsed wave laser. Freshly excised porcine hearts were used, extracted less than six hours before the investigation, and kept at 37°C in a saline solution bath.

The hearts were taken from the saline bath promptly before the power application on the epicardial surface of the left ventricle. Ablations were performed with continuous power settings of 25W for 120s and pulse settings of 40Hz at 85% duty cycle.

The insulating properties of the adipose tissue can lead to extreme temperature build-up during power applications and explosive vaporization identified by an audible acoustic transient (popping sound) [17,18]. As noticed in earlier CW laser investigations, ablation of adipose tissue-covered substrates can cause steam pops at the ablation site. The effects of PW laser on this vaporization and lesion depth in ablation of adipose tissue-covered ventricles were assessed. Ablations were performed with continuous power settings of 25W for 120s and pulse settings of 40Hz at 85% duty cycle. Freshly excised porcine heart were used for this investigation.

Experimental setup to study thermocoagulation of blood (4)

The effect of continuous and pulsed wave applications on the thermocoagulation of blood was assessed by direct irradiation of porcine blood with 980nm laser. Porcine blood was used blood for *ex vivo* experiments serving as substitute to human blood, with similar spectral properties.[19, 20] Approximately 5L freshly drawn porcine blood was circulated in an extracorporeal membrane oxygenator(ECMO). The blood temperature was kept at 37°C, oxygenation saturation was kept at approximately 98%, with a regulated base excess of 0 mEq/L. By EDTA treatment the ACT was kept >1000s[21, 22] avoiding nonthermal coagulation and allowing heat-induced denaturation of blood proteins. Since hemoglobin is the main absorber in blood, a predetermined hematocrit value is vital to promote

comparability between investigations (i.e., higher hematocrit values would lead to increased laser absorption). The hematocrit was set at 55%, 50%, 45%, 40%, and 35% for the investigations with CW and PW applications. The hematocrit value was regulated by adding or extracting plasma from the blood., with an accuracy of ± 1%. **Fig. 4.2**. displays the experimental setup.

The laser applications were conducted with an 8.3 Fr laser loop catheter with a diameter of 28mm and a total laser-active area of 50mm (Herzogenrath, Germany) (Patents: US 2018/0021089, US 2011/0230941, US 2011/0230871). Two configurations with varying energy density were selected, 0,22 W/mm^2 and 0,40 W/mm^2. The irrigated closed tip was flushed with room temperature saline at 16mL/min. A 976nm 40W laser module delivered the laser energy (M1F-SS2.1, Dilas Diodenlaser GmbH, Mainz, Germany), powered by a diode driver (LDD 600, Lumina Power, Bradford (MA), United States of America), and controlled by a laser controller (LDDC 1550, Quantum Composers, Bozeman (MT), United States of America).

The catheter was placed in the middle of a beaker with approx. 150ml of freshly extracted porcine blood. Subsequently the laser energy was delivered to the stagnant blood representing the worst-case condition for endocardial use. This also provides a controllable flow state compared to laminar or pulsatile flows. After power application the catheter was retracted from the beaker and inspected for coagulum formation at the laser active area.

New blood was used after each laser application to prevent sedimentation and overheating of the blood.

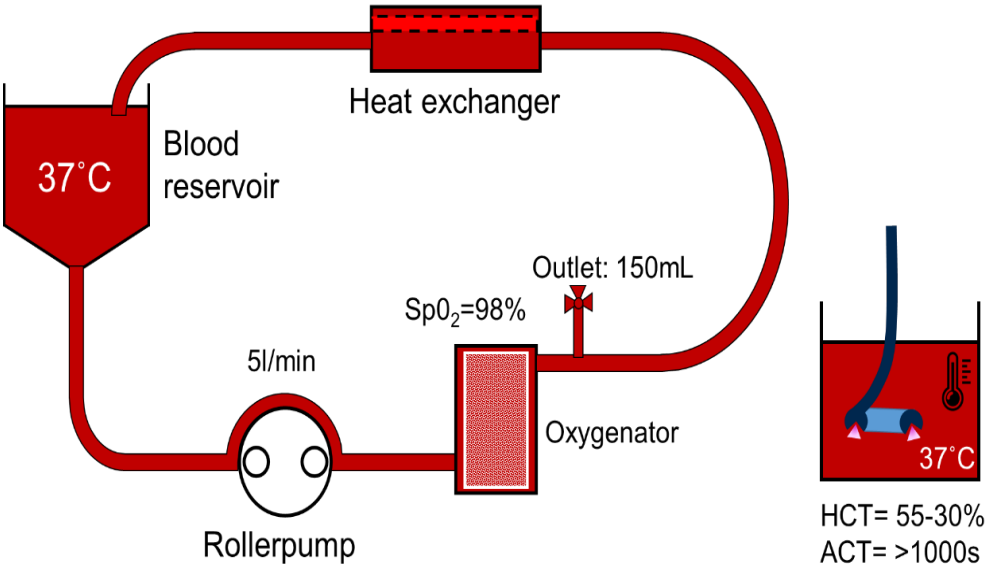

Fig. 4.2 *Schematic ECMO setup, as used for the experiments to define threshold for thermocoagulation of blood.*

To define the threshold of laser induced thermacoagulation of blood, a power setting between 10W and 30W (at 2W steps) and hematocrit value between 55% and 35% (at 5% steps) was chosen. The time setting was stepwise increased in 30s steps (starting at 30s) till coagulum formation was observed on the catheter surface. The same strategy was applied for PW applications, with a frequency of 40Hz, and a duty cycle of 72.5% and 85%. With the gathered threshold points 3D surface plots were created for the CW and PW applications for both catheter types.

Statistical Analysis

A full factorial blocked test plan with the addition of center points was created to analyse various pulse settings (1).[2] Additionally, the linear (first-order) and non-linear (second-order) interactions between the factors were investigated.

The statistical analysis was performed with R-Commander (Version 2.6-0, GNU General Public License). The variability in the data is partitioned by using the built-in ANOVA analysis. The resulting p value for each combination of factors reveals the significance of each interaction — the significance cut-off set at 5%. The main effect plots and surface response plots were also generated with R-Commander.

A Pearson's product-moment correlation was applied to assess the relationship between applied energy and lesion depth in the dose-finding study (2). The obtained data sets for CW and PW applications were compared by means of an ANCOVA analysis (Minitab, Version 18.1) with significance cut-off set at 5%.

[2] *In statistics, a full factorial experiment is an experiment where the design consists of two or more factors, each with discrete possible values or "levels", and whose experimental units take on all possible combinations of these levels across all such factors. In the statistical theory of the design of experiments, blocking is the arranging of similar experimental units in groups (blocks). Blocking reduces unexplained variability. Its principle is variability, which cannot be overcome (e.g., needing two batches of raw material to produce one container of a chemical) is confounded or aliased with a (higher/highest order) interaction to eliminate its influence on the end product. Center points are added to test for non-linear relationships between factors.*

A Mann-Whitney U Test was conducted to assess the difference in catheter surface temperature between continuous and pulsed wave applications (3) with significance cut-off set at 5%.

Results

Pulse parameter finding (1)

In total, 57 data points were collected for the full factorial analysis. The data was used to construct a linear model and derive the main effect plots for each parameter. As displayed in **Fig. 4.3**, these first-order interactions, showed a positive interaction between pulse duty cycle, applied power, application time, and the response value. Variations in pulse frequency did not affect the response value as first-order interaction.

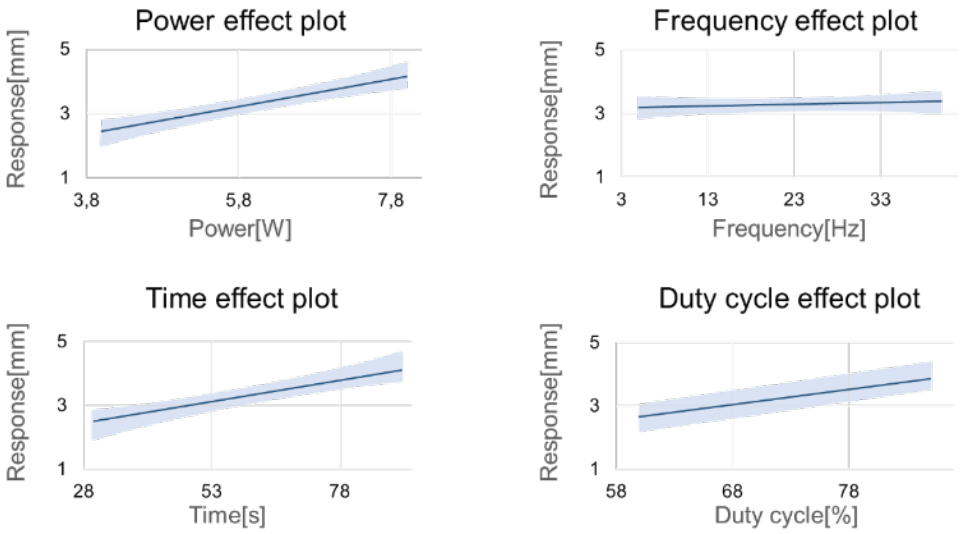

Fig. 4.3 *Main effect plots portraying the first-order interaction between each parameter and the response value (i.e., the lesion depth). A positive interaction between pulse duty cycle, applied power, application time, and the response value were observed. Variations in pulse frequency did not affect the response value as first-order interaction.*

The second-order interactions were also derived from the linear model, providing helpful insight into two-way interactions between the response value parameters. The interactions, also called surface response plots, are displayed in **Fig. 4.4**.

The combined interactions of time and frequency ($p = 0.003$), and time and duty cycle ($p = 0.043$) showed a significant positive interaction with the lesion depth. The pulse parameter combinations 40Hz at 85% duty-cycle and 40Hz at 72.5% duty-cycle were selected for further dose-finding investigations.

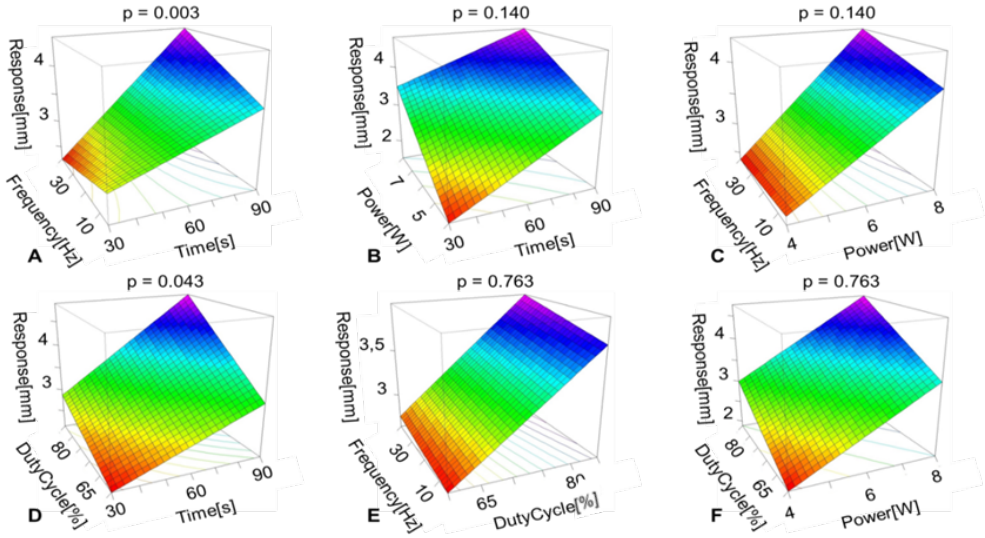

Fig. 4.4 *The surface response plots show the second-order interactions between two parameters and the response value (lesion depth).* ***A:*** *Significant two-way interaction between time- frequency on lesion depth.* ***B – C:*** *Insignificant interactions between power - time / frequency - power on the lesion depth.* ***D:*** *Significant interaction between duty-cycle - time on lesion depth.* ***E – F:*** *Insignificant interactions between frequency - duty-cycle / duty-cycle - power and lesion depth.*

Thermocoagulation of tissue (2)

In total, 52 pulsed power applications were delivered to 10 freshly excised porcine hearts. The continuous wave baseline was established by 138 power applications from previous *ex vivo* dose-finding studies. In the left panel of **Fig. 4.5** the median lesion depth was plotted against the energy. The right panel displays all obtained data points as a scatterplot.

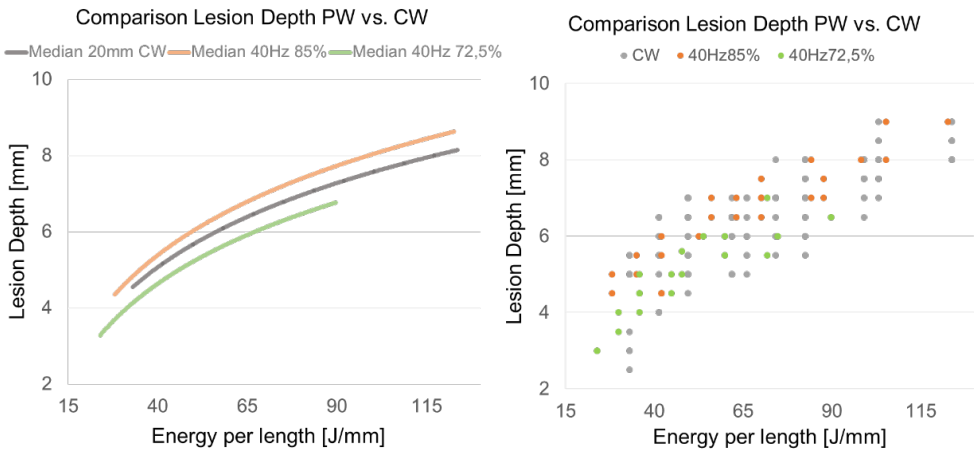

Fig. 4.5 *Left panel: obtained trend lines of the estimated median lesion depth in CW and PW laser applications. Right panel: scatter plot, containing all obtained data points, with orange, representing the PW applications at 40Hz and 85% duty cycle, grey the CW applications, and green the PW applications at 40 Hz and 72.5% duty cycle.*

The pulsed wave power applications showed similar lesion depths compared to continuous-wave applications. The maximum lesion depth of the 72.5% duty cycle group was limited to approximately 7mm and could not be compensated by increasing the power.

The Pearson correlation factor indicates a strong positive correlation between the applied energy and the lesion depth for all groups, with a factor of $r = 0.798$, $p < 0.0001$ for the CW group, $r = 0.928$, $p < 0.0001$ for the PW group with 85% duty cycle, and $r = 0.885$, $p < 0.0001$ for the PW group 72.5% duty cycle.

The ANCOVA results showed no significant difference in lesion depth between the 40Hz/85% PW and the CW application ($p = 0.053$). A significant difference

was found ($p < 0.001$) between the 40Hz/72.5% PW and the CW application ($p = 0.003$) and between both PW applications.

Ablation-related tissue damage (3)

The catheter surface temperature was estimated to assess potential differences in conductive heating by using the pulsed energy applications.

Fig. 4.6 displays the recorded temperatures of the CW and PW applications per power setting. The pulsed-power applications showed significantly lower catheter surface temperatures ($p < 0.001$, Mann-Whitney U Test) than the continuous wave applications.

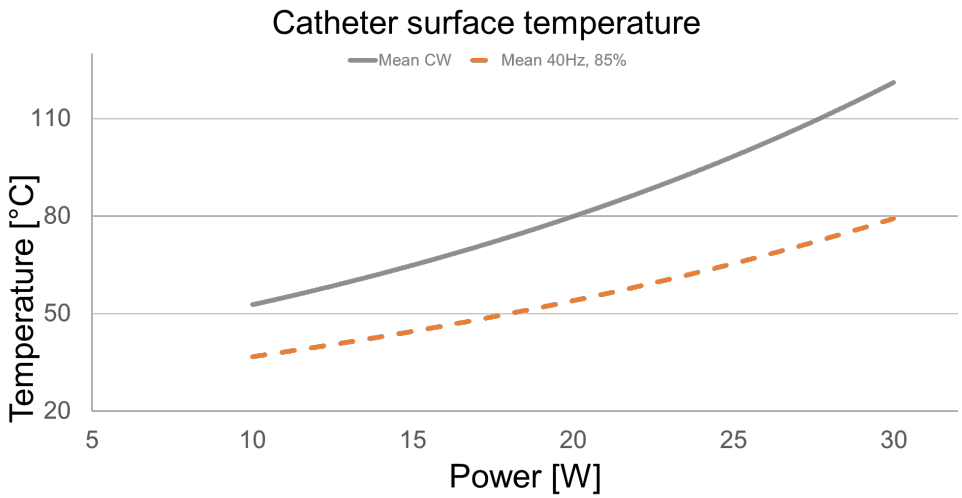

Fig. 4.6 *Recorded surface temperatures for CW and PW laser applications.*

In total, 10 epicardial PW and 10 CW lesions were created to assess the effect of pulsing on carbonization of the epicardial surface. **Fig. 4.7** depicts the observed

difference in tissue discolorations, showing strongly demarcated dark areas in the CW samples. The pulsed applications showed reduced surface discoloration at the ablation site.

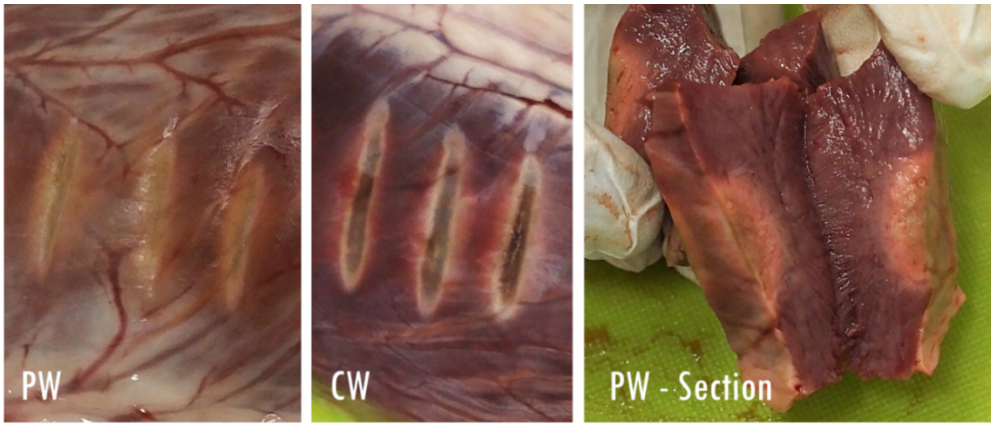

Fig. 4.7 *Left: Effects on tissue surface resulting from pulsed ablations. Middle: Effects on tissue surface from continuous-wave application, with dark demarcated lesions. Right: Cross-section of the pulsed-wave ablation, showing the continuity and linearity of the lesion.*

The effect of PW laser on the ablation of adipose tissue was investigated, by 10 CW and 10 PW ablations. No popping sounds were registered during the PW power application in regard to CW. No significant difference ($p = 0.216$) in lesion depth (6.30±0.75mm) was found in comparison to the non-fat covered tissue (6.88±0.98). **Fig. 4.8** shows the positioning of the catheter on the fat covered ventricle and a cross-section of the created lesions.

Fig. 4.8 *Left: Epicardial view of the catheter positioning in adipose tissue ablation. Right: Cross-section of the formed lesion beneath the adipose layer. The arrows represent the laser application.*

Thermocoagulation of blood (4)

The laser-induced thermocoagulation of blood was assessed by 372 laser applications in stagnant blood, resulting in the power and time threshold per hematocrit value. A baseline of CW power applications was created for both catheter types before the PW applications. The associated data was visualized in **Fig. 4.9** by surface plots of the 72.5% and 85% duty cycle groups against the CW baseline. The catheters with an energy density of 0,22W/mm^2 showed no difference in clotting limit between PW and CW applications, for both 85% and 72.5% duty cycle. All performed laser applications could show clotting at hematocrit values of 55%, regardless of the application time.

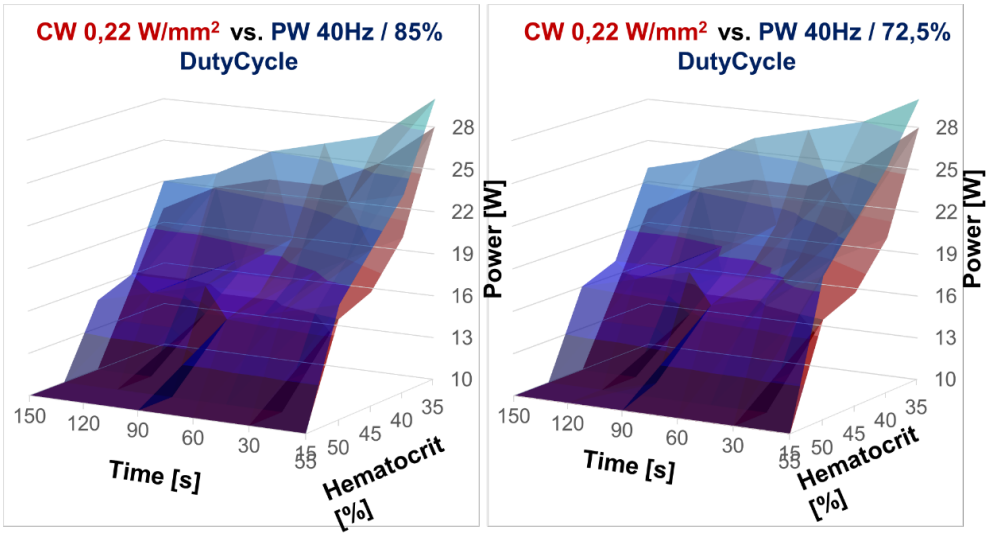

Fig. 4.9 *3D-graphs representing the coagulation limit in stagnant blood for a catheter with an energy density of 0,22W/mm². The red surface represents the CW, and the blue surface the PW applications.*

At an energy density of 0,40W/mm² and a duty cycle of 72.5%, a significant difference in clotting limit was observed between CW and PW applications. A clear upward shift of the PW plane was noted. This effect was less pronounced for pulsed applications with a duty cycle of 85%. The associated data was visualized in **Fig. 4.10** by surface plots for the 72.5% and 85% duty cycle groups.

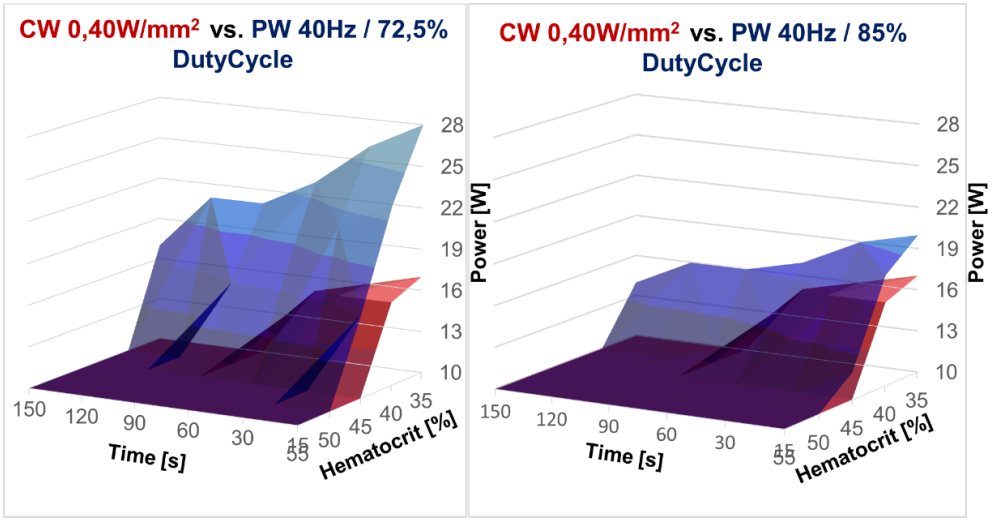

Fig. 4.10 *3D graphs representing the coagulation limit in stagnant blood for a catheter with an energy density of 0,40W/mm². The red surface is the CW, and the blue surface the PW applications.*

Discussion

Benefits of pulsed wave laser in tissue coagulation

In this investigation, the effects of pulsed wave laser on the photothermal coagulation of cardiac tissue and whole blood were evaluated. The results showed no significant difference in lesion depth between continuous wave and pulsed wave applications, for a pulse frequency of 40Hz and duty cycle of 85%. A lower duty cycle of 72,5% demonstrated significantly reduced lesion depth than CW and PW applications with an 85% duty cycle.

Past investigations by Henderson [23] and Hashmi[24] suggested that a pulse-induced cool-down period reduced the energy absorption in the superficial tissue layers, allowing deeper tissue penetration.

Hence, with the same average power, higher penetration depths were obtained.

The findings of this study showed none of the indicated effects on deep-tissue coagulation (>3mm). Discordantly, similar behaviour as in CW applications was seen, where deep coagulation was achieved by heat conduction. Although, Henderson investigated different wavelengths, lower energies, and a different application field.

Beneficial effects were observed in laser absorption in superficial layers and during the ablation of fat-covered tissue. The CW ablation of fat-covered myocardial tissue led to audible steam-pops. The insulating characteristics of the adipose tissue allowed excessive local heating and water evaporation [17,18]. The granted cool-down phase inherent to pulsed applications efficiently reduced the occurrence of steam pops in fat-covered tissue without lesion-depth reduction.

The commonly associated complications, such as cardiac tamponade, barotrauma with dissection of tissue planes, and collateral damage to structures outside the heart [25, 26], could be avoided during epicardial ablation procedures, improving procedural safety. Although the laser applications, in general, showed low collateral damage to surrounding tissue structures, the unique tissue-selective lesion formation properties of PFA [9] could not be achieved.

PFA relies on the biophysical phenomenon of irreversible electroporation, in which the permeability of the cell membrane is increased by nano-scale pores in the lipid bilayer due to the applied electrical field, resulting in apoptosis. [27-29]

Although a laser is an electromagnetic radiation-emitting device consisting of synchronized oscillations of electric and magnetic fields, the electrical field of 980nm laser irradiation, did not have the electrical field strength to induce irreversible electroporation.

The catheter' surface temperature and the absorption of light in the superficial tissue layers could efficiently be reduced by pulsing, limiting the heating of the epicardial surface. There was diminished discoloration of the epicardial tissue surface compared to the current state-of-the-art applications. [30, 31] Pulsing also led to promising results in reduction of charring and damage of the epicardial tissue during ablation procedures, which may reduce the commonly observed increased susceptibility of pericarditis, [32-34] caused by increased friction between the visceral pericardium and the parietal pericardium. In the case of endocardial ablations, preserving an intact endocardial tissue layer is also desirable due to the associated clotting susceptibility and required post-procedural anticoagulation treatment [18, 35] for damaged endocardia.

More chronic *in vivo* studies must investigate the specific clinical benefit of reduced surface damage. Further research is also needed to substantiate these findings and to investigate the influence of frequencies above 40Hz.

Interestingly, the pulsing of laser energy also proved beneficial effects on the optical components of the ablation system. Higher energies could be applied to the optical components without (over)heating the components allowing higher energy transmission into a 200µm fiber in CW applications.

Benefits of pulsed wave laser in the prevention of thermal blood coagulation

The effect of PW laser on the thermocoagulation of whole blood was investigated by direct irradiation of stagnant porcine blood. For low-power applications (0,22W/mm^2), no difference in clotting limit was observed between CW and PW applications. For the high-power applications (0,40W/mm^2), a significant difference in clotting limit was observed if pulsed at 40Hz and 72,5% duty cycle.

Compared to thermally-induced coagulation and charring of blood by radio-frequency ablation catheters, coagulation and charring by laser ablation are mainly caused by light absorption in the erythrocytes. [36, 37, 22]

Research by Black [36] has shown this three-stage mechanism for coagulation involving a heating phase, a primary coagulation phase (70˚C) involving mainly the cytoplasm of the erythrocytes, and a secondary coagulation phase (optical properties of irradiated whole blood continue to evolve even after the laser pulse is removed) involving a more long-range intercellular coagulation.

Apart from coagulation, a chemical modification of oxy-Hb to met-Hb occurs, reducing the light transmission and increasing energy absorption combined with increased scattering. The use of PW laser allows the blood a thermal relaxation time, reducing the probability of coagulum formation.

The findings of this study corroborate the found benefits of pulsed laser irradiation in heparinized whole blood [37-39]: reduced clotting of PW laser applications compared to CW applications. Early research already suggested a reduced damaging effect by pulsed-laser applications with the same energy fluence.[40] Even though pulsed laser applications could reduce clot formation, these effects were

not as significant as observed in studies with irreversible electroporation as ablation modality. [3, 41] Since PFA is a nonthermal coagulation technique, the same absence of thermal coagulation cannot be expected for thermal coagulation devices in PW laser ablation.

The most critical parameter in our investigation was the hematocrit value of the irradiated blood, which predominantly influences the clotting limit. Therefore, the use of swine models for safety studies focussing on laser-induced thermocoagulation of blood [42-44] could be questioned due to the large difference in blood constitution between swine races. Due to lower hematocrit values in porcine blood (35%) compared to human blood (45%),[45, 46] clotting is less likely in porcine species due to the reduced amount of red blood cells. This difference was initially seen by comparing thermal coagulation experiments with both human and porcine blood. With identical power settings clotting was observed in human blood and not in porcine blood.

As shown in these experiments, this is related to the hematocrit level. Pulsing could be helpful in cardiac ablation treatments in areas with low blood flow or patients with high hematocrit values to improve the safety profile of the laser ablation procedures. The validity of the assessed *ex vivo* outcomes of laser-induced coagulation of blood is demonstrated in a clinical setting by *in vivo* trials. In future procedural safety animal studies, the hematocrit effect should be compensated by selecting swine races with higher hematocrit values.

Limitations

Using an *ex vivo* non-perfused porcine tissue model limited the investigation. However, we believe that both CW and PW results are affected identically. Due to physical limitations of the laser source and optical pathway, frequencies above 40Hz could not be tested.

The significance of reduced epicardial surface by PW applications damage needs to be demonstrated by chronic *in vivo* investigations. However, this feasibility study provides useful and necessary initial insights regarding tissue damage. Moreover, additional information is to be gathered by chronic *in vivo* investigations about the efficacy of PW laser applications in the treatment of cardiac arrhythmias.

The use of porcine blood contrary to human blood is an added limitation of this investigation. Despite almost identical properties of the porcine blood, the blood cells are slightly smaller than human blood cells, possibly confounding our results. However, it is undisputed that a higher hematocrit leads to an increased risk of clot formation.

Conclusion

The pulsed wave application is a promising extension of the continuous wave-laser application. At a frequency of 40Hz and a duty cycle of 85%, the achieved lesion depth of the CW application could be maintained while reducing the carbonization of the epicardial tissue surface.

Besides, the benefits of adipose cardiac tissue ablation could be obtained since the researchers observed no steam-pops during PW energy applications. From a safety point of view, the use of a PW laser could increase the safety of endocardial procedures by reduced susceptibility to laser-induced clot formation in high-power applications.

References

[1] Calkins H, Hindricks G, Cappato R, Kim YH, Saad EB et. al. 2017 HRS/EHRA/ECAS/APHRS/SOLAECE expert consensus statement on catheter and surgical ablation of atrial fibrillation. Heart Rhythm. 2017 Oct;14(10):e275-e444. doi: 10.1016/j.hrthm.2017.05.012.

[2] Haegeli LM, Calkins H. Catheter ablation of atrial fibrillation: an update. Eur Heart J. 2014 Sep 21;35(36):2454-9. doi: 10.1093/eurheartj/ehu291.

[3] Reddy VY, Neuzil P, Koruth JS, Petru J, Funosako M et. al. Pulsed Field Ablation for Pulmonary Vein Isolation in Atrial Fibrillation. J Am Coll Cardiol. 2019 Jul 23;74(3):315-326. doi: 10.1016/j.jacc.2019.04.021.

[4] Reddy VY, Anter E, Rackauskas G, Peichl P, Koruth JS et. al. Lattice-Tip Focal Ablation Catheter That Toggles Between Radiofrequency and Pulsed Field Energy to Treat Atrial Fibrillation: A First-in-Human Trial. Circ Arrhythm Electrophysiol. 2020 Jun;13(6):e008718. doi: 10.1161/CIRCEP.120.008718.

[5] Koruth JS, Kuroki K, Kawamura I, Brose R, Viswanathan R et. al. Pulsed Field Ablation Versus Radiofrequency Ablation: Esophageal Injury in a Novel Porcine Model. Circ Arrhythm Electrophysiol. 2020 Mar;13(3):e008303. doi: 10.1161/CIRCEP.119.008303.

[6] Davalos RV, Mir IL, Rubinsky B. Tissue ablation with irreversible electroporation. Ann Biomed Eng. 2005 Feb;33(2):223-31. doi: 10.1007/s10439-005-8981-8.

[7] Rubinsky B, Onik G, Mikus P. Irreversible electroporation: a new ablation modality--clinical implications. Technol Cancer Res Treat. 2007 Feb;6(1):37-48. doi: 10.1177/153303460700600106.

[8] Scheffer HJ, Nielsen K, de Jong MC, van Tilborg AA, Vieveen JM et. al. Irreversible electroporation for nonthermal tumor ablation in the clinical setting: a systematic review of safety and efficacy. J Vasc Interv Radiol. 2014 Jul;25(7):997-1011; quiz 1011. doi: 10.1016/j.jvir.2014.01.028.

[9] Koruth J, Kuroki K, Iwasawa J, Enomoto Y, Viswanathan R et. al. Preclinical Evaluation of Pulsed Field Ablation: Electrophysiological and Histological Assessment of Thoracic Vein Isolation. Circ Arrhythm Electrophysiol. 2019 Dec;12(12):e007781. doi: 10.1161/CIRCEP.119.007781.

[10] van Driel VJ, Neven KG, van Wessel H, du Pré BC, Vink A et. al. Pulmonary vein stenosis after catheter ablation: electroporation versus radiofrequency. Circ Arrhythm Electrophysiol. 2014 Aug;7(4):734-8. doi: 10.1161/CIRCEP.113.001111.

[11] van Driel VJ, Neven K, van Wessel H, Vink A, Doevendans PA, Wittkampf FH. Low vulnerability of the right phrenic nerve to electroporation ablation. Heart Rhythm. 2015 Aug;12(8):1838-44. doi: 10.1016/j.hrthm.2015.05.012.

[12] Neven K, van Es R, van Driel V, van Wessel H, Fidder H et. al. Acute and Long-Term Effects of Full-Power Electroporation Ablation Directly on the Porcine Esophagus. Circ Arrhythm Electrophysiol. 2017 May;10(5):e004672. doi: 10.1161/CIRCEP.116.004672.

[13] Bhardwaj R, Reddy VY. Visually-guided Laser Balloon Ablation of Atrial Fibrillation: A "Real World" Experience. Rev Esp Cardiol (Engl Ed). 2016 May;69(5):474-6. English, Spanish. doi: 10.1016/j.rec.2016.02.006.

[14] Weber H, Sagerer-Gerhardt M, and Heinze A. Laser catheter ablation of long-lasting persistent atrial fibrillation: Longterm results. J Atr Fibrillation. 2017 Aug-Sep; 10(2): 1588.

[15] Sagerer-Gerhardt M and Weber H. Open-irrigated laser catheter ablation: influence of catheter–tissue contact force on lesion formation. J Interv Card Electrophysiol (2015) 42:77–81

[16] Anderson RR, Parrish JA. Selective photothermolysis: precise microsurgery by selective absorption of pulsed radiation. Science. 1983 Apr 29;220(4596):524-7. doi: 10.1126/science.6836297.

[17] Nakagawa H, Yamanashi WS, Pitha JV, Arruda M, Wang X et. al. Comparison of in vivo tissue temperature profile and lesion geometry for radiofrequency ablation with a saline-irrigated electrode versus temperature control in a canine thigh muscle preparation. Circulation. 1995 Apr 15;91(8):2264-73. doi: 10.1161/01.cir.91.8.2264.

[18] Issa Z F, Miller JM, Zipes DP (2012). Clinical Arrhythmology and Electrophysiology: A Companion to Braunwald's Heart Disease: Second Edition. Elsevier Inc. Chapter 7 and Chapter 32. https://doi.org/10.1016/C2010-0-68723-2

[19] Xu X, Yu L, Chen Z. Optical clearing of flowing blood using dextrans with spectral domain optical coherence tomography. J Biomed Opt. 2008 Mar-Apr;13(2):021107. doi: 10.1117/1.2909673.

[20] Cardoso AV, Camargos AO. Geometrical aspects during formation of compact aggregates of red blood cells. Mater. Res. 2002;5(3):263–268.

[21] Verkruysse, W, Nilsson AMK, Milner TE, Beek, JF, Lucassen, GW, and Van Gemert MJC., 'Optical Absorption of Blood Depends on Temperature During a 0.5 ms Laser Pulse at 586 nm. Photochem. Photobiol., 1998; 67, No. 3, pp. 276–281.

[22] Nilsson AMK, Lucassen GW, Verkruysse, W, Andersson-Engels S, and Van Gemert MJC. Changes in Optical Properties of Human Whole Blood ex vivo Due to Slow Heating, Photochem. Photobiol. 1997;65, pp. 366–373.

[23] Henderson TA, Morries LD. Near-infrared photonic energy penetration: can infrared phototherapy effectively reach the human brain? Neuropsychiatr Dis Treat. 2015 Aug 21;11:2191-208. doi: 10.2147/NDT.S78182.

[24] Hashmi JT, Huang YY, Sharma SK, Kurup DB, De Taboada L et. al. Effect of pulsing in low-level light therapy. Lasers Surg Med. 2010 Aug;42(6):450-66. doi: 10.1002/lsm.20950.

[25] Huang S, Mark Wood M. Catheter Ablation of Cardiac Arrhythmias. Chapter 7. 4th Edition, Elsevier 2019. eBook ISBN: 9780323550499

[26] Tokuda M, Kojodjojo P, Epstein LM, Koplan BA, Michaud GF et. al. Outcomes of cardiac perforation complicating catheter ablation of ventricular arrhythmias.Circ Arrhythm Electrophysiol. 2011; 4:660–666.

[27] Weaver JC and Chizmadzhev YA. Theory of electroporation: a review. Bioelectrochem. Bioenergetics, vol. 41, pp. 135–160, 1996. doi:10.1016/S0302-4598(96)05062-3

[28] Chang DC, Chassy BM, Saunders JA, and Sowers AE, Guide to Electroporation and Electrofusion. Academic Press 1992. ISBN: 9780121680411

[29] Tarek M. Membrane electroporation: a molecular dynamics simulation. Biophys J. 2005 Jun;88(6):4045-53. doi: 10.1529/biophysj.104.050617.

[30] Aryana A, d'Avila A. Epicardial Catheter Ablation of Ventricular Tachycardia. Card Electrophysiol Clin. 2017 Mar;9(1):119-131. doi: 10.1016/j.ccep.2016.10.009.

[31] Nazer B, Walters TE, Duggirala S, Gerstenfeld EP. Feasibility of Rapid Linear-Endocardial and Epicardial Ventricular Ablation Using an Irrigated Multipolar Radiofrequency Ablation Catheter. Circ Arrhythm Electrophysiol. 2017 Mar;10(3):e004760. doi: 10.1161/CIRCEP.116.004760.

[32] Tung R, Michowitz Y, Yu R, Mathuria N, Vaseghi M et. al. Epicardial ablation of ventricular tachycardia: an institutional experience of safety and efficacy. Heart Rhythm. 2013 Apr;10(4):490-8. doi: 10.1016/j.hrthm.2012.12.013.

[33] Oesterle A, Singh A, Balkhy H, Husain AN, Moyer D et. al. Late presentation of constrictive pericarditis after limited epicardial ablation for inappropriate sinus tachycardia. HeartRhythm Case Rep. 2016 Jul 16;2(5):441-445. doi: 10.1016/j.hrcr.2016.07.003.

[34] Dar TA, Turagam M, Yarlagadda B, Lakkireddy D. Managing Pericardium in Electrophysiology Procedures. American College of Cardiology. Oct 27, 2017.

[35] Ma J, Cheng G, Xu G, Weng S, Lu X. Effect of radiofrequency catheter ablation on endothelial function and oxidative stress. Acta Cardiol. 2006 Jun;61(3):339-42. doi: 10.2143/AC.61.3.2014838.

[36] Black JF, Barton JK. Chemical and structural changes in blood undergoing laser photocoagulation. Photochem Photobiol. 2004 Jul-Aug;80:89-97. doi: 10.1562/2004-03-05-RA-102.1.

[37] Pfefer TJ, Choi B, Vargas G, McNally-Heintzelman K, Welch A. Mechanisms of Laser-Induced Thermal Coagulation of Whole Blood ex vivo. Proceedings Volume

3590, Lasers in Surgery: Advanced Characterization, Therapeutics, and Systems IX; (1999) https://doi.org/10.1117/12.350970

[38] Kansaku R, Sakakibara N, Amano A, Endo H, Shimabukuro T, Sueishi M. Histological difference between pulsed wave laser and continuous wave laser in endovenous laser ablation. Phlebology. 2015 Jul;30(6):429-34. doi: 10.1177/0268355514538248.

[39] Pfefer TJ, Choi B, Vargas G, McNally KM, Welch AJ. Pulsed laser-induced thermal damage in whole blood. J Biomech Eng. 2000 Apr;122(2):196-202. doi: 10.1115/1.429642.

[40] Flock S, Smith L and Waner M. Quantifying the Effects on Blood of Irradiation with Four Different Vascular-Lesion Lasers. SPIE Vol. 1882 Laser-Tissue Interaction IV(1993)/ 237. https://doi.org/10.1117/12.147664

[41] Wittkampf FHM, van Es R, Neven K. Electroporation and its Relevance for Cardiac Catheter Ablation. JACC Clin Electrophysiol. 2018 Aug;4(8):977-986. doi: 10.1016/j.jacep.2018.06.005.

[42] Stewart MT, Haines DE, Verma A, Kirchhof N, Barka N et. al. Intracardiac pulsed field ablation: Proof of feasibility in a chronic porcine model. Heart Rhythm. 2019 May;16(5):754-764. doi: 10.1016/j.hrthm.2018.10.030.

[43] Hocini M, Condie C, Stewart MT, Kirchhof N, Foell JD. Predictability of lesion durability for AF ablation using phased radiofrequency: Power, temperature, and duration impact creation of transmural lesions. Heart Rhythm. 2016 Jul;13(7):1521-6. doi: 10.1016/j.hrthm.2016.02.012.

[44] Clauss S, Bleyer C, Schüttler D, Tomsits P, Renner S et. al. Animal models of arrhythmia: classic electrophysiology to genetically modified large animals. Nat Rev Cardiol. 2019 Aug;16(8):457-475. doi: 10.1038/s41569-019-0179-0.

[45] Windberger U, Bartholovitsch A, Plasenzotti R, Korak KJ, Heinze G. Whole blood viscosity, plasma viscosity and erythrocyte aggregation in nine mammalian species: reference values and comparison of data. Exp Physiol. 2003 May;88(3):431-40. doi: 10.1113/eph8802496.

[46] Soldin SJ, Rifai N and Hicks JMB. Biochemical Basis of Pediatric Disease. Fourth ed. AACC Press, 1995. ISBN: 9781594251009

5 An analysis of laser and radiofrequency induced tissue damage regarding a thermal threshold for coagulative tissue necrosis.

Dennis Krist, Ulrich Schotten, Stef Zeemering, Dominik Linz

Abstract

Purpose: This study aimed to estimate the required energy to achieve transmural tissue necrosis in laser and RF ablation based on a thermal isotherm of 60.6°C. We assessed the clinical significance of this study by a comparison with the currently used power settings and interlesion distance specifications in catheter ablation.

Methods: Radiofrequency energy was applied to avian tissue samples, with a varying power between 25 and 40W for 30 to 60 seconds in duration. Similarly, laser energy was applied with a varying power between 20 and 25W for 90 to 120 seconds. To promote comparability for the statistical analysis a high and low energy group was formed (high energy: laser > 1700J and RF > 1500; and low energy: laser ≤ 1700J and RF ≤ 1500). Throughout the power applications, the transmural tissue temperature was recorded with an infrared camera to estimate the transmural area surpassing the lethal isotherm of 60.6°C. The estimated areas were compared to the optically estimated coagulated area.

Results: For 89 RF and 48 laser ablations, the transmural areas were estimated. The optical coagulation area was consistently significantly larger($p<0.001$) than the area surpassing the lethal isotherm, regardless of the used energy source or power setting. Less energy was needed to achieve tissue necrosis with laser (55.10±11 J/mm^2) than RF energy (338.71±131 and 311.69±82 J/mm^2) for high energy settings ($p < 0.001$). In the low energy group, this difference was not significant ($p = 0.100$). Moreover, no significant difference in maximum transmural temperature was observed in both the high energy (75.2°C±5.5; 72.7°C±10.0;

74.5°C±9.8; p=0.703) and low energy group (66.9°C±11.6; 63.0°C±11.5; 65.7°C±8.0; 62.4°C±1.9; 61.8°C±2.4; p=0.408).

Conclusion: Analysis of the lesion formation process has shown a difference in the underlying biophysical principle of tissue coagulation between laser and radiofrequency ablation catheters. Comparing applied energy and estimated transmural area with a temperature surpassing the lethal isotherm showed that laser energy heats the tissue more locally. Due to a lower share of the conductive heating component, the tissue is heated more efficiently than with RF.

Introduction

Since the first radio frequency (RF) ablation in the 1990s [1], the transvenous catheter ablation market has witnessed widespread development of ablation devices, techniques, and available energy sources. Despite the emergence of innovative technologies, RF remains one of the most used energy modalities.

Therefore, new energy modalities and ablations devices are commonly compared to current RF devices and procedures. In this case laser energy is compared to RF. Both energy sources achieve tissue necrosis primarily through irreversible thermal injury of the cardiac tissue at the ablation site. [2, 3]

The underlying biophysical principles of tissue heating differ strongly between RF and laser applications. Lesion formation by RF ablation is primarily driven by thermal conduction,[2] as only the surface layers are affected by direct resistive heating. By contrast, laser energy ablation is based on photon absorption in the tissue. [4]

To achieve tissue necrosis for either energy source it is critical to heat the targeted tissue above the thermal threshold. Several studies investigated and determined the thermal threshold for tissue damage, although with different outcomes. [5-8]

This *ex vivo* comparison study used Wood's research [8] as a starting point for setting the lethal isotherm at 60.6°C, by combined visual and thermal estimation of the coagulated area. This temperature also correlated with the threshold as defined by the Arrhenius equation describing the relationship between exposure time, exposure temperature, and thermal necrosis of the tissue.[9]

To date, no study had analyzed the thermal dose requirement for a linear laser catheter for irreversible tissue damage. This study aimed to estimate the required energy to induce transmural tissue necrosis in laser and RF ablation, based on a thermal isotherm of 60.6°C. The results were also used to analyze the underlying biophysical lesion formation principles and to assess the clinical significance in regard to the current power application settings and recommended interlesion distance (ILD) for pulmonary vein isolation by a box lesion. [10-12]

Materials and Methods

Experimental setup

As validated in Chapter 3, avian tissue is well suited as *ex vivo* model for ablation studies. Non-perfused avian tissue was also used for this study. A thickness of 3.5mm ± 0.5mm was aspired, representing the anterior left atrial wall the thickness. [13] The tissue temperature was kept at approximately 37°C by placing the

tissue in a heated saline solution bath (0.9% NaCl solution in distilled water). It was ensured that the transmural tissue surface was maintained above the saline solution surface throughout the power application and temperature recording. Therefore, a support structure for the tissue was created. This prevents artefacts by environmental infrared (IR) radiation reflected on an aqueous surface during the thermal recording.

Fig. 5.1 portrays the experimental setup used for the laser and RF catheters. In both cases, the ablation catheter was inserted in the saline bath through a steerable sheath with a hemostasis valve. Before each ablation, the catheter was positioned perpendicular and centered against the tissue, promoting comparability between ablations. A contact force sensor was placed proximal to the hemostasis valve to set and maintain a contact force of 25±3g for laser and 20g±3g for RF catheters. The infrared camera was placed atop the exposed tissue surface, recording the transmural temperature.

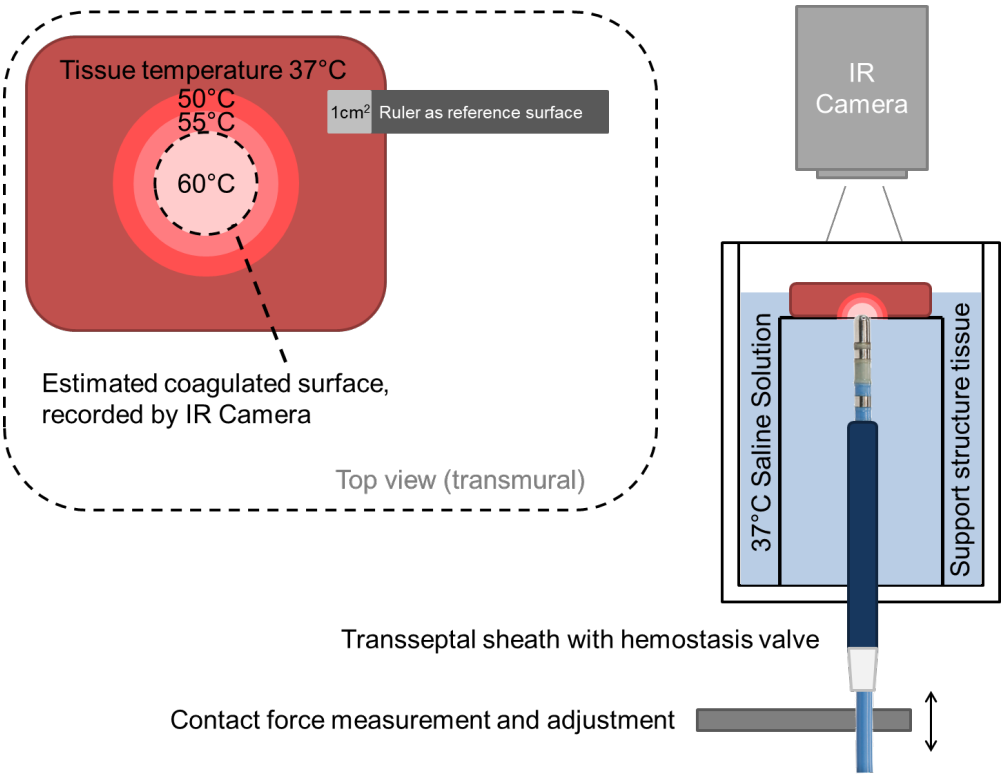

Fig. 5.1 *Schematic view of the experimental setup used to record the transmural tissue surface temperature during power application of laser and RF ablations.*

Laser and radiofrequency ablation

Laser ablations were conducted with an existing 8F, open irrigated, lasso-laser catheter with an active length of 50mm (Laser lasso catheter and Laser console of Vimecon GmbH, Herzogenrath, Germany) (Patents: US 2018/0021089, US 2011/0230941, US 2011/0230871). Catheter flushing was performed at room temperature with saline solution at a flow rate of 16mL/min. Via a fiber-coupled 976nm continuous-wave laser module (Module M1F-SS2.1, DILAS Diode Laser

GmbH, Mainz, Germany), laser energy was introduced in the catheter. The catheter was positioned against the tissue with the shaft perpendicular to the excised tissue. The helical structure of the lasso catheter was fully compressed against the tissue, achieving good contact over the entire length of the laser-active area, using a contact force of 25±3g.

Subsequently, laser energy was applied to the tissue at 20W/120s, 25W/90s, and 25W for 120s. An energy loss of 32.5% in the fiber-optical system translates into actual 13.5W and 18W being delivered to the tissue.

Radiofrequency ablations were conducted with a 7F, open-irrigated, 4 mm platinum or iridium tip catheter (EasyFlush catheter of MedFact Engineering GmbH, Lörrach, Germany). The catheter was connected to a monopolar RF generator (IBI-1500T Series Cardiac Ablation Generator of St. Jude Medical, Saint Paul, United States).

Room temperature saline solution was used as a flushing medium, with a flushing volume of 15 mL/min. The electrical circuit was completed by the placement of copper electrodes in the saline bath. The catheter was pushed to tissue with a contact force of 20g±3g in a perpendicular fashion with a steerable sheath. RF powers of 25W, 35W, and 40W for 30 and 60s were selected, emulating common clinical procedure conditions. [10, 14-20]

Infrared thermometry and optical imaging

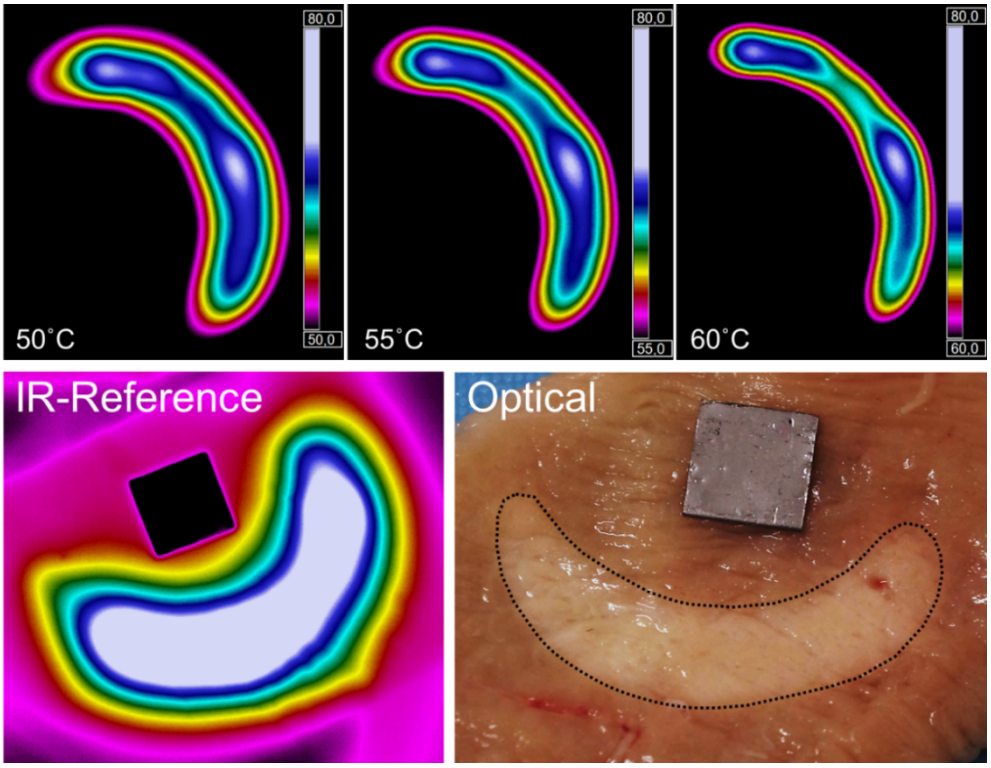

Fig. 5.2 *Recordings for the laser ablation catheter. Top: Infrared recordings (IR) of the transmural temperature, with a lethal isotherm set to 50°C, 55°C, and 60°C. Bottom left: Reference element was placed in the recording for surface estimation (black square). Bottom right: Optical recording of the reference cube and transmural coagulated area.*

The transmural tissue temperature was recorded with a thermal imaging camera (Model PI 640, Optris GmbH, Berlin, Germany). A resolution of 640x480 pixels was achieved for a spectral range of 7.5 to 13µm and a temperature range of 0°C to 250°C. Only the temperature of the tissue sample extending out of the saline

solution bath was captured. As a reference measure, a cooled square piece of stainless steel (108.68 mm^2) was placed in the thermal image at the end of the ablation (displayed as a black square in the reference image). Lastly, an image of the coagulated tissue was taken with an optical camera (Sony NEX-7, 24.3 MP, Sony corp., Japan). The same reference object was placed on the tissue.

Freely available software determined the coagulated area for the optical image and the infrared recordings (ImageJ Version 1.52, public domain). The size of the transmural coagulation area was the primary endpoint for both experiments regarding a lethal isotherm of 60°C to calculate the needed energy for a transmural lesion.

Additionally, an isotherm of 50°C and 55°C were considered. The thermal imaging software allowed the lower limit of the reference bar to be adjusted to the desired temperature cut-off (i.e., tissue with a temperature below the set temperature was displayed as black.)

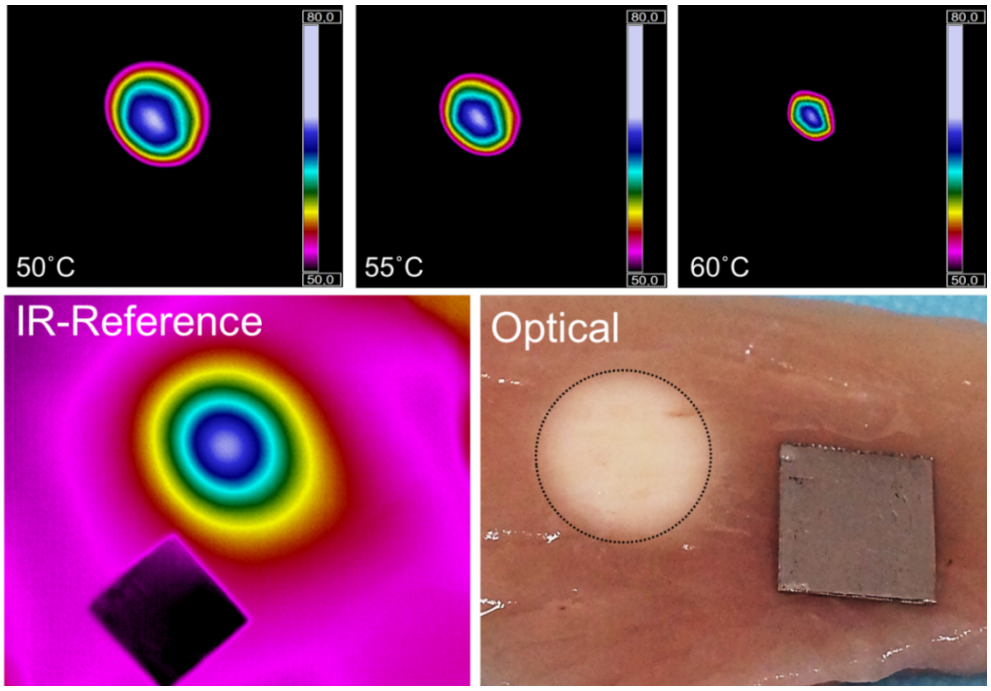

Fig. 5.3 *Recordings for the RF ablation catheter. Top: Infrared recordings (IR) of the transmural temperature, with a lethal isotherm set to 50°C, 55°C, and 60°C. Bottom left: Reference element was placed in the recording for surface estimation (black square). Bottom right: Optical recording of the reference cube and transmural coagulated area.*

Statistical analysis

The recordings of the transmural area were also used to estimate the lesion length using the image processing software. For RF catheters, this translates to lesion diameters, and for the laser-lasso catheter, the linear lesion length. The estimated lethal areas and lengths were transformed to energy per mm^2 and energy per mm to analyze the energy efficiency.

Subsequently, these values were normalized against the laser catheter results at 25W/120s, allowing an easier comparison between used power settings and energy sources.

A paired T-test was conducted comparing the area with temperature succeeding the lethal isotherm of 60°C, and the optically estimated coagulation area per energy source and power setting. A paired T-test compared the obtained lesion lengths. The significance cut-off was set at 5%.

By a one-way analysis of variance (ANOVA) with post-hoc Tukey test the obtained maximum transmural temperatures were compared. The power settings were divided into high- (laser energy > 1700J and RF energy > 1500) and low-energy groups (laser energy ≤ 1700J and RF energy ≤ 1500) to promote comparability.

Similarly, an ANOVA and post-hoc Tukey analysis compared the required energy per mm^2 between laser and RF energy with the same segregation between high and low energy.

Results

For each power settings per energy source, 16 ablations were recorded, resulting in 144 power applications. Some recordings with water partially covering the tissue surface were omitted since superficial fluids lead to artefacts in the IR recording. In total, 137 valid measurements were obtained, including 48 laser ablations and 89 RF ablations. The results for the estimated transmural areas and lengths are shown in **Tab. 5.1** and **Tab 5.2**.

Tab. 5.1 *The first five columns present the estimated areas with a temperature above the set isotherm about the used energy source and power settings. The second to last column shows the optically estimated area of the coagulated tissue, and the last column, the outcome of the paired t-test between the transmural area with a lethal isotherm of 60°C and the optically estimated coagulation area.*

Energy source	Power setting	Transmural Area > 50°C [mm²]	Transmural Area > 55°C [mm²]	Transmural Area > 60°C [mm²]	Transmural optical lesion [mm²]	Isotherm 60°C vs. Optical lesion
Laser	13.5W/120s	272±32.1	125±43.2	23,9±26.4	262±53.5	p < 0.001
Laser	18W/90s	293±55.3	155±50.1	40.3±37.1	270±58.3	p < 0.001
Laser	18W/120s	472±74.9	334±70.4	228±61.5	389±67.9	p < 0.001
RF	25W/30s	55.2±19.5	30.4±21.1	13.4±18,0	59.9±20.4	p < 0.001
RF	25W/60s	90.3±34.8	53.4±30.6	23.9±22.1	101.5±32.6	p < 0.001
RF	35W/30s	53.3±15.7	33.8±13.0	18.8±14.0	60.5±18.6	p < 0.001
RF	35W/60s	106.2±37.5	69.2±29.6	43.4±27.2	122.5±37.1	p < 0.001
RF	40W/30s	64.6±33.2	45.3±27.6	28.1±22.3	77.9±31.3	p < 0.001
RF	40W/60s	125.7±48.8	88.4±39.4	64.1±38.2	118.9±51.3	p < 0.001

Tab. 5.2 *The first five columns present the estimated lesion length with a temperature above the set isotherm about the used energy source and power settings. The second to last column shows the optically estimated lesion length of the coagulated tissue and the last column, the outcome of the paired t-test between the transmural length with a lethal isotherm of 60°C and the optically estimated coagulation length.*

Energy source	Power setting	Transmural Length > 50°C [mm]	Transmural Length > 55°C [mm]	Transmural Length > 60°C [mm]	Transmural length lesion [mm]	Length isotherm 60°C vs. Optical lesion
Laser	13.5W/120s	40.2±2.8	28.3±6.6	9.0±8.0	39.5±3.7	$p < 0.001$
Laser	18W/90s	43.7±2.3	33.1±6.7	14.4±10.2	40.7±4.4	$p < 0.001$
Laser	18W/120s	48.3±3.9	42.3±4.6	39.2±7.0	44.6±3.0	$p < 0.001$
RF	25W/30s	7.9±1.8	5.1±3.0	2.5±3.0	7.4±1.4	$p < 0.001$
RF	25W/60s	10.1±2.1	7.1±3.0	4.0±3.0	9.0±1.3	$p < 0.001$
RF	35W/30s	7.5±1.3	5.2±1.9	3.5±2.1	7.5±1.3	$p < 0.001$
RF	35W/60s	10.7±2.6	8.3±3.2	6.2±3.6	8.7±0.8	$p = 0.016$
RF	40W/30s	8.4±2.7	6.1±3.4	4.3±3.4	8.7±2.4	$p < 0.001$
RF	40W/60s	11.7±2.6	9.9±2.2	7.7±2.2	8.5±1.2	$p = 0.177$

The estimated transmural areas with a temperature above the lethal isotherm of 60°C are consistently significantly smaller than the optically established coagulation areas ($p < 0.001$ for all applications). The estimated lengths showed a similar outcome. However, at 40W/60s RF applications, no significant difference ($p = 0.177$) was found between the optical and the 60°C lethal isotherm group.

Tab. 5.3 lists the transmurally recorded maximum temperatures alongside the average tissue thickness and number of ablations regarding the energy source and power setting. The temperatures were compared by analyzing variance for the low and high energy groups.

In both groups, no significant difference was seen ($p = 0.408$ and $p = 0.703$). Since there was no significant difference between the means of any pair, the post-hoc Tukey analysis was not conducted. A difference between RF and laser applications was observed after cessation of the power application. Where the transmural temperature of laser energy applications instantly dropped after the cessation treatment, the highest RF temperature was recorded approximately 10s after cessation of the power application.

Tab. 5.3 *Overview of the number of ablations, the mean tissue thickness, and the recorded maximum temperature per power setting. The right section shows the analysis of variance between the low-energy maximum temperatures and the high-energy maximum temperatures.*

Energy source	Power setting	Number of Ablations	Tissue Thickness	Max. Temp. [°C]	ANOVA Outcome	Post-hoc Tukey Analysis
Laser	13.5W/120s	n = 16	3.5±0.4	66.9±11.6	Low energy applications p = 0.408	Not necessary
Laser	18W/90s	n = 16	3.5±0.2	61.8±2.4		
RF	25W/30s	n = 13*	3.6±0.3	63.0±11.5		
RF	25W/60s	n = 16	3.5±0.2	65.7±8.8		
RF	35W/30s	n = 16	3.6±0.3	65.7±8.0		
RF	40W/30s	n = 16	3.5±0.3	66.9±11.6		
Laser	18W/120s	n = 16	3.5±0.4	75.2±5.5	High energy applications p = 0.703	Not necessary
RF	35W/60s	n = 16	3.6±0.3	72.7±10.0		
RF	40W/60s	n = 16	3.6±0.2	74.5±9.8		

** Some recording with water partially covering the tissue surface were omitted since superficial fluids lead to artefacts in the IR recording.*

Tab. 5.4 portrays the transformed values for the needed energy per mm² to heat the transmural tissue surface above the set isotherm of the used energy source and power settings. Moreover, the needed energy per mm² is depicted concerning the optically assessed coagulation area.

Tab. 5.5 lists the needed energy per mm to heat the transmural tissue surface above the isotherm of the energy source and power settings. Furthermore, the needed energy per mm for the optically assessed lesion length is depicted.

Tab. 5.4 *The first five columns present the needed energy per mm² to heat the transmural tissue surface above the set isotherm of the used energy source and power settings. The last column shows the needed energy per mm² concerning the optically assessed coagulation area.*

Energy source	Power setting	Energy per mm² at 50°C [J/mm²]	Energy per mm² at 55°C [J/mm²]	Energy per mm² at 60°C [J/mm²]	Energy per mm² Optical [J/mm²]
Laser	13.5W/120s	5.96	12.96	67.78	6.18
Laser	18W/90s	5.53	10.45	40.20	6.00
Laser	18W/120s	4.58	6.47	9.47	5.55
RF	25W/30s	13.59	24.67	55.97	12.52
RF	25W/60s	16.61	28.09	62.76	14.78
RF	35W/30s	19.70	31.07	55.85	17.36
RF	35W/60s	19.77	30.35	48.39	17.14
RF	40W/30s	18.58	26.49	42.70	15.40
RF	40W/60s	19.09	27.15	37.44	20.19

Tab. 5.5 *The first five columns present the needed energy per mm to heat the transmural tissue surface above the set isotherm of the used energy source and power settings. The last column shows the needed energy per mm concerning the optically assessed lesion length.*

Energy source	Power setting	Energy per mm at 50°C [J/mm]	Energy per mm at 55°C [J/mm]	Energy per mm at 60°C [J/mm]	Energy per mm Optical [J/mm]
Laser	13.5W/120s	40.30	57.24	180.00	41.01
Laser	18W/90s	37.07	48.94	112.50	39.80
Laser	18W/120s	44.72	51.06	55.10	48.43
RF	25W/30s	94.94	147.06	300.00	101.35
RF	25W/60s	148.51	211.27	375.00	166.67
RF	35W/30s	140.37	201.92	302.59	140.75
RF	35W/60s	210.00	253.01	338.71	241.38
RF	40W/30s	142.86	196.72	279.07	137.93
RF	40W/60s	205.13	242.42	311.69	282.35

The energy per area and length calculations showed that tissue heating by direct irradiation is more efficient than heating by conduction, regardless of the set lethal isotherm or the selected power setting.

By analyzing the variance, divided into low and high-energy groups, the required energies to achieve a transmural area with a temperature above 60°C were compared in **Tab. 5.6**.

In the low-energy group, no significant difference was observed ($p = 0.100$). Therefore, the posthoc Tukey analysis was not conducted for the low-energy group. In the high-energy group, a significant difference was observed ($p < 0.001$). More detailed information was obtained by a posthoc Tukey analysis, showing a significantly lower J/mm^2-value for laser energy compared to RF ($p < 0.001$). No significant difference was observed between RF applications ($p = 0.154$).

Tab. 5.6 *Overview of the needed energy per mm² to obtain an area with a temperature above 60°C. An ANOVA test was performed with subsequent Tukey Analysis to assess the differences between the acquired means.*

Energy source	Power setting	Energy per mm² at 60°C [J/mm²]	ANOVA Outcome	Post-hoc Tukey Analysis
Laser	13.5W/120s	67.78±32.4	Low energy applications p = 0.100	Not necessary
Laser	18W/90s	40.20±23.7		
RF	25W/30s	55.97±19.3		
RF	25W/60s	62.76±40.3		
RF	35W/30s	55.85±37.3		
RF	40W/30s	42.70±24.8		
Laser	18W/120s	9.47±2.3	High energy applications p < 0.001	18W/120s (Laser) - 35W/60s (RF) p < 0.001
RF	35W/60s	48.39±22.0		18W/120s (Laser) - 40W/60s (RF) p < 0.001
RF	40W/60s	37.44±16.3		35W/60s (RF) - 40W/60s (RF) p = 0.154

Tab. 5.7 compared the needed energy per mm lesion length with a temperature surpassing the lethal isotherm of 60°C for RF and laser-induced coagulation, divided in low- and high-energy groups. In both groups significant differences were observed with $p < 0.001$. In the low-energy group, the results varied

between significantly lower energy per mm and no difference for the laser ablation compared to RF. In the high-energy group, the needed energy was significantly lower for the laser applications compared to RF ($p<0.001$).

Tab. 5.7 *Overview of the needed energy per mm lesion length with a temperature above 60°C. An ANOVA test was performed with subsequent Tukey Analysis to assess the differences between the acquired means.*

Energy source	Power setting	Energy per mm at 60°C [J/mm]	ANOVA Outcome	Post-hoc Tukey Analysis
Laser	13.5W/ 120s	180.00±114	Low energy applications $p < 0.001$	13,5W/120s(Laser) - 18W/90s(Laser) $p = 0.578$
Laser	18W/90s	112.50±50		18W/90s(Laser) - 25W/60s(RF) $p < 0.001$
RF	25W/30s	300.00±170		18W/90s(Laser) - 35W/30s(RF) $p < 0.001$
RF	25W/60s	375.00±112		18W/90s(Laser) - 40W/30s(RF) $p = 0.002$
RF	35W/30s	302.59±122		18W/90s(Laser) - 25W/30s(RF) $p < 0.001$
RF	40W/30s	279.07±114		13,5W/120s(Laser) - 25W/60s(RF) $p < 0.001$
				13,5W/120s(Laser) - 35W/30s(RF) $p = 0.043$
				13,5W/120s(Laser) - 40W/30s(RF) $p = 0.168$
				13,5W/120s(Laser) - 25W/30s(RF) $p = 0.066$
Laser	18W/120s	55.10±11	High energy applications $p < 0.001$	18W/120s(Laser) - 35W/60s(RF) $p < 0.001$
RF	35W/60s	338.71±131		18W/120s(Laser) - 40W/60s(RF) $p < 0.001$
RF	40W/60s	311.69±82		35W/60s(RF) - 40W/60s(RF) | $p = 0.689$

The required number of ablations to complete a box lesion with a perimeter of 115.7±22.3mm were calculated for each power setting and lethal isotherm as displayed in **Tab. 5.8**. An increase in power or application time consistently leads to decreased ablations to complete a box lesion.

Tab. 5.8 *Listing of the required number of applications to complete a box lesion with a perimeter of 115.7±22.3mm, for both energy sources and settings.*

Energy source	Power setting	Needed abl. 50°C	Needed abl. 55°C	Needed abl. 60°C	Needed abl. Optical
Laser	13.5W/120s	3±1	5±1	13±3	3±1
Laser	18W/90s	3±1	4±1	9±2	3±1
Laser	18W/120s	3±1	3±1	3±1	3±1
RF	25W/30s	15±3	23±5	47±9	16±4
RF	25W/60s	12±3	17±4	29±6	13±3
RF	35W/30s	16±3	23±5	34±7	16±3
RF	35W/60s	11±3	14±3	19±4	14±3
RF	40W/30s	14±3	19±4	27±6	14±3
RF	40W/60s	10±2	12±3	16±3	14±3

Discussion

This study has shown the difference in underlying biophysical principles of tissue coagulation between laser and radiofrequency ablation catheters. Although both rely on tissue heating to achieve tissue necrosis, RF primarily relies on

direct resistive heating of the superficial tissue layers. As electrical current passes through the tissue, the voltage drops, and heat is generated. Deeper tissue layers are only heated passively by heat conduction.[3] By increasing power levels, this resistive heating can reach in deeper tissue layers. Conversely, laser relies upon heating via direct irradiation, scattering, and subsequent absorption of light.[9]

This biophysical difference in heating principle was noticed by the divergent thermal latency[3] after power cessation. After cessation of the RF power application, the transmural tissue temperature continued to increase for at least 10 seconds. By contrast, this effect was not observed with laser energy.

Both observations suggest a strongly reduced presence of thermal latency in laser-energy applications. The main explanation for this difference was that laser applications reach the highest temperatures in the tissue (approximately 2mm) due to penetration and scattering of light in the tissue. This component is less pronounced in laser applications regarding the superficial heating of RF and resulting conductive heating.

Thermal analysis of RF applications showed large and unpredictable in ablation-areas (area with a temperature above 40˚C). In laser applications the affected area was smaller and more focused, related to the conductive heating component

[3] *Starting the RF energy delivery, a high superficial temperature is reached, falling off rapidly over a short distance. As time progresses, more thermal energy is transferred to deeper tissue layers by thermal conduction. Interruption of the RF power before achieving a steady state, leads to continued tissue temperature rise in deeper tissue as a result of thermal conduction from more superficial layers. This is termed thermal latency and has important clinical implications on ablation treatment, with beneficial or adverse effects, due to the continued temperature rise despite cessation of RF power.*

in tissue heating beyond the superficial layer, resulting in more radially directed heat transfer. Laser energy mainly heats the directly irradiated tissue (either by direct irradiation or by scattering) with a relatively minor border zone of conductive heating. This is reflected in the needed energy per mm^2 surface area and per mm lesion length if comparing laser and RF energy. RF used up to six times more energy to achieve the same coagulation. Direct irradiation advocates being a more effective approach than resistive superficial heating and following conductive heating into deep tissue layers. With less energy, a more focused and selective tissue heating was achieved.

Compared to the results obtained by Wood et al.,[8] aiming to estimate the lethal isotherm, a difference was observed between optically and IR-thermometry based estimation of the coagulation area. In the investigation of Wood, the optical zone corresponded with the area of a lethal isotherm of 60˚C. In this investigation, the optically estimated lesion size was between the surface areas estimated for 50˚C and 55˚C.

In general, protein denaturation and tissue discoloration start at lower temperatures. The lack of tissue perfusion in this *ex vivo* investigation could play a role in the observed difference. The perfusion would limit the effect of the conductive heating and reduce the optical lesion size.

Contrastingly, could these new results indicate that optically coagulated tissue is not always irreversible damaged? Underestimating the lethal myocardial temperature or overestimating the lesion size would lead to inadequate power delivery during clinical use.

Overall, the RF ablation results seem to be following the results obtained by Taghji[10] where the lesion contiguity was optimized by limiting the interlesion distance (ILD) to <6 mm and by implementing an ablation index for the posterior and anterior wall. It was found that an ablation protocol with reduced ILD and strict criteria for lesion depth resulted in high acute and short-term (1 year) success rates. On average, 28±5 ablations were needed to enclose a perimeter of 115.7 ± 22.3 mm, in pulmonary vein isolation. According to this investigation, between 16±3 (40W/60s) and 34±7 (35W/30s) ablations would be needed to realize a geometrically ideal box lesion, depending on the power and time setting.

Limitations

The use of an *ex vivo* tissue model and setup facilitated perpendicular catheter tissue contact accommodates a near-ideal energy transfer and heat dispersion in the tissue for both energy sources. This will not always be the case for *in vivo* studies with the ventricular or atrial wall's perfused cardiac tissue and motion. The perfusion of the tissue also affects the parameters of heat conduction and absorption. Though the *in vivo* investigations of Chapter 3 have shown a strong correlation between *ex vivo* and in *vivo* applications.

Imperfect registration between the optical and thermal images is a potential source of error. The use of a reference surface, a high-resolution IR camera, and subsequent analysis of the recordings with image processing software minimizes the potential for image registration errors.

Conclusion

Analysis of the lesion formation process has shown a difference in underlying biophysical principles of tissue coagulation between laser and radiofrequency ablation catheters. Comparing applied energy and estimated transmural area with a temperature surpassing the lethal isotherm showed that laser energy heats the tissue more focused. The tissue is heated more efficiently than RF due to a lower share of the conductive heating component.

Interestingly the observed optical coagulation area was consistently larger than the estimated area with a temperature above the lethal isotherm. Nonetheless, the commonly applied interlesion distance values of ≤6 mm for point-by-point RF ablations aligned with the outcome of this investigation, applying a lethal isotherm of 60.6°C.

References

[1] Joseph JP, Rajappan K. Radiofrequency ablation of cardiac arrhythmias: past, present and future. QJM. 2012 Apr;105(4):303-14. doi: 10.1093/qjmed/hcr189.

[2] Huang S and Miller J. Catheter ablation of cardiac arrhythmias. Chapter 5 - Alternative Energy Sources and Ablative Techniques: Ultrasound, Laser, and Microwave—Biophysics and Applications. Elsevier 2014. ISBN-13: 978-0323244299

[3] David E. Haines. Book: Catheter Ablation of Cardiac Arrhythmias 2006, Chapter 1 - Biophysics of Radiofrequency Lesion Formation, Pages 3-21. Paperback ISBN: 9781416003120

[4] Raulin C and Karsai S (eds.), Book: Laser and IPL Technology in Dermatology and Aesthetic Medicine 2011. Chapter 2 - Laser-Tissue Interactions (Rudolf Steiner). DOI: 10.1007/978-3-642-03438-1_2, © Springer-Verlag Berlin Heidelberg

[5] Whayne JG, Nath S, Haines DE. Microwave catheter ablation of myocardium ex vivo. Assessment of the characteristics of tissue heating and injury. Circulation. 1994 May;89(5):2390-5. doi: 10.1161/01.cir.89.5.2390.

[6] Nath S, Lynch C 3rd, Whayne JG, Haines DE. Cellular electrophysiological effects of hyperthermia on isolated guinea pig papillary muscle. Implications for catheter ablation. Circulation. 1993 Oct;88(4 Pt 1):1826-31. doi: 10.1161/01.cir.88.4.1826.

[7] Haines DE, Watson DD. Tissue heating during radiofrequency catheter ablation: a thermodynamic model and observations in isolated perfused and superfused canine right ventricular free wall. Pacing Clin Electrophysiol. 1989 Jun;12(6):962-76. doi: 10.1111/j.1540-8159.1989.tb05034.x.

[8] ood M, Goldberg S, Lau M, Goel A, Alexander D, Han F, Feinstein S. Direct measurement of the lethal isotherm for radiofrequency ablation of myocardial tissue. Circ Arrhythm Electrophysiol. 2011 Jun;4(3):373-8. doi: 10.1161/CIRCEP.110.961169.

[9] Jürgen Eichler and Theo Seiler. Book: Lasertechnik in der Medizin. Springer 1991. https://doi.org/10.1007/978-3-662-08272-0

[10] Taghji P, El Haddad M, Phlips T, Wolf M, Knecht S et. al. Evaluation of a Strategy Aiming to Enclose the Pulmonary Veins With Contiguous and Optimized Radiofrequency Lesions in Paroxysmal Atrial Fibrillation: A Pilot Study. JACC Clin Electrophysiol. 2018 Jan;4(1):99-108. doi: 10.1016/j.jacep.2017.06.023.

[11] Phlips T, Taghji P, El Haddad M, Wolf M, Knecht S et. al. Improving procedural and one-year outcome after contact force-guided pulmonary vein isolation: the role of interlesion distance, ablation index, and contact force variability in the 'CLOSE'-protocol. Europace. 2018 Nov 1;20(FI_3):f419-f427. doi: 10.1093/europace/eux376.

[12] Kobayashi S, Fukaya H, Oikawa J, Saito D, Sato T et. al. Optimal interlesion distance in ablation index-guided pulmonary vein isolation for atrial fibrillation. J Interv Card Electrophysiol. 2020 Sep 25. doi: 10.1007/s10840-020-00881-0.

[13] Tan HW, Wang XH, Shi HF, Zhou L, Gu JN, Liu X. Left atrial wall thickness: anatomic aspects relevant to catheter ablation of atrial fibrillation. Chin Med J (Engl). 2012 Jan;125(1):12-5.

[14] Guler TE, Aksu T, Yalin K, Golcuk SE, Mutluer FO, Bozyel S. Combined Cryoballoon and Radiofrequency Ablation Versus Radiofrequency Ablation Alone for Long-Standing Persistent Atrial Fibrillation. Am J Med Sci. 2017 Dec;354(6):586-596. doi: 10.1016/j.amjms.2017.08.010.

[15] Laish-Farkash A, Suleiman M. Comparison of the Efficacy of PVAC® and nMARQ™ for paroxysmal atrial fibrillation. J Atr Fibrillation. 2017 Apr 30;9(6):1550. doi: 10.4022/jafib.1550.

[16] Schmidt B, Neuzil P, Luik A, Osca Asensi J, Schrickel JW et. al. Laser Balloon or Wide-Area Circumferential Irrigated Radiofrequency Ablation for Persistent Atrial Fibrillation: A Multicenter Prospective Randomized Study. Circ Arrhythm Electrophysiol. 2017 Dec;10(12):e005767. doi: 10.1161/CIRCEP.117.005767.

[17] Winkle RA, Moskovitz R, Hardwin Mead R, Engel G, Kong MH et. al. Atrial fibrillation ablation using very short duration 50 W ablations and contact force sensing catheters. J Interv Card Electrophysiol. 2018 Jun;52(1):1-8. doi: 10.1007/s10840-018-0322-6.

[18] Reddy VY, Dukkipati SR, Neuzil P, Natale A, Albenque JP et. al. Randomized, Controlled Trial of the Safety and Effectiveness of a Contact Force-Sensing Irrigated Catheter for Ablation of Paroxysmal Atrial Fibrillation: Results of the TactiCath Contact Force Ablation Catheter Study for Atrial Fibrillation (TOCCASTAR) Study. Circulation. 2015 Sep 8;132(10):907-15. doi: 10.1161/CIRCULATIONAHA.114.014092.

[19] Hamaya R, Miyazaki S, Kajiyama T, Watanabe T, Kusa S et. al. Efficacy and safety comparison between different types of novel design enhanced open-irrigated ablation catheters in creating cavo-tricuspid isthmus block. J Cardiol. 2018 May;71(5):513-516. doi: 10.1016/j.jjcc.2017.10.015.

[20] Ücer E, Janeczko Y, Seegers J, Fredersdorf S, Friemel S et. al. A RAndomized Trial to compare the acute reconnection after pulmonary vein ISolation with Laser-BalloON versus radiofrequency Ablation: RATISBONA trial. J Cardiovasc Electrophysiol. 2018 May;29(5):733-739. doi: 10.1111/jce.13465.

6 Feasibility assessment of catheter-based diffuse reflectance spectroscopy for detection of thermal tissue damage

Dennis Krist, Ulrich Schotten, Stef Zeemering, Dominik Linz

Abstract

Purpose: This feasibility study investigates the visualization of laser-induced thermal tissue damage by diffuse reflectance spectroscopy.

Methods: A linear laser ablation catheter was used to induce thermal tissue damage in non-perfused bovine tissue. An added modified optical fiber was integrated in the catheter design to capture the diffuse reflectance spectrum, illuminated by the already integrated emitting fiber. The *in situ* recorded spectra prior and after ablation were analyzed to discriminate between treated and untreated tissue. A direct comparison between both data sets was made after the recorded distributions were brought into alignment by normalization in the wavelength range of 600-750nm. Comparably, this process was applied to differentiate between treated, partially treated, and untreated tissue. Recordings of the partial lesions were created by repositioning the catheter after the ablation for spectrum collection.

Results: In total, 90 reflectance spectra were recorded, resulting in 127,980 data points. Spectra for fully treated and untreated tissue were compared, showing a significant drop of the normalized response value (Mean difference (MD)=0.415) in the wavelength range of 600-750nm ($p<0.001$). The same experiment was repeated to assess the lesion formation of semi lesion-formed lesions (MD=0.130, $p<0.001$), quarter lesions (MD=0.288, $p<0.001$), and orthogonal lesions (MD=0.080, $p>0.061$).

Conclusion: Diffuse reflectance spectroscopy is a promising lesion visualization tool for cardiac arrhythmia ablation. A clear distinction could be made between treated and untreated tissue with *in situ* spectroscopic analysis. Whether the

addition of a second optical fiber to a linear laser ablation catheter can assess lesion formation by reflectance spectroscopy warrants further investigations.

Introduction

Despite significant advances in ablation catheter technologies, the success rates of catheter ablation can still be improved. Intraprocedural visualization of the catheter's surroundings could improve ablation outcome due to enhanced catheter guidance and assessment of lesion formation. Wall contact and lesion formation can be confirmed directly. Direct visualization would be integral in creating linear lesions with a laser ablation catheter since wall contact is indispensable to achieve thermal tissue coagulation.

Most commonly indirect means of lesion visualization are used to visualize lesions, based on local electrogram (EGM) data, lesion prediction algorithms, [5-8, 12] or more elaborated methods as dynamic contrast-enhanced (DynCE) MRI. [9,10] Only a laser balloon catheter with integrated endoscope is able to visualize the lesion directly. Since the laser ablation catheter already has an optical fiber, reflectance spectroscopy is the clearest option to achieve direct visualization of wall contact and lesion formation for this catheter type.

Spectroscopy analyzes the interaction between chemical structures and electromagnetic radiation. It is commonly used to analyze matter in chemistry, biology, and medical engineering.

In this case, diffuse reflectance spectroscopy is applied to assess wall contact and confirm tissue coagulation. Therefore, a spectrometer is connected to the catheter to measure and records the reflected intensity per wavelength of the subject

under investigation. This spectroscopic application allows the possibility to differentiate and study the chemical structures and tissue compositions by their characteristic absorption. [18] To a certain extent, the incident light is absorbed by both endo- and exogenous chromophores and scattered by cells, organelles, and fibers.

First investigations concerning the changes of the optical property of slowly heated myocardium were conducted in the early nineties. [1] An increase of light absorption at a wavelength of 632,8nm was found at temperatures above 45°C and even stronger increase above 55°C. Subsequent studies [13,14] noticed the discoloration of a trial tissue upon ablation treatment by radiofrequency in the recorded spectrum. These effects were later also shown for laser ablation catheters [15-17] with *in vivo* studies.

This discoloration of the cardiac tissue has been used to assess the lesion formation process through optical spectroscopy and radiofrequency catheter ablation. [2-4, 11] Transmitting and receiving optical fibers were added to the tip electrode for RF catheters.

To realize this spectroscopy-based monitoring system for the linear laser ablation catheter two fibers were integrated in the laser active area. One to homogeneously coagulate or illuminate the tissue over the entire length of the active area and one to collect the reflected light.

This feasibility study aims to investigate the visualization of thermocoagulated tissue by diffuse reflectance spectroscopy in a linear laser ablation catheter.

Materials and Methods

Tissue preparation and laser catheter

Non-perfused porcine cardiac tissue was selected for the *ex vivo* feasibility study, given the similar cardiac structure and tissue color. The tissue was placed in a heated saline solution bath (0,9% NaCl solution in distilled water) to maintain a temperature of 37°C. For the laser-induced tissue coagulation, an 8F, open irrigated, straight catheter with active ablation length of 50mm was used (50mm linear laser ablation catheter and laser console of Vimecon GmbH, Herzogenrath, Germany)(Patents: US 2018/0021089, US 2011/0230941, US 2011/0230871) combined with a fiber-coupled 976nm continuous wave-laser diode (Module M1F-SS2.1, DILAS Diode Laser GmbH, Mainz, Germany). **Fig. 6.1** shows the laser-lasso catheter, the laser source, and a microscopic capture of a modified optical fiber.

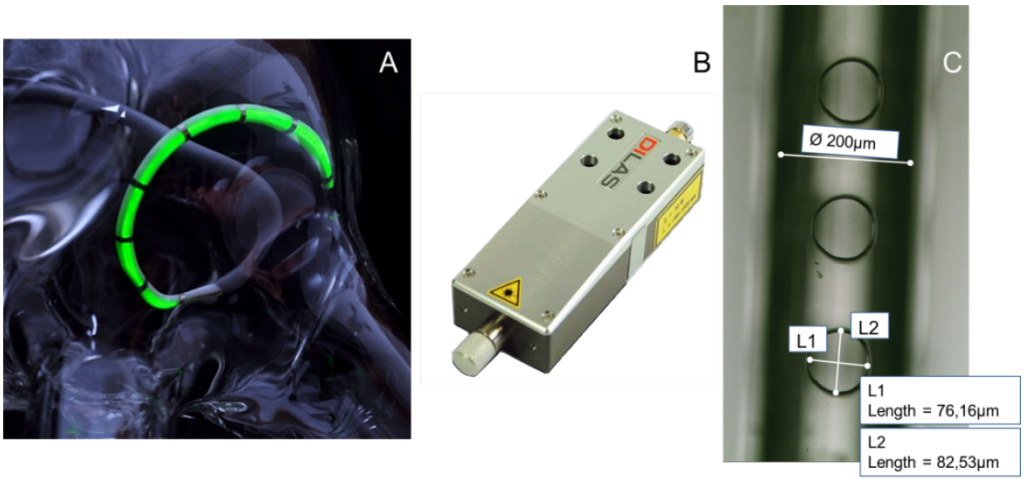

Fig. 6.1 *A: The laser ablation catheter is shown. For visualization purposes only, a green laser is used to visualize the laser-active area. B: The Dilas laser module M1F-SS2.1 as used in the experimental setup is shown. C: Enhanced view of the modified optical fiber.*

For the spectroscopic analysis, a second identically 200µm modified[4] fiber was integrated into the catheter, dedicating one fiber as illuminating fiber and the other as collecting fiber.

Fig. 6.2 shows the design used to record the spectroscopic data. A double V-shaped[5] profile was used, each holding a modified fiber. The illuminating fiber was used to apply the therapeutic dose (laser) to the ablation site and for

[4] *Modified fiber is a fiber modified so that lateral emission of laser light is possible over a length of 50mm, with a homogeneous emission distribution. The modification entails a single-sided partial removal of the fiber's cladding, uncovering the fiber core.*

[5] *The V-Shaped profile serves as a support frame for the optical fiber (embedded with resin) and to effectuate unilateral laser emission.*

consecutive illumination with a halogen light source. The second fiber was solely used as collecting fiber to record the diffuse reflectance spectrum.

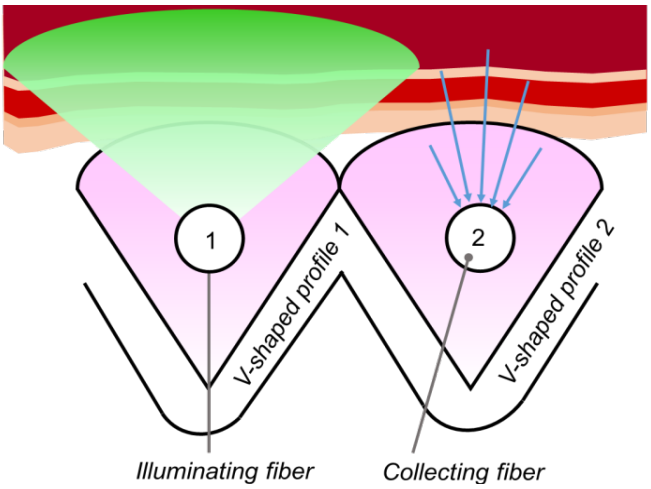

Fig. 6.2 *Schematic visualization of the used catheter design. Two modified fibers are embedded in two separate profiles, the illuminating fiber marked with 1 and the collecting fiber with 2.*

Diffuse Reflectance Spectroscopy setup

A spectrometer (AvaSpec-ULS2048L-EVO, Avantes BV, Apeldoorn, Netherlands) with a 200-1100nm wavelength range was coupled with the collecting fiber. A resolution of 0,06-20nm was achieved, depending on the device configuration. The sensitivity of the device was 470000 counts/microwatt per ms integration time.

The halogen light source (AvaLight-HAL-S-Mini, Avantes BV, Apeldoorn, Netherlands) was coupled with the 200µm illuminating fiber. The light source covered

a wavelength range of 360-2500nm with an intensity of 0.35mW for a 200 fiber μm. The measurements were analyzed with the software provided by Avantes (AvaSoft 8.8.0.0).

Protocol

The tissue was placed in a heated saline bath to maintain the tissue temperature during the laser ablation and following diffuse reflectance spectroscopy. For the entire duration of the power application and subsequent spectroscopy, the laser-active area of the catheter was pressed against the tissue. The spectra were always recorded in dark surroundings to minimize environmental noise. The power settings were set at 25W for 120s.

The spectrum of the untreated tissue was continually recorded before the power application, while the spectrum of the treated tissue was recorded directly after power application. The diffuse reflectance spectra of semi (50% of total lesion length), quarter (25% of total lesion length), and orthogonal (8% of total lesion length) lesions were similarly recorded directly after ablation by catheter repositioning; as displayed in **Fig. 6.3**.

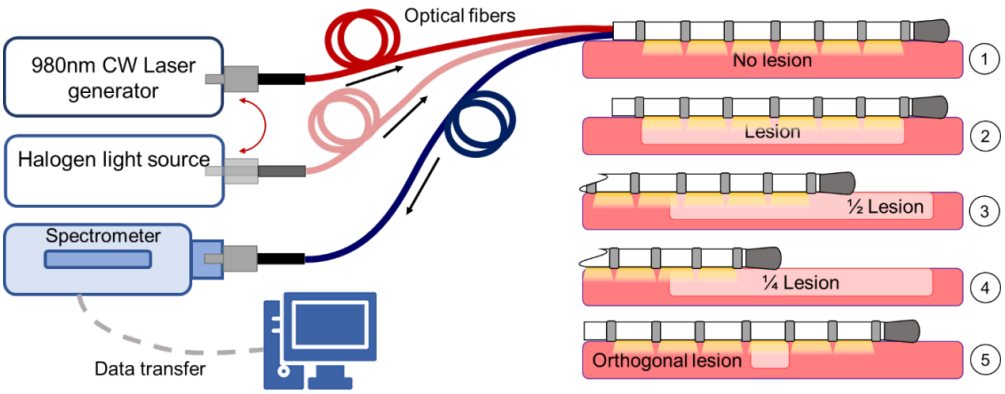

Fig. 6.3 *Schematic experimental setup to 'visualize' the coagulated tissue. Step 1 displays the measurement of the 'no lesion' reflectance data, step 2 -5 display the measurement of the reflectance data of (partially) treated tissue.*

Data analysis

To combine and compare all captured spectra, the distributions of the recorded values were aligned by normalization[6] to promote comparability. Subsequently, the normalized values of the wavelength range 600-750nm were averaged (i.e., each measurement results in a single normalized average), leading to the mean value per group (untreated, full lesion, half lesion, and quarter lesion). Differences in mean reflectance were tested with a paired two-tailed t-test using a significance level of 0.05 (H_0= no statistically significant difference between the compared groups). Where multiple comparisons were made in the same data set, a Bonferroni correction was applied to obtain an adjusted significance cut-off.

[6] *Normalization is conducted according to the following scheme: 1 – Recording of the reflected spectrum; 2 – export of data to PC; 3 – Normalize each spectrum against min/max values according to the function* $f(x)_{norm}=(f(x)-f_{min})/f_{max}-f_{min})$*; 4 – Calculate the average and standard deviation per group.*

Results

Similar tissue discoloration as observed in the past studies [13-17] was reproduced by laser ablation of non-perfused bovine tissue. In total, 90 spectra were recorded, obtaining 127,980 data points.

Fig. 6.4 plots the recorded spectra of treated and untreated tissue over the entire length of the laser-active area. The untreated tissue is marked as 'no lesion' and the treated tissue as 'lesion.' For this group, 20 spectra were recorded, of which 10 prior to the ablation and 10 immediately after.

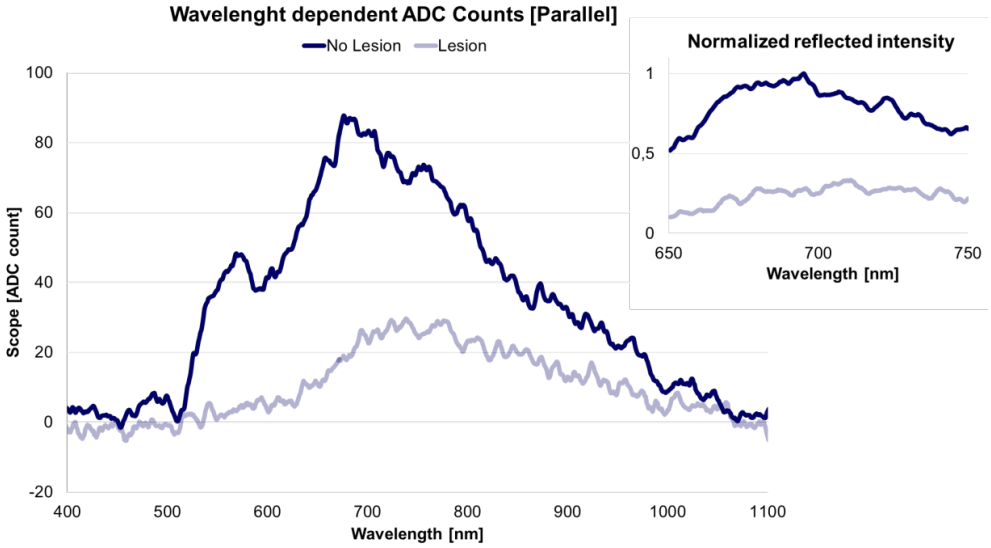

Fig. 6.4 *Recorded spectra prior, and after ablation. A clear distinction can be made between treated (light blue) and untreated tissue (dark blue). The lesion graph demonstrates reduced reflection intensity in the wavelength range of 500 to 1000nm. The normalized graph in the top right corner shows a detailed comparison in the wavelength range of 650 to 750nm.*

A clear distinction could be made between treated and untreated tissue by comparison of the recorded spectrum just before ablation and immediately after ablation..

The recorded spectra were normalized and compared before and after ablation for the wavelength ranges of 500 to 800nm and 650 to 750nm to perform statistical analysis. **Tab. 6.1** lists the mean difference (MD) and standard error (SE) of the treated and untreated tissue and the corresponding estimated p-values for each range. In the range 650 to 750nm, an MD of 0.4155 with a SE of 0.0344 was obtained. In the range 500 to 800nm, an MD of 0.1963 with a SE of 0.0288 was obtained. The mean difference between treated and untreated tissue is significantly different for each wavelength range with p-values < 0.001.

Tab. 6.1 *This table lists the results and statistical outcome of the recorded normalized reflectance spectra for the wavelength ranges 650 to 750nm and 500 to 800nm. The MD and SE between the treated and untreated tissue are subjected to a paired t-test.*

Wavelength range	Sample size	Mean Difference	Standard Error	p-value
650 to 750 nm	n=10	0.4155	0.0344	<0.001
500 to 800 nm	n=10	0.1963	0.0288	<0.001

Fig. 6.5 plots the results for the second group, comparing the recorded spectra of untreated tissue, quarter lesions, semi lesion, and full lesions. In total, 40 spectra were recorded, ten just before the ablation, ten immediately after the ablation, ten of a semi lesion and ten of a quarter lesion. A distinction could also be

made between the recorded spectra of the full, semi, quarter and no lesion recordings. The recorded spectra of semi and quarter lesions were consistently located between the response of the treated and untreated tissue. The difference between the recorded spectra was best noticeable in the wavelength range of 650 to 750nm.

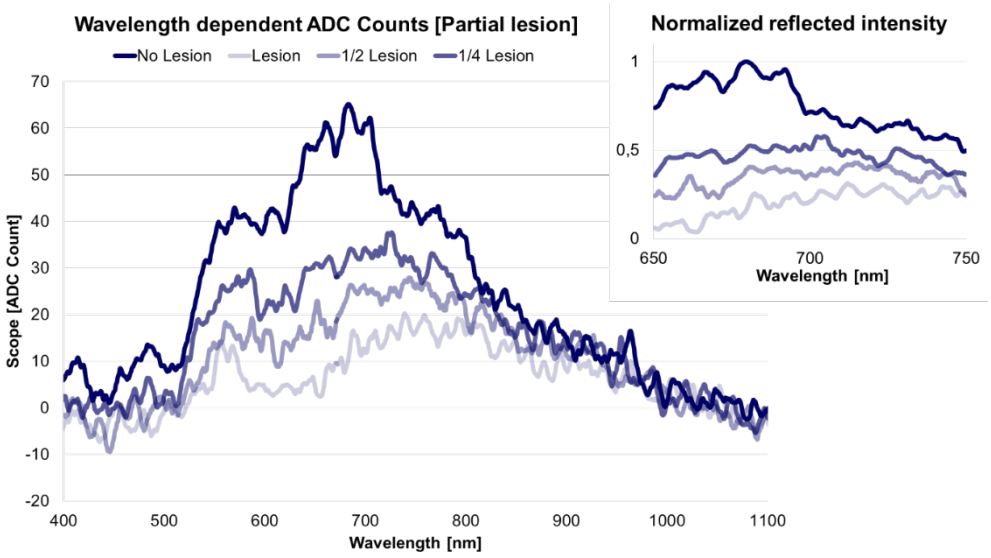

Fig. 6.5 *Recorded spectra prior and after ablation. Besides the difference between treated (light blue), and untreated (dark blue), a difference with the partial lesion could also be observed (middle blue tones) in the wavelength range 500 to 800nm. The reduction is clearly visible in the normalized plot in the top right corner.*

Tab. 6.2 displays the MD, SE, and statistical outcome of the recorded normalized reflectance spectra, comparing the partial lesions with the treated and untreated tissue. The calculated mean differences and corresponding t-test results confirm the observed differences in the graph. Since multiple comparisons were made

with the same data, a Bonferroni correction was applied to adjust the significance cut-off, resulting in a critical value of 0.01 instead of 0.05. The t-tests between the groups result in p-values < 0.01, showing a statistically significant difference.

Tab. 6.2 *Lists the calculated MD and SD of the treated and untreated tissue and the partial lesions. The corresponding p-values per comparison group in the wavelength range of 650 to 750nm are estimated via a paired t-test with a corrected significance cut-off of 0.01.*

Groups compared	Sample size	Mean Difference	Standard Error	p-value
Semi vs. Full Lesion	n=10	0.1305	0.0329	0.00326
Quarter vs. Full Lesion	n=10	0.2883	0.0078	<0.001
Semi Lesion vs. Untreated	n=10	0.4589	0.0292	<0.001
Quarter Lesion vs. Untreated	n=10	0.2611	0.0121	<0.001
Quarter vs. Semi Lesion	n=10	0.1578	0.0275	<0.001

Fig. 6.6 plots the third group results, comparing the recorded spectra of untreated tissue, orthogonal, and full lesions. In total, 30 additional spectra were retrieved for the orthogonal placement of the catheter, ten just before the ablation, ten immediately after the ablation, and ten of an orthogonal lesion.

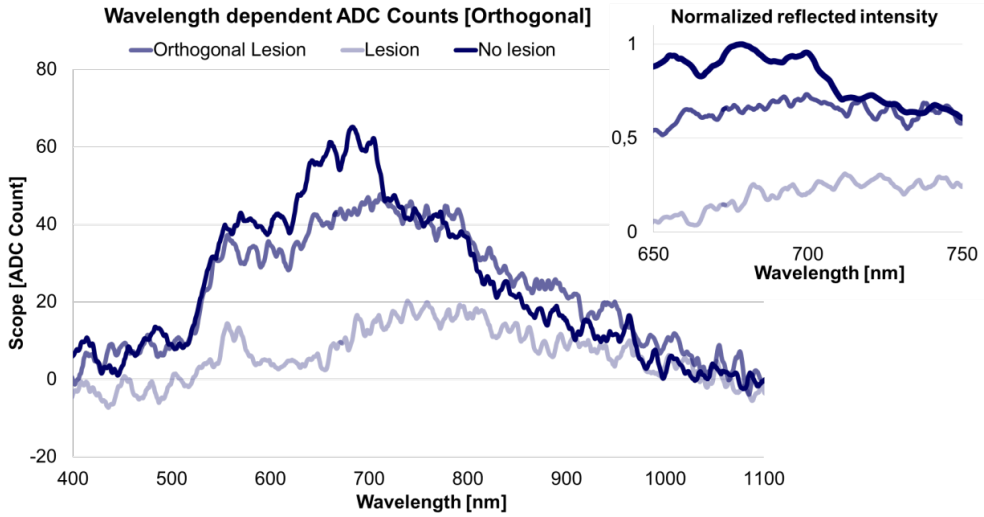

Fig. 6.6 *The graph represents one of the spectra as recorded. In this case, a minor reduction can be observed in the wavelength range of 600 to 700nm but not as evident as in other configurations. The reduction is clearly visible in the normalized plot in the top right corner.*

The plotted graph shows an unclear difference between the untreated tissue and the orthogonal lesion. In all measurements, the difference was small, though the spectra had a slightly flatter profile. This observation is reflected in the statistical analysis, depicted in **Tab. 6.3**. A Bonferroni correction was also applied to adjust the significance cut-off, reducing the critical value to 0.025

In both wavelength ranges, the differences are insignificant, with p=0.0608 (650 to 750nm) and p=0.4006 (500 to 800nm).

Tab. 6.3 *lists the results and statistical outcome of the recorded normalized reflectance spectra for the wavelength ranges 650 to 750nm and 500 to 800nm. The MD*

and SE between the orthogonal lesions and untreated tissue are subjected to a paired t-test.

Wavelength range [nm]	Sample size	Mean Difference	Standard Error	p-value
650 to 750	n=10	0.0799	0.0373	0.0608
500 to 800	n=10	0.0249	0.0282	0.4006

Discussion

The experiments showed that integration of a second modified optical fiber allowed diffuse reflectance spectroscopy of the investigated tissue. A significant difference between the reflected spectra of the partially treated, fully treated, and untreated tissue was observed. If the treated tissue only represented 8% of the reflected spectrum (i.e., orthogonal to the lesion), no significant difference could be observed between treated and untreated tissue.

The recordings demonstrated the clinical relevance of diffuse reflectance spectroscopy, providing valuable information about thermal tissue damage (i.e., lesion formation). The technology is easily integrated into a laser ablation catheter.

An ADC count drop in the recorded spectra allowed discrimination between treated and untreated tissue. The ADC count drop relates to the observed paleness of treated tissue. As Pickering [1] has shown, pale tissue possesses reduced reflective properties in the visible spectrum and increased scatter. Due to the tissue's low density of reflective components in the 400 to 550nm wavelength range, no ADC count drop was observed in this range. Consequently, both treated and untreated tissue equally absorb or scatter the light, as observed.

The ability to discriminate between full, half, and a quarter lesions provides a great clinical benefit. With an empirically constructed baseline, a clear distinction can be made between (partially) treated and untreated tissue. This information allows the physician to assess if the lesion is fully or only partially created.

Similarly, gaps in linear lesion schemes can be detected, potentially increasing the treatment efficacy and reducing the recurrence rate. Lesions formed below 25% of the total catheter length will be hard to distinguish, as depicted by the reflectance spectrum of the orthogonal lesion. In this case, the untreated component of the reflected spectrum is too dominant, preventing the detection of small, treated areas. The detection sensitivity can be increased by integrating multiple collecting fibers in series.

As Rajinder P. Singh-Moon [3] already showed in his experiments, where he combined a radiofrequency ablation catheter with an integrated near-infrared spectroscopy system, it is also possible to assess wall contact and measure the transmurality of the lesion. Especially for laser ablation, it is crucial to obtain good wall contact to ensure full lesion formation. The spectroscopic analysis could provide the necessary confirmation of wall contact.

Studies by Demos and Sharareh[4] suggested that detection of thrombus formation and carbonization of the endocardium can be detected by diffuse reflectance spectroscopy. Not only would this increase the safety of standard ablation procedures, but it would be extremely helpful for the treatment of trabeculated surfaces or morphology with pouch-like recesses. [19 – 21]. These two features need to be confirmed for the linear ablation catheter, with integrated modified optical

fiber for reflectance spectroscopy. Moreover, in future investigations, the sensitivity and specificity of the lesion recognition are to be assessed.

Limitations

Changes in reflective properties of tissue measured *ex vivo* may not wholly represent the expected *in vivo* reflective changes. The perfusion affects the color of the untreated and treated tissue. Additionally, the laser tissue interaction and the lesion characteristics may slightly differ from *in vivo* conditions. The lesion width is reduced, due to the convective cooling effect of the blood flow. The influence of cardiac contractions during the ablation and spectrum recording can also not be assessed in *ex vivo* conditions.

Due to the small sample size, more data is required to further substantiate the study results and to provide a good baseline as reference for implementation in a clinical setting.

Conclusion

Diffuse reflectance spectroscopy is a promising lesion visualization tool for cardiac arrhythmia ablation. By *in situ* spectroscopic analysis, a clear distinction could be made between treated and untreated tissue. Whether the addition of a second optical fiber to a linear laser ablation catheter can be used to assess lesion formation by reflectance spectroscopy in a clinical setting warrants further investigation.

References

[1] Linte CA, Camp JJ, Rettmann ME, Haemmerich D, Aktas MK et. al. echnical Note: On Cardiac Ablation Lesion Visualization for Image-guided Therapy Monitoring. Proc SPIE Int Soc Opt Eng. 2018 Feb;10576:105760N. doi: 10.1117/12.2322523.

[2] Havranek S, Alfredova H, Fingrova Z, Souckova L, and Wichterle D. Early and Delayed Alteration of Atrial Electrograms Around Single Radiofrequency Ablation Lesion. Front Cardiovasc Med. 2018; 5: 190

[3] Malik R, Malik B, Hunter TD. Touch-up and recurrence rates after voltage mapping for verification of pulmonary vein isolation following cryoablation of paroxysmal atrial fibrillation. J Interv Card Electrophysiol. 2019; 56(3): 307-312

[4] Rottner L, Bellmann B, Lin T, Reissmann B, Tönnis T et. al. Catheter Ablation of Atrial Fibrillation: State of the Art and Future Perspectives. Cardiol Ther 2020 Jun;9(1):45-58. doi: 10.1007/s40119-019-00158-2.

[5] Wood MA. Exposing gaps in linear radiofrequency lesions: form before function. Circ Arrhythm Electrophysiol 2011; 4(3): 257–259

[6] Shmatukha, A., Sundaram, B., Qi, X. Oduneye S, Stainsby J et al. Visualization of ablation lesions by dynamic contrast-enhanced (DynCE) MRI. J Cardiovasc Magn Reson 12, O25 (2010). https://doi.org/10.1186/1532-429X-12-S1-O25

[7] Grant EK, Berul CI, Cross RR, Moak JP, Hamann KS et.al. Acute Cardiac MRI Assessment of Radiofrequency Ablation Lesions for Pediatric Ventricular Arrhythmia: Feasibility and Clinical Correlation. J Cardiovasc Electrophysiol. 2017 May;28(5):517-522. doi: 10.1111/jce.13197.

[8] Häggblad E. In Vivo Diffuce Reflectance Spectroscopy of Human Tissue. ISBN 978-91-7393-809-9, Linköping Studies in Science and Technology. Dissertations, No. 1210

[9] Pickering JW, Bosman S, Posthumus P, Blokland P, Beek JF and van Gemert MJ. Changes in the optical properties (at 632.8 nm) of slowly heated myocardium. Applied Optics 1993; 32(4): 367-71

[10] Ahmed H, Neuzil P, Skoda J, Petru J, Sediva L, Kralovec S, Reddy VY. Initial clinical experience with a novel visualization and virtual electrode radiofrequency ablation catheter to treat atrial flutter. Heart Rhythm 2011; 8(3): 361–367

[11] William C. Stoffregen, Serge D. Rousselle, Marian K. Rippy. Pathology Approaches to Determine Safety and Efficacy of Cardiac Ablation Catheters. Toxicologic Pathology 2019; 47(3): 311-328

[12] Reddy VY, Neuzil P, Themistoclakis S, Danik SB, Bonso A et. al. Visually-Guided Balloon Catheter Ablation of Atrial Fibrillation. Experimental Feasability and First-in-Human Multicenter Clinical Outcome. Circulation 2019; 120: 12-20

[13] Sagerer-Gerhardt M, Weber HP. Open-irrigated laser catheter ablation: influence of catheter-tissue contact force on lesion formation. J Interv Card Electrophysiol. 2015 Mar;42(2):77-81. doi: 10.1007/s10840-015-9977-4.

[14] Sagerer-Gerhardt M , Weber H. Influence of catheter orientation on lesion formation in bovine myocardium by using an open-irrigated laser ablation catheter. Lasers Med Sci 2016; 31: 1333-1338

[15] Moon RP and Hendon CP. Cardiac tissue characterization using near-infrared spectroscopy. Proc. SPIE 8926, Photonic Therapeutics and Diagnostics X, 89263N; 2014

[16] Moon RP, Marboe CC, and Hendon CP. Near-infrared spectroscopy integrated catheter for characterization of myocardial tissues: preliminary

demonstrations to radiofrequency ablation therapy for atrial fibrillation. Biomedical optic express 2015; 6(7): 2494-511

[17] Demos SG and Sharareh S. Real time assessment of RF cardiac tissue ablation with optical spectroscopy. Optics Express 2008; 16(19): 15286-96

[18] Tanis E, Spliethoff JW, Evers DJ, Langhout GC, Snaebjornsson P, Prevoo W, Hendriks BH, Ruers TJ. Real-time in vivo assessment of radiofrequency ablation of human colorectal liver metastases using diffuse reflectance spectroscopy. Eur J Surg Oncol. 2016 ;42(2): 251-9

[19] Cabrera JA, Sanchez-Quintana D, Ho SY, Medina A, Anderson RH. The architecture of the atrial musculature between the orifice of the inferior caval vein and the tricuspid valve: the anatomy of the isthmus. J Cardiovasc Electrophysiol. 1998 Nov;9(11):1186-95. doi: 10.1111/j.1540-8167.1998.tb00091.x.

[20] Schwartzman D, Michele JJ, Trankiem CT, Ren JF. Electrogram-guided radiofrequency catheter ablation of atrial tissue comparison with thermometry-guide ablation: comparison with thermometry-guide ablation. J Interv Card Electrophysiol. 2001; 5(3): 253-66.

[21] Barkagan M, Contreras-Valdes FM, Leshem E, Buxton AE, Nakagawa H, Anter E. High-power and short-duration ablation for pulmonary vein isolation: Safety, efficacy, and long-term durability. J Cardiovasc Electrophysiol. 2018; 29(9): 1287-1296

7 General discussion and concluding remarks

This thesis reports on a series of studies investigating the feasibility of laser-induced tissue coagulation in a clinical setting, the effects of pulsed wave laser, and the use of reflectance spectroscopy to visualize lesions.

Chapter 1 describes the treatment of cardiac arrhythmias and the catheter ablation of atrial flutter and ventricular tachycardia (VT). For the ablation treatment of atrial flutter, usually a transmural linear conduction block is created in the right atrium between the tricuspid valve and the cavotricuspid isthmus (CTI) by catheter-based application of cryo- or radiofrequency energy to the targeted substrate. The energy applications result in regions of myocardial necrosis, disrupting the circular conduction pattern in the right atrium, hence preventing the continuation of the re-entrant circuit that causes atrial flutter. These lesions need to be continuous and transmural. [1-3] to achieve acute conduction block and reduce the recurrence of the atrial tachycardia after ablation.

The ablation of VT has shown to be effective for post-infarction scar homogenization. [4]. The border zone of scars, regions where myocardial scars are adjacent to surviving myocardium, represent regions of slow conduction and sources of VT. High-density delineation of the scar by catheter ablation is commonly the first step to eliminate all abnormal electrograms. [5-7]. Also ablation of idiopathic VT in the absence of structural heart disease is now well accepted as a safe and effective procedure.

The electrical homogenization of myocardial scars achieved by catheter ablation eliminates the heterogeneous low-voltage regions and converts them into electrically silent areas preventing the continuation of the re-entrant circuit that causes ventricular tachycardia.

More extensive and linear ablation schemes are associated with a better success rate and lower recurrence rate during ablation of large scar-related ventricular tachycardia.[8]

Biophysical limitations of ablation are constituted by the thick ventricular walls with transmural circuits, where, besides the wall thickness, trabeculations and fat serve as barriers to effective power delivery into the scar. [9, 10] Therefore, deep and linear lesions are required to treat VT by catheter ablation effectively.[11]

In both fields, the use of different energy sources could overcome current limitations of point-by-point RF ablations and the collateral damage to surrounding tissues associated with cryotherapies.

Since lesion formation is a crucial factor in ablation therapy success, the lesion formation process and its principles form the basics of each procedure. The energy-based lesion formation relies on the exceedance of the tissue-specific thermal threshold, either by removing or adding thermal energy, resulting in irreversible tissue necrosis (e.g., in RF resistive heating of the cardiac tissue exceeds applications the thermal threshold).

In cryotherapies, energy deprivation exceeds the threshold due to local freezing. The created regions of tissue necrosis need to be big enough to incorporate the target but small enough to minimize collateral damage to achieve the desired therapeutic effect.

Ex *vivo* investigations most commonly assess the first tissue interaction of new energy sources or ablation devices. The controllable environment of *ex vivo* investigations allows precise and identical energy applications, promoting comparability between device settings and catheter design regarding lesion formation.

These investigations provide a first indication of the required treatment dose and an initial impression of device safety regarding tissue damage and thermal blood coagulation. Subsequently, these *ex vivo* findings are typically confirmed by *in vivo* animal investigations, focusing on lesion formation, procedural safety, and device handling in a clinical setting.

Laser energy ablation

For every energy source, the main challenge is finding the correct balance between therapeutic effect and safety. Lesion continuity and transmurality are required to effectively prevent the continuation of the re-entrant circuit from achieving the desired therapeutic effect in CTI and VT ablation.

Concurrently, the applied therapeutic dose may not lead to myocardial disruption at the target site, extracardiac damage, or acute periprocedural complications related to the energy application. These aspects are to be assessed experimentally and confirmed via *in vivo* studies.

This thesis chose laser energy as an energy source for the endocardial ablation of the cavotricuspid isthmus and the epicardial ablation of ventricles. Laser energy is known for its precise lesion formation [12] and can be shaped to create unidirectional linear lesions.

In the thermo-ablative treatment of cardiac tissue by laser energy, the targeted tissue is heated by the absorption of laser light until a lesion is formed, resulting in regions of myocardial necrosis.

A deflectable linear laser ablation catheter with a side-firing laser-active area of 20mm, was developed as described in *Chapter 2*. The potential linearity of the created lesions could be beneficial in the ablation of the cavotricuspid isthmus that requires a linear lesion between 27±3,3 mm and 37±8 mm, [13] or in the

case of a VT scar, homogenization that demands a unidirectional energy emission preventing excessive thermal effects on surrounding tissues.

By its bidirectional steering and diameter of only 8.5 Fr, this catheter design allows transfemoral access for endocardial ablations and subxiphoidal access for epicardial ablations. However, the uniqueness of this linear laser ablation catheter lies in the homogeneous unilateral laser emission over a length of 20mm. This is achieved by modification of optical fiber, allowing laser light to escape from a single side of the fiber. The length of this lateral emission can be varied between 20 and 100mm, depending on the desired application. This lateral extraction of laser light defers strongly from the currently available laser ablation devices solely relying upon emission at the tip[14] or reflection of the tip emission.[15]

Compared to existing linear multipolar RF catheters[16] and RF balloon catheters [17], this kind of homogeneous laser emission is unique since the lesion formation occurs contemporaneous and homogeneous over the entire length of the catheter. Lesions created by RF catheters expand from the electrodes, achieving linearity by lesion connection between two electrodes. Hence, RF relies on lesion creation by resistive electrical heating between two poles, while laser relies on heating by absorption of the homogeneously emitted laser energy over the entire catheter length at once.

The effects of laterally emitted laser light on cardiac tissue by the 20mm linear laser ablation catheter were initially assessed in an *ex vivo* dose-finding study. Laser energy was applied to a freshly excised porcine heart between 60 and 150s with power varying between 20W and 30W. Power applications at the CTI lead to transmural atrial lesions at a power of 25W and application time of 60s. Power applications on the ventricular surface led to a maximum lesion depth of 9mm at a power of 30W and applications time of 120s.

These outcomes were validated by a subsequent *in vivo* proof of concept study, as reported and discussed in *Chapter 3*. In this study, eight endocardial CTI ablations and 26 epicardial ventricle ablations were created. Complete transmural CTI lesions could be achieved by connecting between two and three power applications, extending from inside the tricuspid valve towards the inferior vena cava. Between applications, the catheter was incrementally retracted towards the sheath.

After the procedure, the right atrium was dissected and opened, allowing macroscopic assessment of transmurality and lesion size by an experienced pathologist. The linear laser catheter created homogeneous and transmural lesions at the CTI. As past studies have shown, this lesion homogeneity and transmurality are essential for procedural success. [1-3]

A direct relationship between confirmed bidirectional conduction block at the isthmus and macroscopically assessed lesion homogeneity and transmurality was established by several animal studies. [18-20] Therefore, the results reported in *Chapter 3* indicate the strong feasibility of CTI conduction block by linear laser lesion ablation, despite the absence of conduction block confirmation by mapping or pacing.

Admittedly, the ideal morphology presented by the swine model supplies a preferable substrate to target, compared to the complex and diverse CTI anatomy of humans. Typical anatomical peculiarities, such as a prominent Eustachian ridge, pouchlike recesses, and pectinate muscles, can make the ablation of the CTI in humans challenging. The suitability of the linear laser ablation catheter to achieve conduction block in challenging CTI anatomy is to be confirmed.

Besides the benefits of homogeneous and transmural lesions, the procedure times could be reduced. The required laser time between 120s and 180s is

shorter than current RF ablation times. [21] The reduction is mainly driven by the linear fashion of the energy application, overcoming the necessity of time-consuming point-by-point energy applications as customary for RF ablation catheters.

A midline sternotomy was performed to allow free access to the epicardial surface of the ventricles to investigate the ventricular lesion formation in the porcine animal model. The left and right ventricle were targeted for catheter ablation, aiming to assess the maximum lesion depth and lesion linearity. After the procedure, the right and left ventricle were dissected and opened, allowing macroscopic assessment of lesion size by an experienced pathologist. In most cases, the RV ablations resulted in transmural lesions, depending on the thickness and presence of papillary muscles. A maximum lesion depth of 9mm In the left ventricle could be achieved, insufficient to obtain lesion transmurality.

As past studies have shown, deep and linear lesions are essential for procedural success.[9-11] A direct relationship between areas of reduced voltage due to epicardial ablation and macroscopically assessed lesion homogeneity and depth was established by several animal studies.[22-24]

Therefore, the deep and linear ventricular lesions reported in this study indicate strong feasibility of electrical homogenization of myocardial scars by linear laser-lesion ablation, despite the absence of confirmed voltage reduction by electroanatomic mapping. Compared to past epicardial RF ablation studies, [23, 25] the obtained laser-induced LV lesions were deeper and more homogeneous. Increased lesion depth could provide a solution to overcome current challenges in the ablation of intramural sites of the left ventricular summit, papillary muscles, or interventricular septum. [9-11]

The linearity and homogeneity of the laser ablations could effectively minimize the risk of lesion and conduction gaps, increasing the likelihood of durable

lesions, improving procedural success. The procedural advantage is in the unidirectional laser emission preventing damage to the parietal pericardium, underlying tissues, or phrenic nerve.

Complications related to catheter-ablation-induced injuries to the visceral pericardium are commonly reported in minimally invasive procedures with RF and cryo-energy. [26-28] By its unilateral emission, only the epicardial surface is irradiated with laser energy, leaving the visceral pericardium and underlying tissue structures unaffected and reducing the risk of ablation related post-procedural complications.

In general, the observed safety profile of the endo- and epicardial ablations aligned with those of current state-of-the-art procedures, presenting no recordable incidents or signs of blood clot formation or charring. Therefore, laser energy provides a great alternative to current RF and Cryo-devices regarding lesion formation while presenting a similar intra-procedural safety profile to state-of-the-art devices.

Future studies need to elaborate on these findings. This *in vivo* study did not assess long-term safety and should be considered in follow-up studies with this linear laser ablation catheter.

By comparing the energy-dependent *in vivo* lesion depth with the *ex vivo* dose-finding study, the *ex vivo* lesion formation model could be validated. Since no significant difference in lesion depth was seen, it was concluded that the *ex vivo* model can be well used to predict the energy-dependent *in vivo* lesion depth. This is significant to define the ideal energy settings to achieve the desired therapeutical effect while limiting the effect to underlying tissue structures.

Pulsed wave laser

In past laser ablation investigations, a laser was applied in a continuous manner. [29-31] The pulsed-laser application could improve epicardial lesion formation and reduce susceptibility to endocardial blood-clot formation. [39-41] Similar effects on the safety profile, selective tissue necrosis, and increased procedural efficacy as recently observed in pulsed-field ablations [35-38] may be observed with PW laser applications.

We investigated the effects of pulsed wave (PW) laser on lesion formation and thermal coagulation of blood compared to continuous wave (CW) laser as described in *Chapter 4*.

A parameter-finding study was conducted on avian tissue to define suitable pulsing parameters for pulsing duty cycle and frequency regarding lesion depth. The parameter study showed satisfactory results at a duty cycle of 85%, leading to reduced heating of the superficial tissue layers and equal-lesion depth compared to continuous-wave power applications. The lesion depth was assessed macroscopically by an orthogonal section at the lesion site, which confirmed the predicted cool-down phase and lower temperature at superficial tissue layers while maintaining tissue heating in deeper layers.

In later steps, the lesion homogeneity was assessed by measuring the lesion depth over the entire length of the linear ablation catheter. Pulsing also did not affect the lesion homogeneity compared to continuous wave applications. This result confirmed that pulsed laser applications provide a superior alternative to continuous-wave applications, lowering the superficial tissue temperature while maintaining identical-lesion depth.

The clotting limits for continuous and pulsed wave-power applications were assessed in stagnant oxygenated blood to establish the influence of pulsed-wave laser on the thermal coagulation of blood. These investigations showed that pulsing allowed higher power applications than continuous wave before

clot formation was observed. This finding confirmed that pulsing also provided a cool-down phase for red blood cells, the main absorbing component in blood, reducing overheating and coagulation of proteins.

The provided cool-down phase primarily increases the safety profile of laser-based catheter ablation procedures and allows higher application powers. In this case, higher power applications could reduce application times since transmurality is achieved quicker. This principle could also be applied to existing laser ablation devices, such as the visually-guided laser balloon, to increase the safety profile of endocardial pulmonary vein isolation procedures without affecting the lesion formation and procedural outcome.

Pericarditis presents a well-known post-procedural complication in epicardial catheter-ablation procedures caused by initial damage to the pericardial and superficial myocardial tissue through trauma or ablation.[39]

Therefore, it is vital to minimize ablation-related damage to the visceral and parietal pericardial surface. This can be achieved by reduced absorption in the superficial layers of the epicardium due to pulsing, utilizing directed laser emission preventing unwanted side effects on the parietal pericardial tissue. Applications on freshly excised porcine hearts showed reduced heating and less surface charring for pulsed-wave laser applications than continuous-wave laser and current state-of-the-art RF applications. [40, 41] These findings also confirmed the cool-down phase of the superficial tissue layers evoked by pulsing, as observed in the heating of red blood cells. Hence, pulsed laser applications could reduce the risk of post-procedural pericarditis due to reduced damage to the pericardial tissue. This assumption needs to be investigated by chronic *in vivo* studies comparing pulsed laser applications to RF.

Although the laser applications showed low collateral damage to surrounding tissue structures, the unique tissue-selective lesion formation properties of

PFA[2] could not be achieved. PFA relies on the biophysical phenomenon of irreversible electroporation, which increases the cell membrane permeability of the by nano-scale pores in the lipid bilayer due to the applied electrical field, resulting in apoptosis.[20-22] The laser is an electromagnetic radiation emitting device consisting of synchronized oscillations of electric and magnetic fields. However, the electrical field of 980nm laser irradiation did not have the electrical field strength to induce irreversible electroporation.

Besides the identified catheter-dependent effects of pulsed-wave laser on the thermal coagulation of blood, this investigation showed that hematocrit was the crucial factor in laser-induced blood clot formation. For a 980nm laser, red blood cells are the main absorbing components in blood. The absorption-related excessive heating of red blood cells triggers coagulation of comprised proteins, such as hemoglobin, leading to thrombus formation. Thus, the hematocrit directly determines the number of absorbing components that could result in blood clots. Future *in vivo* animal studies concerning the procedural safety of laser ablation devices need to address this factor.

Properties of laser-ablation catheters

The earlier investigations compared many properties of the laser-ablation catheter to current RF catheters. *Chapter 5 extended* this comparison by estimating the required energy to achieve transmural tissue necrosis, based on a thermal isotherm of 60.6°C for an RF and laser ablation catheter. In general, the required energy to produce transmural lesions of equal length and volume was lower for laser applications. This finding showed that the underlying biophysical principle of laser-induced tissue coagulation differs strongly from thermal coagulation by RF energy. The observed thermal latency characterized by the rising transmural temperature after cessation of the RF energy application supported

this conclusion. However, it which was not observed in laser energy applications.

Increased understanding of the heating process resulting in a more accurate prediction of the extent of necrotic tissue prevents underestimation of the lethal myocardial temperature or overestimation of the lesion size. This increased understanding allows exact selection of power settings and specification of the maximum interlesion distance (ILD), minimizing the occurrence of conduction gaps. The results of this investigation corroborated the findings of Taghji, [42] where the lesion contiguity was optimized by limiting the inter-lesion distance (ILD) to <6 mm, and by implementing an ablation index for the posterior and anterior wall. This study confirmed that an ILD <6 is necessary to reduce lesion gaps and increase the long-term procedural efficacy. The observations for laser applications can define the required lesion overlap to promote continuous transmural lesions for future and current laser energy devices.

An additional optical fiber was added to the laser ablation catheter to improve the procedural success of ablation therapies further, allowing intraprocedural assessment and confirmation of the lesion continuity. Both integrated optical fibers could be used to subject the cardiac tissue to reflectance spectroscopy.

Chapter 6 investigated the visualization of thermally-induced tissue damage by diffuse reflectance spectroscopy via a modified optical fiber. For this purpose, the integrated illuminating fiber irradiated the tissue. The reflected spectrum was recorded by the additional collecting fiber, resulting into a wavelength-dependent ADC count. A clear ADC-count drop could be observed in the range of 650 to 750nm (red light) between treated and untreated tissue. This drop corresponds to the commonly observed tissue discoloration induced by thermal-ablation therapy, containing fewer red components. Through the recorded

ADC-count drop, discrimination between treated and untreated tissue is possible.

The use of reflectance spectroscopy in a clinical setting could improve the procedural efficacy of linear laser-ablation catheters since lesions and lesion formation can be observed directly over the entire application length. It can also be applied to localize previously treated or untreated areas identifying suitable target sites and lesion gaps for touch-up procedures.

Conclusions

Overall, the investigations showed that the 20mm linear laser-ablation catheter can produce homogenous and transmural atrial lesions and deep linear ventricular lesions. The catheter could fill a device gap in the current ablation-catheter market by its lesion characteristics and flexible design. Improvements in procedural safety and lesion continuity can be made using pulsed laser and integration of reflectance spectroscopy.

References

[1] Ouyang F, Tilz R, Chun J, Schmidt B, Wissner E, et. Al. Long-term results of catheter ablation in paroxysmal atrial fibrillation: lessons from a 5-year follow-up. Circulation 2010; 122:2368-2377.

[2] Hussein AA, Saliba WI, Martin DO, Bhargava M, Sherman M, et. al. Natural history and long-term outcomes of ablated atrial fibrillation. Circ Arrhythm Electrophysiol. 2011; 4:271-278.

[3] Medi C. Sparks PB, Morton JB, Kistler PM, Halloran K, et. al. Pulmonary vein antral isolation for paroxysmal atrial fibrillation: results from long-term follow-up. J Cardiovasc Electrophysiol. 2011; 22:137-141.

[4] Aryana A, Tung R, d'Avila A. Percutaneous Epicardial Approach to Catheter Ablation of Cardiac Arrhythmias. JACC Clin Electrophysiol. 2020 Jan;6(1):1-20. doi: 10.1016/j.jacep.2019.10.016.

[5] Di Biase L, Santangeli P, Burkhardt DJ, Bai R, Mohanty P et. al. Endo-epicardial homogenization of the scar versus limited substrate ablation for the treatment of electrical storms in patients with ischemic cardiomyopathy. J Am Coll Cardiol. 2012 Jul 10;60(2):132-41. doi: 10.1016/j.jacc.2012.03.044.

[6] Vergara P, Trevisi N, Ricco A, Petracca F, Baratto F et. al. Late potentials abolition as an additional technique for reduction of arrhythmia recurrence in scar

related ventricular tachycardia ablation. J Cardiovasc Electrophysiol. 2012 Jun;23(6):621-7. doi: 10.1111/j.1540-8167.2011.02246.x.

[7] Ghanem MT, Ahmed RS, Abd El Moteleb AM, Zarif JK. Predictors of success in ablation of scar-related ventricular tachycardia. Clin Med Insights Cardiol. 2013 May 7;7:87-95. doi: 10.4137/CMC.S11501.

[8] Thomsen AF, Pehrson S, Chen X, Jons C, Jacobsen PK. Challenges in catheter ablation of deep myocardial substrate for ventricular tachycardia. Journal of Interventional Cardiac Electrophysiology 2021; 60:349–351

[9] Soejima K, Stevenson WG, Sapp JL, Andrew P Selwyn AP, Couper G, Epstein LM. Endocardial and epicardial radiofrequency ablation of ventricular tachycardia associated with dilated cardiomyopathy: The importance of low-voltage scars, Journal of the American College of Cardiology 2004; 43(10):1834-1842

[10] De Cobelli F, Pieroni M, Esposito A, Chimenti C, Belloni E, et. al. Delayed Gadolinium-Enhanced Cardiac Magnetic Resonance in Patients With Chronic Myocarditis Presenting With Heart Failure or Recurrent Arrhythmias, Journal of the American College of Cardiology 2006; 47(8):1649-1654

[11] Koruth JS, Dukkipai S, Miller MA, Neuzil P, d'Avila A, et. al. Bipolar irrigated radiofrequency ablation: a therapeutic option for refractory intramural atrial and ventricular tachycardia circuits. Heart Rhythm 2012;9:1932-41

[12] Reddy VY, Neuzil P, Themistoclakis S, Danik SB, Bonso A et. al. Visually-Guided Balloon Catheter Ablation of Atrial Fibrillation. Experimental Feasability and First-in-Human Multicenter Clinical Outcome. Circulation 2019; 120: 12-20

[13] Cabrera JA, Sanchez-Quintana D, Ho SY, Medina A, Wanguemert F et. al. Angiographic anatomy of the inferior right atrial isthmus in patients with and without history of common atrial flutter. Circulation 1999; 99:3017-3023.

[14] Weber H, Sagerer-Gerhardt M and Heinze A. Laser catheter ablation of long- lasting persistent atrial fibrillation: Longterm results. J Atr Fibrillation. 2017; 10(2): 1588.

[15] Dukkipati SR, Cuoco F, Kutinsky I, Aryana A, Bahnson TD et. al. Pulmonary Vein Isolation Using the Visually Guided Laser Balloon: A Prospective, Multicenter, and Randomized Comparison to Standard Radiofrequency Ablation. J Am Coll Cardiol. 2015; 66(12):1350-60. doi: 10.1016/j.jacc.2015.07.036.

[16] Nazer B, Walters TE, Duggirala S, Gerstenfeld EP. Feasibility of Rapid Linear-Endocardial and Epicardial Ventricular Ablation Using an Irrigated Multipolar Radiofrequency Ablation Catheter. Circ Arrhythm Electrophysiol. 2017; 10(3).

[17] Reddy VY, Neuzil P, Peichl P, Rackauskas G, Anter E, et. al. A Lattice-Tip Temperature-Controlled Radiofrequency Ablation Catheter: Durability of Pulmonary Vein Isolation and Linear Lesion Block. JACC 2020; 6(6):623-635.

[18] Nordbeck P, Hiller KH, Fidler F, Warmuth M, Burkard N, et. al. Feasibility of contrast-enhanced and nonenhanced MRI for intraprocedural and postprocedural lesion visualization in interventional electrophysiology: animal studies and early delineation of isthmus ablation lesions in patients with typical atrial flutter. Circ Cardiovasc Imaging. 2011 May;4(3):282-94.

[19] Hoffmann BA, Koops A, Rostock T, Müllerleile K, Steven D, et. al. Interactive real-time mapping and catheter ablation of the cavotricuspid isthmus guided by magnetic resonance imaging in a porcine model. Eur Heart J. 2010 Feb;31(4):450-6.

[20] Ganesan AN, Selvanayagam JB, Mahajan R, Grover S, Nayyar S, et. al. Mapping and ablation of the pulmonary veins and cavo-tricuspid isthmus with a magnetic resonance imaging-compatible externally irrigated ablation catheter and integrated electrophysiology system. Circ Arrhythm Electrophysiol. 2012 Dec;5(6):1136-42.

[21] Zhang T, Wang Y, Han Z, Zhao H, Liang Z, et. al. Cavotricuspid isthmus ablation using ablation index in typical right atrial flutter. J Cardiovasc Electrophysiol. 2019; 30(11):2414-2419.

[22] d'Avila A, Houghtaling C, Gutierrez P, Vragovic O, Ruskin JN, et. al. Catheter ablation of ventricular epicardial tissue: a comparison of standard and cooled-tip radiofrequency energy. Circulation. 2004 May 18;109(19):2363-9.

[23] Nazer B, Walter TE, Duggirala S and Gerstenfeld E. Feasibility of Rapid Linear-Endocardial and Epicardial Ventricular Ablation Using an Irrigated Multipolar Radiofrequency Ablation Catheter. Circulation: Arrhythmia and Electrophysiology. 2017;10:1-9.

[24] Aryana A, O'Neill PG, Pujara DK, Singh SK, Bowers MR, et. al. Impact of irrigation flow rate and intrapericardial fluid on cooled-tip epicardial radiofrequency ablation. Heart Rhythm. 2016 Aug;13(8):1602-11.

[25] Tung R. Epicardial Approach to Catheter Ablation of Ventricular Tachycardia. Elsevier, Part 7 – Catheter ablation of ventricular tachycardia 2017;Chapter 33:649-670.

[26] Tung R, Michowitz Y, Yu R, Mathuria N, Vaseghi M et. al. Epicardial ablation of ventricular tachycardia: an institutional experience of safety and efficacy. Heart Rhythm. 2013 Apr;10(4):490-8. doi: 10.1016/j.hrthm.2012.12.013.

[27] Oesterle A, Singh A, Balkhy H, Husain AN, Moyer D et. al. Late presentation of con-strictive pericarditis after limited epicardial ablation for inappropriate sinus tachycar-dia. HeartRhythm Case Rep. 2016 Jul 16;2(5):441-445. doi: 10.1016/j.hrcr.2016.07.003.

[28] Dar TA, Turagam M, Yarlagadda B, Lakkireddy D. Managing Pericardium in Elec-trophysiology Procedures. American College of Cardiology. Oct 27, 2017.

[29] Bhardwaj R, Reddy VY. Visually-guided Laser Balloon Ablation of Atrial Fi-brilla-tion: A "Real World" Experience. Rev Esp Cardiol (Engl Ed). 2016 May;69(5):474-6. English, Spanish. doi: 10.1016/j.rec.2016.02.006.

[30] Weber H, Sagerer-Gerhardt M, and Heinze A. Laser catheter ablation of long- last-ing persistent atrial fibrillation: Longterm results. J Atr Fibrillation. 2017 Aug-Sep; 10(2): 1588.

[31] Sagerer-Gerhardt M and Weber H. Open-irrigated laser catheter ablation: influ-ence of catheter–tissue contact force on lesion formation. J Interv Card Electrophysiol (2015) 42:77–81

[32] Anderson RR, Parrish JA. Selective photothermolysis: precise microsur-gery by selective absorption of pulsed radiation. Science. 1983 Apr 29;220(4596):524-7. doi: 10.1126/science.6836297.

[33] Henderson TA, Morries LD. Near-infrared photonic energy penetration: can infra-red phototherapy effectively reach the human brain? Neuropsychiatr Dis Treat. 2015 Aug 21;11:2191-208. doi: 10.2147/NDT.S78182.

[34] Hashmi JT, Huang YY, Sharma SK, Kurup DB, De Taboada L et. al. Effect of pulsing in low-level light therapy. Lasers Surg Med. 2010 Aug;42(6):450-66. doi: 10.1002/lsm.20950.

[35] Reddy VY, Neuzil P, Koruth JS, Petru J, Funosako M et. al. Pulsed Field Ablation for Pulmonary Vein Isolation in Atrial Fibrillation. J Am Coll Cardiol. 2019 Jul 23;74(3):315-326. doi: 10.1016/j.jacc.2019.04.021.

[36] Reddy VY, Anter E, Rackauskas G, Peichl P, Koruth JS et. al. Lattice-Tip Focal Abla-tion Catheter That Toggles Between Radiofrequency and Pulsed Field Energy to Treat Atrial Fibrillation: A First-in-Human Trial. Circ Arrhythm Electrophysiol. 2020 Jun;13(6):e008718. doi: 10.1161/CIRCEP.120.008718.

[37] Koruth JS, Kuroki K, Kawamura I, Brose R, Viswanathan R et. al. Pulsed Field Abla-tion Versus Radiofrequency Ablation: Esophageal Injury in a Novel Porcine Model. Circ Arrhythm Electrophysiol. 2020 Mar;13(3):e008303. doi: 10.1161/CIRCEP.119.008303.

[38] Koruth J, Kuroki K, Iwasawa J, Enomoto Y, Viswanathan R et. al. Preclinical Evaluation of Pulsed Field Ablation: Electrophysiological and Histological Assessment of Thoracic Vein Isolation. Circ Arrhythm Electrophysiol. 2019 Dec;12(12):e007781. doi: 10.1161/CIRCEP.119.007781.

[39] Dar TA, Turagam M, Yarlagadda B, Lakkireddy DR. Managing Pericardium in Electrophysiology Procedures. American College of Cardiology Oct 2017.

[40] Aryana A, d'Avila A. Epicardial Catheter Ablation of Ventricular Tachycardia. Card Electrophysiol Clin. 2017 Mar;9(1):119-131. doi: 10.1016/j.ccep.2016.10.009.

[41] Nazer B, Walters TE, Duggirala S, Gerstenfeld EP. Feasibility of Rapid Linear-Endocardial and Epicardial Ventricular Ablation Using an Irrigated Multipolar Radiofrequency Ablation Catheter. Circ Arrhythm Electrophysiol. 2017 Mar;10(3):e004760. doi: 10.1161/CIRCEP.116.004760.

[42] Taghji P, El Haddad M, Phlips T, Wolf M, Knecht S et. al. Evaluation of a Strategy Aiming to Enclose the Pulmonary Veins With Contiguous and Optimized Radiofrequency Lesions in Paroxysmal Atrial Fibrillation: A Pilot Study. JACC Clin Electrophysiol. 2018 Jan;4(1):99-108. doi: 10.1016/j.jacep.2017.06.023.

Summary

Novel laser energy applications for the treatment of cardiac arrhythmias

Over the years, ablation therapy has been introduced into treatment of a variety of cardiac arrhythmias.

Traditionally, radiofrequency or cryo-devices are used to place lesions in the myocardium to interrupt specific arrhythmogenic mechanisms.

In this thesis, we investigated the use of laser energy as an ablation modality with a novel, linear, laser-ablation catheter. This steerable 8.5 Fr laser catheter allows homogeneous unilateral laser emission over a length of 20mm. Through *ex vivo* experiments with this catheter, the parameter settings were defined to achieve transmural atrial lesions.

In animal experiments, characteristics of lesion formation were investigated while at the same time assessing aspects with potential relevance for procedural safety. The cava-tricuspid isthmus was targeted for endocardial power applications under fluoroscopic guidance in these studies. Subsequently, a complete sternotomy was performed to allow epicardial ablations on both ventricles.

After the procedure, the atria and ventricles were dissected to perform macroscopic analysis of both lesion sets. Well-defined transmural linear lesions were found in the atria and lesions up to 9mm in the ventricles. We compared the lesion formation process in laser and radiofrequency energy applications to put these results into perspective. The underlying tissue coagulation principles differed strongly between both energy modalities, although both could achieve irreversible tissue damage.

The pulsed-wave laser was compared to continuous-wave application to improve the lesion formation and potentially safety of endocardial laser-ablation procedures. Therefore, we investigated the effects of pulsed-wave laser on tissue coagulation and thermally-induced blood clot formation. Pulsing reduced the absorption in superficial tissue layers, diminished the risk of blood clot formation, and prevented steam pops during ablation of fat-covered tissues.

In the final investigation, we fitted an additional optical fiber to the laser ablation catheter, allowing direct visualization of the created lesions by reflectance spectroscopy. A clear distinction could be made between treated and untreated tissue by illuminating the target site with one fiber and capturing the reflected spectrum with the additional fiber.

Overall, the catheter could create linear transmural atrial and deep ventricular lesions in the performed animal studies. The use of pulsed-wave laser applications improved the lesion formations process and reduced thermally induced blood clot formation compared to continuous-wave applications. The integration of an added optical fiber allowed spectroscopical analysis of the target site, allowing direct visualization of the lesion-formation process, supplying a useful tool to prevent lesion gaps.

Significance of Investigation

In this thesis, the studies' aimed to investigate the technical feasibility of laser energy in the treatment of cardiac arrhythmias. These energy-based treatments are called ablation therapy.

Several arrhythmias can be treated by ablation therapy, selectively destroying abnormal tissue to inhibit cardiac arrhythmia. In current ablation therapies, a catheter heats or cools the cardiac tissue to prevent the occurrence and sustainment of the arrhythmia. In the past, laser energy was already explored as feasible energy source for this treatment of cardiac arrhythmias. The linear laser catheter developed and investigated in this thesis could provide an alternative to the existing ablation devices, by delivering the necessary energy to the tissue, achieving the required tissue coagulation.

To deliver the necessary laser energy to the target site, the light needs to be transported and emitted at the desired location. Via an optical fiber the light can be transported from the laser source into the heart. By creating small openings at the end of the optical fiber light is emitted laterally over 20mm. The ability to extract laser light laterally in a linear fashion by creating small holes in the fiber is unique. The completeness of linear ablation is positively associated with ablation success and can be difficult to obtain with current ablation devices. Compared to focal treatment linear emission allows a homogeneous tissue treatment over a longer area, fostering improved procedural outcome and reduced duration.

The technical feasibility, laser interaction and preliminary safety of the catheter design was tested in lab conditions with freshly excised animal tissue (*ex vivo*) and later confirmed during animal studies (*in vivo*). *In vivo* studies showed good results in energy applications from inside (endocardial) and from outside (epicardial) the heart suggesting suitability as alternative to

existing treatment devices. The presented results in this thesis contain important new information regarding fast and linear creation of lesions by laser energy, with a small and flexible ablation catheter.

In contrast to the previous *ex vivo* and *in vivo* investigations, laser can also be applied in a pulsed fashion. In these applications optical power appears in pulses of some duration at some repetition rate.
In past research the beneficial properties of pulsed laser sources were investigated. The inherent cool down period between the pulses can reduce or even prevent excessive tissue damage, and increases the safety of energy applications. By *ex vivo* studies these beneficial properties could be confirmed for the developed laser ablation catheter. Damage to the cardiac tissue, and susceptibility to blood clot formation due to laser ablation could be reduced. These findings also of interest for presently existing laser ablation devices to increase procedural safety.

Finally, a possibility was sought, to visualize the lesion formation process. The utilized optical fiber of the ablation catheter also allowed normal light to be transported to the target site, besides the usual laser energy dose. By integrating an extra fiber, the reflection of the normal light could be captured. The recorded spectrum can provide information about the examined tissue. High reflection of red light indicates untreated tissue and low reflection treated tissue. Analysis of the spectra before and after successful treatment showed this reduced reflection of red light, indicating tissue ablation. This could provide the physician with useful information about the catheter position and the successful execution of the ablation procedure.

Overall, the obtained results contribute to understanding how laser can treat arrhythmias by ablation therapy and improve catheter ablation procedures. Furthermore, the results uncovered new capabilities of fiber-based optical systems, allowing lateral extraction of light from an optical fiber. Thus, general interest is created for the physician-scientist in the field of catheter ablations but also for the physicist studying fiber-based optical systems.